



ΕΛΛΗΝΙΚΗ
ΕΠΙΣΤΗΜΟΝΙΚΗ
ΕΤΑΙΡΕΙΑ
ΕΔΑΦΟΜΗΧΑΝΙΚΗΣ
& ΓΕΩΤΕΧΝΙΚΗΣ
ΜΗΧΑΝΙΚΗΣ

Τα Νέα

της Ε Ε Ε Ε Γ Μ

24

Αρ. 24 - ΟΚΤΩΒΡΙΟΣ 2009

17th INTERNATIONAL CONFERENCE ON SOIL MECHANICS AND GEOTECHNICAL ENGINEERING

Το συνέδριο δεξήχθη στο συνεδριακό κέντρο της νέας Βιβλιοθήκης Αλεξάνδρειας, στην Αίγυπτο, από την Δευτέρα, 5 Οκτωβρίου μέχρι την Πέμπτη, 8 Οκτωβρίου, ενώ την Παρασκευή έγιναν επισκέψεις σε τεχνικά έργα από την Αλεξάνδρεια μέχρι το Κάιρο.

Του συνεδρίου προηγήθηκε η Γενική Συνέλευση της International Society for Soil Mechanics and Geotechnical Engineering, την Κυριακή 4 Οκτωβρίου, κατά την οποία εξελέγη ο Πρόεδρος της ISSMGE για την περίοδο 2009 - 2013.

Από τις 2 μέχρι τις 6 Οκτωβρίου διεξήχθη το International Young Geotechnical Engineers Conference σε ξενοδοχείο της Αλεξάνδρειας, με διπλή Ελληνική εκπροσώπηση.

Επίσης, το διήμερο 2 και 3 Οκτωβρίου διεξήχθη το Satellite Conference της Technical Committee TC 4 "Earthquake Geotechnical Engineering".

Τέλος, πριν και κατά τη διάρκεια του συνεδρίου διεξήχθησαν workshops καθώς και ανοικτές συνεδριάσεις πολλών τεχνικών επιτροπών της ISSMGE.

Το επόμενο 18th International Conference on Soil Mechanics and Geotechnical Engineering θα διεξαχθεί στο Παρίσι, 1 - 5 Σεπτεμβρίου 2013.



Π Ε Ρ Ι Ε Χ Ο Μ Ε Ν Α

17 th International Conference on Soil Mechanics and Geotechnical Engineering	1	- Pipelines Conference 2010	61
Γιάννης Βαρδουλάκης (1049 – 2009)	3	- II International Congress on Dam Maintenance and Rehabilitation	62
Ανασκόπηση Γεγονότων Γεωτεχνικού Ενδιαφέροντος	4	- 2nd International Conference on Geotechnical Engineering - ICGE 2010 Innovative Geotechnical Engineering	63
- 4 th International Young Geotechnical Engineers Conference - 4 iYGEC'09	4	- ISCE-5 5 th International Conference on Scour and Erosion	63
- TC4 Satellite Conference Earthquake Geotechnical Engineering	4	- Fifth International Symposium on Deformation Characteristics of Geomaterials (IS-Seoul 2011)	64
- Council Meeting of International Society for Soil Mechanics and Geotechnical Engineering	5	Ηλεκτρονικά Περιοδικά	65
- 17 th International European Conference on Soil Mechanics and Geotechnical Engineering	6	- ISSMGE Bulletin	65
Άρθρα Εκπροσώπων ΕΕΕΕΓΜ στο 4 th iYGEC	9	- Geoengineer	65
- P. Fortsakis " <i>Estimation of tunnel final lining loads</i> "	9	- ISRM Newsletter	65
- K. Kakderi & K. Pitilakis " <i>Fragility curves for the seismic vulnerability assessment of waterfront structures</i> "	13	- ITA News	65
Άρθρα Μελών ΕΕΕΕΓΜ στο 17 th ICSMGE	17	- British Tunnelling Society Newsletter	65
- D.N. Christodoulou, A.I. Droudakis, I.A. Pantazopoulos, I.N. Markou and D.K. Atmatzidis " <i>Groutability and effectiveness of microfine cement grout</i> "	17	- International Journal of Geoengineering Case Histories Volume 1, Issue #3, October 2008	65
- I. Mihalios, S. Konstantis, A. Anagnostopoulos, G. Vliavianos and G. Doulis " <i>Tunnel Stability Factor – A new controlling parameter for the face stability conditions of shallow tunnels in weak rock environment</i> "	21		
- D.K. Atmatzidis, D.A. Chrysikos & I.M. Papaefstathiou " <i>Installation damage of nonwoven polypropylene geotextiles</i> "	25		
- K. Pitilakis & S. Bandis and S. Hemeda " <i>Geotechnical investigation and seismic analysis of underground monuments in Alexandria, Egypt</i> "	29		
- Z. R. Papachatzaki, K. Anastasopoulos, C. Oikonomidis, S. Siachou and G. Dounias " <i>Experiences from the installation of geotechnical instruments in dams</i> "	33		
- M. Pantazidou " <i>Student understanding of the concept of soil structure guides instructional interventions</i> "	37		
- A. Valsamis, G. Bouckovalas and E. Drakopoulos " <i>Design charts for single piles under lateral spreading of liquefied soil</i> "	41		
- E. Papageorgiou, N. Boussoulas, F. Karaoulanis and S. Tsotsos " <i>Ground movements during tunnel construction by EPB method along the southern extension of Athens Metro Line 2, Greece</i> "	46		
- Bardanis, M., Cavounidis, S. and Dounias, G. " <i>Numerical simulation of the pore pressure regime in landslides with underdrainage</i> "	51		
- M. Kavvadas, M. Karlaftis, P. Fortsakis, E. Stylianidi " <i>Probabilistic analysis in slope stability</i> "	55		
Προσεχείς Επιστημονικές Εκδηλώσεις	59		
- 5 th Congress on Forensic Engineering	59		
- The Seventh South Asian Geotechnical Conference	60		

ΓΙΑΝΝΗΣ ΒΑΡΔΟΥΛΑΚΗΣ

1949 ÷ 2009

Τις πρωινές ώρες του Σαββάτου 19 Σεπτεμβρίου 2009 πέθανε ο Γιάννης Βαρδουλάκης μετά από κρανιοεγκεφαλικό κάταγμα από πτώση στις 6 Σεπτεμβρίου. Η κηδεία του έγινε την Τρίτη 22 Σεπτεμβρίου από το Α΄ Νεκροταφείο Αθηνών.



Ο Γιάννης ήταν Καθηγητής Μηχανικής του Ε.Μ.Π. και μέλος της ΕΕΕΕΓΜ. Ήταν δάσκαλος και φίλος πολλών εκ των μελών μας και ερευνητής με παγκόσμια ακτινοβολία.

Ο Γιάννης Βαρδουλάκης γεννήθηκε στις 22 Μαρτίου 1949 στα Χανιά. Έλαβε το δίπλωμα Πολιτικού Μηχανικού από το ΕΜΠ το 1972 και το Διδακτορικό Δίπλωμα Μηχανικού στην Εδαφομηχανική από το Πανεπιστήμιο της Καρλσρούης της Γερμανίας το 1977.

Διετέλεσε ερευνητής στην Karlsruhe και Καθηγητής της Γεωμηχανικής στο Πανεπιστήμιο της Minnesota των ΗΠΑ, μέχρι την εκλογή του σε θέση Καθηγητή στο ΕΜΠ το 1990.

Η ερευνητική δραστηριότητα του εκλιπόντος επηρέασε βαθύτατα τις διεθνείς επιστημονικές κοινότητες τόσο της Εδαφομηχανικής όσο και της Μηχανικής γενικότερα. Είναι αξιοθαύμαστη η ευρύτητα των περιοχών στις οποίες είχε όχι απλώς συνεισφέρει αλλά κυρίως δημιουργήσει νέες βάσεις και εισηγηθεί επαναστατικές μεθόδους επίλυσης και αντιμετώπισης τόσο θεωρητικών όσο και εφαρμοσμένων προβλημάτων. Τέτοιες περιοχές ήταν η Γεωμηχανική με έμφαση στην αστάθεια, διακλάδωση, συγκέντρωση παραμορφώσεων και υγροποίηση της άμμου, η θερμοπορομηχανική, η θεωρία βαθμίδων και η επέκταση και εφαρμογή των θεωριών Cosserat και Mindlin τόσο σε θέματα εδαφομηχανικής και πλαστικότητας όσο και σε ελαστικότητα και θραύση, η θερμομηχανική γεωμαζών και οι συνέπειες της σε κατολισθήσεις, η διάδοση κυμάτων σε συνεχή μέσα με μικρομηχανική, η μελέτη της σταθερότητας και συμπεριφοράς αρχαίων μνημείων με κολοφώνα την έρευνα στα μάρμαρα του Παρθενώνα, και πλείστες άλλες ερευνητικές περιοχές. Το ιδιαίτερω καταπληκτικό ήταν ότι στα περισσότερα από αυτά τα ερευνητικά πεδία ο Βαρδουλάκης συνέβαλε όχι μόνο θεωρητικά αλλά και πειραματικά με διατάξεις εντελώς πρωτότυπες για τις οποίες είχε τιμηθεί με διεθνή αναγνώριση και πατέντες ευρεσιτεχνίας.

Για την προσφορά του τιμήθηκε με το βραβείο Bishop για τη γεωτεχνική έρευνα από το Ίδρυμα Πολιτικών Μηχανικών του Ηνωμένου Βασιλείου και το μετάλλιο «Εξαιρετής Έρευνας στην Γεωμηχανική» από τον Ιαπωνικό Γεωτεχνικό Σύλλογο. Η σημαντική επιστημονική του συμβολή όμως, εκτός από τις διακρίσεις, αποδεικνύεται από τις πολλές στον αριθμό, αλλά κυρίως εκτενείς και ουσιαστικές αναφορές στις εργασίες του από άλλους ερευνητές.

Για την έρευνά του διεκδίκησε και έλαβε χρηματοδότηση, με σημαντικές ερευνητικές προτάσεις, η κορωνίδα των οποίων ήταν το τελευταίο μεγάλο ευρωπαϊκό του πρόγραμμα στο

πλαίσιο του IDEAS. Με τις προσπάθειες του έστησε ένα σπουδαίο ερευνητικό εργαστήριο στο ΕΜΠ άρτια εξοπλισμένο.

Το σπουδαιότερο όμως για τη δράση ενός ακαδημαϊκού δασκάλου ήταν ότι ο Γιάννης Βαρδουλάκης δημιούργησε ερευνητική ομάδα. Έχοντας σπουδαία επιστημονική επάρκεια ο ίδιος, αφιερώθηκε στην εκπαίδευση των μαθητών του, τους μετέδιδε τη γνώση, τους καθοδηγούσε, τους ενέπνευσε τον ενθουσιασμό του για την έρευνα, τους μύησε στην περιπέτειά της. Έχοντας και ο ίδιος ένα εξαιρετικό υπόβαθρο στα μαθηματικά, πίστευε ότι δεν είναι δυνατόν να νοηθεί γόνιμη έρευνα βασική ή εφαρμοσμένη, χωρίς υψηλής ποιότητας εκπαίδευση στις βασικές επιστήμες. Και έκανε υποδειγματική δουλειά στους μαθητές του, επένδυε πολύ σε αυτό τον τομέα. Η λαμπρή ερευνητική πορεία των μαθητών του αποτελούν την καλύτερη απόδειξη της προσφοράς του και σε αυτή την κατεύθυνση.

Η συμβολή του Γιάννη στη Σχολή Ε.Μ.Φ.Ε. ως μέλους της Επιτροπής Προπτυχιακών Σπουδών με ουσιαστικές προτάσεις, στις οποίες αποτυπώνονταν και η εμπειρία του ως μηχανικού και οι διεθνείς του εμπειρίες ήταν σημαντική. Στο Μεταπτυχιακό Πρόγραμμα του Τομέα Μηχανικής έχοντας διατελέσει ο πρώτος διευθυντής του έπαιξε καθοριστικό ρόλο στη διαμόρφωσή του. Ως εκπρόσωπος της Σχολής στην επιτροπή Βασικής Έρευνας του Ίδρυματος διετέλεσε πρόεδρος της και παρήγαγε τα τελευταία χρόνια ένα σημαντικό έργο θέτοντας κανόνες αξιοκρατικής αξιολόγησης. Μειχρε επίσης στα κοινά του Ίδρυματος από τη θέση του εκλεγμένου μέλους του συνδικαλιστικού οργάνου των διδασκόντων.



Ο Γιάννης Βαρδουλάκης ήταν ένας καλλιεργημένος άνθρωπος με παιδεία, άριστος γνώστης της ελληνικής γλώσσας που τη χρησιμοποιούσε με περίτεχνο τρόπο, που πάλευε με ζωντάνια για τα πιστεύω του. Ήταν ένας άνθρωπος με ποιότητα ο οποίος αγάπησε το Πολυτεχνείο, αφιερώθηκε σε αυτό και το τίμησε με την παρουσία του.

(από την ανακοίνωση της Πρυτανείας του ΕΜΠ)

ΑΝΑΣΚΟΠΗΣΗ ΓΕΓΟΝΟΤΩΝ ΓΕΩΤΕΧΝΙΚΟΥ ΕΝΔΙΑΦΕΡΟΝΤΟΣ



4 IYGEC'09 4th International Young Geotechnical Engineers Conference 2 – 6 October 2009, Alexandria, Egypt

Το 4^ο Διεθνές Συνέδριο Νέων Γεωτεχνικών Μηχανικών (4 IYGEC'09) πραγματοποιήθηκε από τις 2 έως τις 6 Οκτωβρίου, 2009, στην Αλεξάνδρεια Αιγύπτου. Το 4 IYGEC'09 ξεκίνησε δύο μέρες πριν την έναρξη του 17^{ου} Διεθνούς Συνεδρίου Εδαφομηχανικής και Γεωτεχνικής Μηχανικής (17th International Conference on Soil Mechanics and Geotechnical Engineering - 17th ICSMGE 2009).

Μετά τις δύο πρώτες μέρες του 4 IYGEC, οι συμμετέχοντες νέοι μηχανικοί έλαβαν μέρος στις εργασίες του 17th ICSMGE για τις δύο πρώτες μέρες (5-6 Οκτωβρίου) για την παρακολούθηση των state-of-the art και κύριων διαλέξεων.

Στο 4ο Διεθνές Συνέδριο Νέων Γεωτεχνικών Μηχανικών έλαβαν μέρος 89 σύνεδροι από 43 χώρες, ηλικίας έως 35 ετών, που δραστηριοποιούνται στους τομείς της γεωτεχνικής μηχανικής και τεχνικής γεωλογίας. Την Ελλάδα εκπροσώπησαν οι Καλλιόπη Κακδέρη, Πολιτικός Μηχανικός Α.Π.Θ., MSc, που παρουσίασε την εργασία με τίτλο "Fragility Curves for the Seismic Vulnerability Assessment of Waterfront Structures", και ο Πέτρος Φορτσάκης, Πολιτικός Μηχανικός Ε.Μ.Π., MSc, που παρουσίασε την εργασία με τίτλο "Estimation of Tunnel Final Lining Loads".

Τις εργασίες του συνεδρίου άνοιξαν η Πρόεδρος του συνεδρίου, Καθ. Fatma El-Zahraa Baligh, ο Πρόεδρος της οργανωτικής επιτροπής του 17th ICSMGE, Καθ. Mamdouh Hamza, ο Γραμματέας της ISSMGE, Καθ. Neil Taylor και ο Πρόεδρος της ISSMGE, Καθ. Pedro Sêco e Pinto, ενώ διάλεξε με θέμα "Scenario-focused three-dimensional computational modeling in geomechanics" δόθηκε από τον Καθ. Ahmed W. Elgamal.

Τα θέματα που παρουσιάστηκαν και συζητήθηκαν τις δύο πρώτες μέρες του συνεδρίου εντάσσονται στις παρακάτω γενικές θεματικές ενότητες:

- Συμπεριφορά και ιδιότητες εδαφικών υλικών, νέες αρχές και σχέσεις
- Βελτίωση εδάφους: χημική, μηχανική και ενίσχυση
- Ροή εντός του εδάφους, Αντιμετώπιση μολυσμένων εδαφικών σχηματισμών
- Κατολισθήσεις και ευστάθεια πρανών
- Βαθιές θεμελιώσεις - σχεδίαση και εφαρμογή
- Συμπεριφορά διαφόρων τύπων κατασκευών αντιστήριξης
- Αλληλεπίδραση εδάφους-κατασκευής, διαχείριση κρίσης
- Υπόγειες κατασκευές

Τα τελικά συμπεράσματα του 4 IYGEC καθώς και ιδέες για το μέλλον της γεωτεχνικής μηχανικής παρουσιάστηκαν σε ειδική συνεδρία στο 17th ICSMGE.

Καλλιόπη Κακδέρη και Πέτρος Φορτσάκης

Έχει αποδειχθεί ότι τα συνέδρια των νέων γεωτεχνικών μηχανικών αποτελούν μια σημαντική δραστηριότητα, που ενθαρρύνει τη νέα γενιά των γεωτεχνικών μηχανικών στη διάδοση των στόχων της International Society for Soil Mechanics and Geotechnical Engineering.

Τα διεθνή συνέδρια των νέων γεωτεχνικών μηχανικών διεξάγονται ανά τετρατία, αμέσως πριν από την διεξαγωγή των ICSMGE. Οι επιστημονικοί φορείς - μέλη της ISSMGE καλούνται να επιλέξουν δύο νέους γεωτεχνικούς μηχανικούς για να τους αντιπροσωπεύσουν στα συνέδρια.

Η συμμετοχή στα IYGEC είναι περιορισμένη σε γεωτεχνικούς μηχανικούς ηλικίας μικρότερης των 35 ετών τον Δεκέμβριο του έτους διεξαγωγής του συνεδρίου.

Η επιλογή των Ελλήνων εκπροσώπων έγινε από την Εκτελεστική Επιτροπή της ΕΕΕΕΓΜ τον Φεβρουάριο 2009 μετά από πρόσκληση και αξιολόγηση των υποβληθεισών περιλήψεων των παρακάτω άρθρων:

Zania V., Tsompanakis Y. and Psarropoulos P. "Issues on the seismic slope stability of earth dams and soil embankments"

Kakderi K., Dimitriou I., Pitilakis K. "Fragility Curves for the Seismic Vulnerability Assessment of Waterfront Structures"

Ktenidou O.-J., Chavez-Garcia F.J., Raptakis D., Pitilakis K., Diagourtas D. "Experimental and numerical studies of site effects in the city of Aegion, Greece"

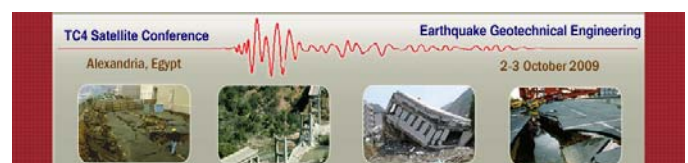
Manou D., Anastasiadis A. and Pitilakis K. "Elastic Demand Spectra based on Strong Ground Motion Processing"

Bournta Z. and Georgiadis K. "3D numerical analysis of undrained lateral loading of barrettes"

Papazafeiropoulos G. and Psarropoulos P. "Analytical evaluation of the dynamic distress of rigid fixed-base retaining systems"

Fortsakis P. "Estimation of tunnel final lining loads"

Τα άρθρα των Ελλήνων εκπροσώπων δημοσιεύονται σε επόμενες σελίδες των ΝΕΩΝ.



**TC4 Satellite Conference
Earthquake Geotechnical Engineering
Alexandria, Egypt, 2 – 3 October 2009**
www.tanta.edu.eg/ar/Conf/TC4/index.html

Το συνέδριο διοργανώθηκε από την Egyptian National Society of Soil Mechanics and Geotechnical Engineering και την Technical Committee (TC4) on Earthquake Geotechnical Engi-

neering της International Society for Soil Mechanics and Geotechnical Engineering.

Στην International Advisory Committee του συνεδρίου συμμετείχαν τα μέλη της ΕΕΕΕΓΜ Καθηγητές Γ. Γκαζέτας, Γ. Μπουκοβάλας και Κ. Πιπιλάκης, ενώ παρουσιάστηκαν προσκελημένες εισηγήσεις και πολλά άρθρα μελών της ΕΕΕΕΓΜ:

- George Gazetas "*Dynamics of Batter Piles*" (προσκεκλημένη εισήγηση)
- Kyriazis Pitilakis "*Experimental and theoretical SSI studies in a model structure in Euroseistest*" (προσκεκλημένη εισήγηση)
- Dimitris Pitilakis "*Equivalent Linear Soil-Foundation-Structure Interaction and Performance Based Design*"
- Asterios Liolios, George Michaltsos, & Konstantinos Liolios "*A Numerical Approach to the Seismic Problem of Steel Pile-Soil Interaction under Environmental and Second-Order Geometric Effects*"
- George Papazafeiropoulos, Prodromos N. Psarropoulos, & Yiannis Tsompanakis "*Retaining Wall-Soil-Structure Interaction Effects Due To Seismic Excitation*"
- Spyros Pavlides, Theodoros Tsapanos, Nikos Zouros, Sotiris Sboras, George Koravos, & Alexandros Chatzipeiros "*Using Active Fault Data For Assessing Seismic Hazard: A Case Study From NE Aegean Sea, Greece*"
- Emilius Comodromos, Mello Papadopoulou, & Ioannis Rentzeperis "*Degradation Of Pile Foundations' Response Due To Cracking: Advanced And Simplified Numerical Approach*"
- Anastasios Anastasiadis, Kyriazis Pitilakis & Kostas Senetakis "*Dynamic Shear Modulus and Damping Ratio Curves of Sand/Rubber Mixtures*"
- Varvara Zania, Ioanna Tzavara, Yiannis Tsompanakis, & Prodromos N. Psarropoulos "*Geosynthetics As Mitigation Measure For Seismic Hazard on Geostructures*"

Τα παραπάνω άρθρα θα παρουσιαστούν σε επόμενο τεύχος των ΝΕΩΝ.

Πληροφορίες για τα πρακτικά του συνεδρίου από Conference Organiser:

A./Prof. Dr. Mohamed A. Sakr
Director, Geotechnical Engineering Research Laboratory
Faculty of Engineering, Tanta University, Tanta, EGYPT
Fax: +2040-3420330 Mobile: +2012-3168002 E-mail:
mamsakr@yahoo.com



**Council Meeting of the International Society for
Soil Mechanics and Geotechnical Engineering
Bibliotheca Alexandrina, Alexandria, Egypt
4 October 2009**

Η Γενική Συνέλευση της ISSMGE διεγάζεται κάθε δύο χρόνια, την προηγούμενη ημέρα της έναρξης του ICSMGE και την

προηγούμενη της έναρξης κάποιου από τα Regional Conferences on Soil Mechanics and Geotechnical Engineering. Κατά την διάρκεια της Γενικής Συνέλευσης πριν από το ICSMGE αφ' ενός εκλέγεται ο Πρόεδρος της ISSMGE για την επόμενη τετραετία, αφ' ετέρου επιλέγεται η πόλη για την διοργάνωση του επομένου ICSMGE.

Στη συνέλευση της Αλεξάνδρειας κατά την ψηφοφορία για την ανάδειξη του Προέδρου της ISSMGE για την περίοδο 2009 – 2013 πλειοψήφισε ο Jean-Louis Briaud / USA.

Το επόμενο, 18th ICSMGE θα διεξαχθεί στο Παρίσι, Γαλλία, 1 – 5 Σεπτεμβρίου 2013.

Τέλος, η επόμενη Γενική Συνέλευση της ISSMGE θα γίνει στο Toronto, Canada, στις 2 Οκτωβρίου 2011, με την ευκαιρία της διεξαγωγής του XIV Panamerican Conference on Soil Mechanics and Geotechnical Engineering.

The President - Professor Jean-Louis Briaud

Jean-Louis Briaud was born in France. He received his Bachelor's degree from the Ecole Speciale des Travaux Publics in Paris in 1972. Then, he went to Canada and earned his Master's degree from the University of New Brunswick in 1974, completed his military service, and received his Doctorate from the University of Ottawa in 1978. He married his Canadian wife Janet in 1975; they have two children Natalie, born in 1980, and Patrick, born in 1983. Jean-Louis speaks English and French fluently. He has some very rudimentary knowledge in Spanish and in German.



In 1978, Professor Briaud moved to the USA to be an Assistant Professor at Texas A&M University. There, he progressed through the ranks of Associate Professor, Professor, Professorship Professor, and now Chair Professor. Indeed he holds the Spencer J. Buchanan Chair in the Zachry Department of Civil Engineering at Texas A&M University. This chair gives him significant financial support which will be used in part to support the significant travel required of an ISSMGE President.

Professor Briaud has a broad range of geotechnical interests from soil mechanics to rock mechanics, from in situ testing to laboratory testing, from saturated soils and offshore problems to unsaturated soils and shrink-swell soils problems, from classical geotechnical engineering topics to little known geoproblems such as soil erosion and roadside safety. He is a firm believer in the value of continuing education and offers regular short courses on topics emanating from his research work.

Professor Briaud has published one book on the pressuremeter, edited six books, published close to 300 Journals articles, conference papers, and research reports. He has advised 84 Master students and 37 Ph.D. students and managed 63 research projects totaling over 8.5 million dollars on foundations, retaining walls, pavements, in situ testing, load testing, compaction, software development, scour of bridges, levee erosion, unsaturated soils. He has developed 13 software packages and 11 videotapes. He has chaired the organization of 3 international conferences and conducted many short courses and webinars on in situ testing, geotechnical engineering software, bridge scour, shrink-swell soils. He has delivered over 150 lectures worldwide and is an international consultant on various topics including bridge scour, cliff erosion, slope stability, highway embankments, oil tank foundations, deep foundations, shallow foundations, docking facilities, tunnels, pressuremeter testing onshore and offshore.

For his innovative contributions in these various fields, Professor Briaud has received among other awards The ASCE Ralph B. Peck Lecture Award, The Canadian Geotechnical Society G. Geoffrey Meyerhof Award, The ASCE Martin Kapp Award, the ASCE Huber Research Prize, and The ASTM Hogenotglar Award. He holds two formal patents and one commercial agreement.

In 2004, Professor Briaud became President of the American Association of Geotechnical Professors (USUCGER) which regroups about 500 professors in the USA and abroad. As President of USUCGER, he generated much enhanced participation of the members in education and research activities. In 2008, Professor Briaud became President of the Geo-Institute (G-I) of the American Society of Civil Engineers in the USA after serving several years on the G-I Board of Governors. The G-I has about 12,000 members worldwide with most of them being from the USA. Working with the G-I Board of Governors, he promoted many ideas dear to the G-I members and remained very responsive to their concerns. The ISSMGE has 84 member countries, some 18000 individual members, and the ISSMGE budget is of the same order of magnitude as the Geo-Institute budget. Professor Briaud has been a member of ISSMGE since 1980 and has attended most ICSMGE conferences since 1985. He was chosen by President Ishihara in 1997, President Van Impe in 2001, and President Seco e Pinto in 2005 to chair ISSMGE Technical Committee 33 on Geotechnics of Soil Erosion. Therefore his experience in previous leadership positions has prepared him well to be the next President of ISSMGE, and his demonstrated commitment to ISSMGE through 12 years of chairing a very successful TC33 Committee indicates that he will give it all his energy.

Jean-Louis plays tennis daily, he was an avid rugby and soccer (football) player, and plays classic and jazz piano at the amateur level.



**17th International Conference on Soil Mechanics and Geotechnical Engineering
Future of Academia & Practice in Geotechnical Engineering
www.2009icsmge-egypt.org**

Το συνέδριο διεξήχθη στο Συνεδριακό Κέντρο της Βιβλιοθήκης της Αλεξάνδρειας στην Αίγυπτο από τις 5 έως τις 9 Οκτωβρίου 2009 με γενικό θέμα «Future of Academia & Practice in Geotechnical Engineering».

Οι εργασίες του συνεδρίου διεξήχθησαν σε ολομέλεια τις δύο πρώτες ημέρες, ενώ τις επόμενες διεξήχθησαν σε παράλληλες συνεδριάσεις. Επίσης υπήρχε η δυνατότητα παρουσίασης των άρθρων με μορφή poster.

Πιο συγκεκριμένα, των πρόγραμμα των εργασιών του συνεδρίου είχε ως εξής:

MONDAY, OCTOBER 5

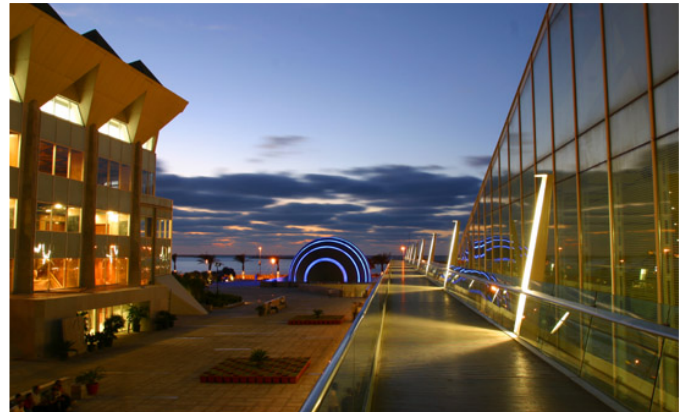
Opening Ceremony

Terzaghi Oration : Lecturer H. Poulos

State-of-the-Art Lecture #1: Materia Behavior and Testing

State-of-the-Art Lecture #2: Analysis and Design

Practinioners / Academia Forum



Συνεδριακό Κέντρο, Πλανητάριο και Βιβλιοθήκη Αλεξανδρείας

TUESDAY, OCTOBER 6

State-of-the-Art Lecture #3: Prediction, Monitoring and performance

Heritage Lecture: Hidden Egypt, by Z. Hawass

State-of-the-Art Lecture #4: Construction Process

State-of-the-Art Lecture #5: Management, Training and Education

iYGEC: Thoughts and Observations

Great Projects Lecture #1: Safeguarding Venice from High Tides: Site Characterization and Geotechnical problems, by M. Jamiolkowski

Great Projects Lecture #2: Development of Foundation Construction Techniques Over the Past 5.000 Years

Obituary of Late Prof. R.B.Peck and Late Prof. V.De Mello

WEDNESDAY, OCTOBER 7

Technical Session 1A: Laboratory Testing

Technical Session 2C: Underground Structures

Technical Session 4B: Deep Excavation, Tunnelling / Groundwater Control

Presentation and Poster Discussion Session 1A: Laboratory Testing

Presentation and Poster Discussion Session 2C: Underground Structures

Presentation and Poster Discussion Session 4B: Deep Excavation, Tunnelling / Groundwater Control

Technical Session 2A: Deep Foundation / Retaining Structures

Technical Session 1D: In Situ Testing

Technical Session 3B: Monitoring and Performance

Presentation and Poster Discussion Session 2A: Deep Foundation / Retaining Structures

Presentation and Poster Discussion Session 1D: In Situ Testing

Presentation and Poster Discussion Session 3B: Monitoring and Performance

Technical Session 1B: Physical / Constitutive Modelling

Technical Session 4A: Ground Improvement / Grouting / Dredging

Technical Session 5B: Management of Geotechnical Data and Processes



Συνεδριακό Κέντρο Βιβλιοθήκης Αλεξανδρείας

THURSDAY, OCTOBER 8

Technical Session 1C: Problematic Soils and Geosynthetics

Technical Session 3A: Instrumentation

Technical Session 5A: Owner / Engineer / Contractor / Public Awareness

Technical Session 5C: Training of Geotechnical Engineers / Future of Geotechnical Engineering

Presentation and Poster Discussion Session 1B: Physical / Constitutive Modelling

Presentation and Poster Discussion Session 4A: Ground Improvement / Grouting / Dredging

Presentation and Poster Discussion Session 5B: Management of Geotechnical Data and Processes

Presentation and Poster Discussion Session 1C: Problematic Soils and Geosynthetics

Presentation and Poster Discussion Session 3A: Instrumentation

Presentation and Poster Discussion Session 5A: Owner / Engineer / Contractor / Public Awareness

Presentation and Poster Discussion Session 5C: Training of Geotechnical Engineers / Future of Geotechnical Engineering

Technical Session 2B: Slopes and Embankments

Technical Session 3C: Interactive Design

Technical Session 4C: Natural Hazard Mitigation

Presentation and Poster Discussion Session 2B: Slopes and Embankments

Presentation and Poster Discussion Session 3C: Interactive Design

Presentation and Poster Discussion Session 4C: Natural Hazard Mitigation

Closing Ceremony

FRIDAY, October 9

Technical Visits

- Alexandria Port
- East Port Said Port
- Cairo Metro
- Giza Pyramids Archaeology
- Aswan Dams

Παράλληλα με το συνέδριο διοργανώθηκαν τα παρακάτω Workshops και συνεδριάσεις των Technical Committees της ISSMGE πριν και κατά την διάρκεια των εργασιών του:

TC 2 – Physical Modelling in Geomechanics

TC 5 – Environmental Geotechnics

TC 6 – Applications of Unsaturated Soil Mechanics in Geotechnical Engineering

TC 8 – Frost Geotechnics

TC17 – Ground Improvement

TC19 – Preservation of Monuments and Historic Sites

TC23 – Limit State Design in Geotechnical Engineering Practice

TC28 – Underground Construction in Soft Ground

TC29 – Laboratory Stress Strain Strength Testing of Geomaterials

TC34 - Prediction and Simulation Methods in Geomechanics

TC38 - Soil-Structure Interaction

JTC2 – Geo-Engineering Data: Representation and Applications

JTC3 – Education and Training

JTC7 – Soft Rocks and Endurated Soils

ATC 17 – Waste Management in Geoenvironmental Engineering

Στο συνέδριο συμμετείχαν πλέον των 1,000 σύνεδροι από 81 χώρες και μεταξύ αυτών τα μέλη μας Α. Αναγνωστόπουλος, Δ. Ατματζίδης, Γ. Γκαζέτας, Σ. Καβουνίδης, Π. Μαρίνος, Μ. Μπαρδάνης, Γ. Ντουριάς, Μ. Πανταζίδου, Χ. Παπαχατζάκη, Μ. Παχάκης, Α. Πλατής, Σ. Σχινά, Χ. Τσατσάνιφος, Σ. Τσότσος, Π. Φορτσάκης, Ε. Χαρδαλούπα και Δ. Χρυσικός.

Ο Καθηγητής Γ. Γκαζέτας συμμετέσχε ως «contributor» στην State-of-the-Art Lecture #2: Analysis and Design.

Ο Καθηγητής Π. Μαρίνος ήταν συμπρόεδρος στην Τεχνική Συνεδρία TS 2C και στην αντίστοιχη συνεδρία παρουσίασης poster PDS 2C: Underground Structures.

Τέλος, ο Π. Φορτσάκης ήταν panelist στην Τεχνική Συνεδρία TS 2B: Slopes and Embankments.

Στα πλαίσια της προβολής της διεξαγωγής του European Conference on Soil Mechanics and Geotechnical Engineering στην Αθήνα, τον Σεπτέμβριο 2009, η ΕΕΕΕΓΜ διαμόρφωσε περίπτερο σε χώρο που ευγενώς της παραχωρήθηκε απ τους διοργανωτές του συνεδρίου, όπου γινόταν προβολή σχετικής ενημερωτικής ταινίας και διενέμετο το Πληροφοριακό Φυλλάδιο του συνεδρίου και αναμνηστικό δώρο.

Επίσης, η ΕΕΕΕΓΜ συμμετέχε στην διοργάνωση πολιτιστικής εκδήλωσης στο Εθνικό Μουσείο Αλεξανδρείας, την Τετάρτη 7 Οκτωβρίου, όπου έγινε η πρώτη παρουσίαση προσφάτως ανακαφέντος μαρμάρινου αγάλματος της Ελληνιστικής εποχής. Στην εκδήλωση και στην επακολουθήσασα δεξίωση στους κήπους το μουσείου παρέστη πολύ μεγάλος αριθμός συνέδρων από διάφορες χώρες.



Τέλος, υποβλήθηκαν και δημοσιεύθηκαν στα πρακτικά του συνεδρίου τα παρακάτω άρθρα μελών της ΕΕΕΕΓΜ:

GREECE 01

D.N. Christodoulou, A.I. Droudakis, I.A. Pantazopoulos, I.N. Markou and D.K. Atmatzidis "Groutability and effectiveness of microfine cement grout"

GREECE 04

I. Mihalidis, S. Konstantis, A. Anagnostopoulos, G. Vlavianos and G. Doulis "Tunnel Stability Factor – A new controlling parameter for the face stability conditions of shallow tunnels in weak rock environment"

GREECE 05

D.K. Atmatzidis, D.A. Chrysikos & I.M. Papaefstathiou "Installation damage of nonwoven polypropylene geotextiles"

GREECE 06

K. Pitilakis & S. Bandis and S. Hemedat "Geotechnical investigation and seismic analysis of underground monuments in Alexandria, Egypt"

GREECE 08

Z. R. Papachatzaki, K. Anastasopoulos, C. Oikonomidis, S. Siachou and G. Dounias "Experiences from the installation of geotechnical instruments in dams"

GREECE 09

M. Pantazidou "Student understanding of the concept of soil structure guides instructional interventions"

GREECE 10

A. Valsamis, G. Bouckovalas and E. Drakopoulos "Design charts for single piles under lateral spreading of liquefied soil"

GREECE 11

E. Papageorgiou, N. Boussoulas, F. Karaoulanis and S. Tsotsos "Ground movements during tunnel construction by EPB method along the southern extension of Athens Metro Line 2, Greece"

GREECE 12

Bardanis, M., Cavounidis, S. and Dounias, G. "Numerical simulation of the pore pressure regime in landslides with underdrainage"

GREECE 13

M. Kavvadas, M. Karlaftis, P. Fortsakis, E. Stylianidi "Probabilistic analysis in slope stability"

Τα άρθρα των Ελλήνων συνέδρων δημοσιεύονται στις επόμενες σελίδες.

ΑΡΘΡΑ ΕΚΠΡΟΣΩΠΩΝ ΕΕΕΕΓΜ ΣΤΟ 4TH ΙΥΓΕC

Estimation of tunnel final lining loads

Estimation de charges du revêtement final des tunnels

P. Fortsakis National Technical University of Athens, Greece

ABSTRACT

Tunnel final lining is designed to undertake all the loads during the tunnel service life, such as pressure from the geomaterial due to time dependent phenomena, part of the loads which are initially undertaken from temporary support measures, accidental loads, temperature loads, water pressure and seismic loads.

The most important of the final lining loads is the pressure applied from the surrounding geomaterial. According to data from a large number of tunnels in Egnatia Highway, in northern Greece, final lining loads were mainly estimated through empirical and analytical methods and it was observed that there is not a rational correlation between the geotechnical conditions and the final lining design proposed.

In the present paper a comparative parametric study for tunnel final lining loads is carried out in order to compare the results of empirical and analytical methods with numerical analyses performed with the finite element code ABAQUS, for a great variety of geotechnical parameters. Comparing the results of empirical and analytical methods, which are widely used in practice, it is evident that there is a large scatter, because of the different assumptions they are based on. Furthermore the comparison with the results of the numerical analyses shows that empirical and analytical methods can be considered reliable, only in specific geotechnical conditions, because they can only partially describe the problem mechanism.

RÉSUMÉ

Le revêtement définitif est dimensionné à prendre tous les chargements appliqués pendant la durée d'opération des tunnels, tels que les pressions de terrain à long terme dues de phénomènes rhéologiques, les charges accidentelles, les charges dues à la température, à l'eau environnante, au séisme, ainsi qu'une part des charges qui initialement étaient prises par le soutènement provisoire.

La charge la plus importante pour le revêtement définitif est celle appliquée par les terrains environnants. Selon les données prises par les tunnels construits à l'autoroute Egnatia, qui se trouve en Grèce du Nord, les méthodes de l'évaluation des charges du revêtement définitif sont soit empiriques, soit analytiques. Après l'observation des mêmes données, nous avons conclu qu'il n'y pas de corrélation logique entre les conditions géotechniques et le dimensionnement proposé du revêtement définitif.

Dans ce rapport, une étude paramétrique sur les charges du revêtement définitif des tunnels s'effectue, afin que nous comparions les résultats provenant des méthodes empiriques et analytiques avec les résultats du code des éléments finis ABAQUS, en fonction des paramètres géotechniques différents. Après la comparaison entre les méthodes analytiques et empiriques, qui sont couramment utilisées, il est évident que les valeurs calculées des charges du revêtement définitif sont très dispersées à cause des hypothèses différentes adoptées par chaque méthode. Finalement, la comparaison avec les résultats de la méthode

numérique montre que les méthodes empiriques et analytiques peuvent être considérées fiables seulement sous conditions géotechniques spécifiques, parce qu'elles peuvent décrire partiellement les mécanismes du problème.

Keywords: Tunnel, Final lining, Design methods, Numerical analyses

1 INTRODUCTION

The conventional tunnel excavation method consists of two main phases. The first is the excavation and installation of the temporary support measures and the second is the construction of the final lining. Tunnel final lining, which is constructed using plain or reinforced concrete, is designed to undertake all loads during tunnel service life, such as pressure from the geomaterial due to time dependent phenomena (creep of the geomaterial, swelling and consolidation), part of the loads which are initially undertaken from temporary support measures, accidental loads, temperature loads, water pressure and seismic loads. The issue of final lining design has been a controversial one and much disputed subject within the field of tunnel engineering.

The most important of the final lining loads is the pressure applied by the surrounding geomaterial. The magnitude of this load depends on the interaction of the system surrounding geomaterial - temporary support measures - final lining and the construction procedure as well, in case of weak geomaterials (time interval between excavation and final lining construction).

According to data from Tunnel Information and Analysis System (Marinos et al 2006) for a large number of tunnels designed and constructed through a great variety of geological formations, in Egnatia Highway, in northern Greece, final lining loads were mainly estimated with empirical and analytical methods which do not take into account most of the problem parameters, since tunnel final lining is mainly approached as a structural engineering project. Due to these simplifications there is not an orthological correlation between the final lining design proposed (concrete thickness and weight of reinforcement per tunnel meter) and the geotechnical conditions (Fortsakis et al 2006).

In the present paper tunnel final lining loads are calculated through empirical and analytical methods and numerical analyses performed with finite elements code ABAQUS as well, for a great variety of geotechnical parameters. Based on these results the empirical and analytical methods are criticised and suggestions are presented for tunnel final lining load estimation.

2 ANALYSES DESCRIPTION

The calculations were performed for a 10m diameter circular tunnel. The strength and deformation properties of the rock-mass were quantified through GSI (Marinos & Hoek 2000) and Hoek -Brown failure criterion (Hoek et al 2002).

A wide range of tunnel cases was analysed using the following ranges of geometrical, geotechnical and support parameters:

Table 1. Range of analysed parameters

Parameters	Range of values	Number of values
Overburden height, H, m	50 - 500	4
Tunnel diameter, D, m	10	1
Stress ratio, K	0.7, 1.0, 1.3	3
Unit weight, γ , MN/m ³	0.025	1
GSI	15-75	11
Uniaxial compressive strength of intact rock, σ_{ci} , MPa	5-50	9
Constant of geomaterial, m_i	6-17	4
σ_{cm}/p_0	0.08-16.3	

Excavation step (m)		
(According to σ_{cm}/p_0 ratio)	1.0, 1.5, 2.0	3
Shotcrete thickness, d (m)	0.1, 0.2, 0.3	3
Shotcrete Elastic Modulus (MPa)	20000	1
Number of tunnels examined		795

where the ratio σ_{cm}/p_0 quantifies how severe the geotechnical conditions are. Rockmass strength (σ_{cm}) is calculated according to Hoek et al (2002) and in situ stress is expressed as:

$$p_0 = \frac{(1 + K)\gamma H}{2} \quad (1)$$

The equivalent Mohr – Coulomb strength parameters and the deformation modulus of the geomaterial were calculated according to Hoek et al (2002), since most of the methods are based on Mohr-Coulomb failure criterion.

The calculations were based on the assumption that final lining load is equal to the temporary support measures load. This assumption is reasonable for rockmasses with insignificant creep behaviour and it has always been adopted in final lining designs studied, since temporary support measures have low construction reliability and are not considered as a permanent structure.

2.1 EMPIRICAL AND ANALYTICAL METHODS

Empirical and analytical methods are based on the geological characteristics of the surrounding rockmass or an equilibrium demand of the rockmass-support system. Time dependent behaviour of the rockmass which is very important in case of weak geomaterials under high overburden is not taken into account through these methods.

Apart from the methods discussed in the present paper, which were used in tunnel final lining design in Egnatia Highway, there are also several approaches from other researchers as Bierbaumer (1913), Barton (1975), Wickham (1972) and Wickham et al (1974).

2.1.1 Terzaghi empirical method (M1)

This method, suggested by Terzaghi (1946), is based on a qualitative description of the rockmass and the final lining load is estimated according to the rockmass structure and weathering. It is recommended, for tunnels with section width up to 5m and overburden height larger than $1.5(b+h)$, where b is section width and h is section height. In order to quantify the method criteria the rockmass description was corresponded to a GSI field.

2.1.2 Terzaghi analytical method (M2)

The analytical method proposed by Terzaghi (1946) is based on the assumption that final lining load can be calculated through the equilibrium of the prism above the tunnel section.

2.1.3 Protodyanov method (M3)

The "Russian method", suggested by Protodyanov (1960), indicates that final lining is loaded from a vault above the tunnel, the height of which depends on the rockmass quality. It is recommended for tunnels excavated in rockmass with $RMR > 40$.

2.1.4 Unal method (M4)

According to this method proposed by Unal (1983) final lining load can be estimated with RMR value of the rockmass, for tunnels with section width 5-10m, overburden height up to 100m and RMR values of surrounding rockmass larger than 50. Since the initial input parameters for rockmass classification in this paper were considered according to GSI, the RMR

values were calculated as $GSI+5$, for $GSI > 30$ and $GSI+10$ for $GSI \leq 30$, because RMR tends to overestimate rockmass quality especially in weak rockmasses.

2.1.5 Convergence-Confinement method (S1, S2, U1, U2)

Convergence – confinement methodology is based on the assumption of a circular tunnel excavated in an axisymmetric stress field. According to this methodology the equivalent pressure on temporary support measures can be calculated based on design criteria imposed. In this paper two different analyses were performed to estimate the equilibrium point of the rockmass and the support measures. In the first one, a shotcrete layer with the characteristics mentioned in Table 1 is assumed and the pressure is calculated from the equilibrium point of the rockmass and shotcrete curve (Method S). In the second, pressure is calculated so that the final convergence, during the excavation, is smaller than a critical value which depends on how severe the geotechnical conditions are (Method U).

Final lining load was estimated with two different assumptions for the load mechanism for each equilibrium point. In the first one, it was considered equal to the equivalent pressure on temporary support measures (Assumption 1). The second relies on the assumption that tunnel final lining is loaded from the "dead weight" of plastic zone created in the rockmass due to tunnel excavation (Assumption 2).

The confinement of the rockmass due to face advance was estimated through the relationship suggested by Chern et al (1998). The temporary support measures were simulated according to Rabsewicz & Golser (1973). Additionally an equivalent pressure on tunnel face was estimated with the presupposition that the factor of safety against tunnel face failure is larger than 1.0.

The excavation step and the maximum allowable convergence after temporary support measure installation were set based on the geotechnical conditions in order the analyses to be realistic.

Consequently, founded on the convergence-confinement theory, tunnel final lining load was calculated with four different ways, which are illustrated in Figure 1. Each one is named from the combination of the method which is used for the equilibrium (U, S) and the assumption for the load mechanism (1, 2).

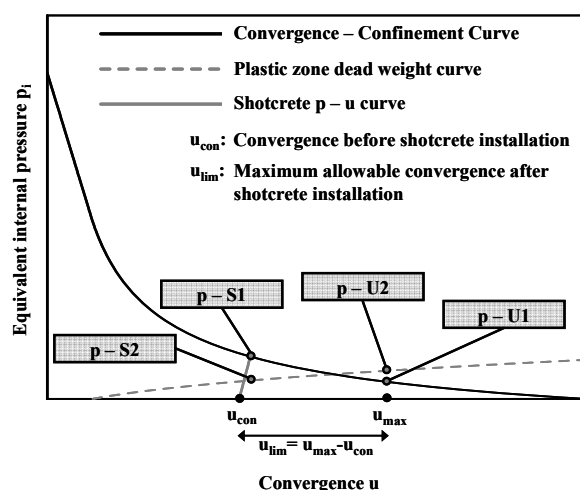


Figure 1. Final lining load estimation based on convergence-confinement theory.

2.2 NUMERICAL ANALYSES

Numerical 2D analyses with finite element code ABAQUS were carried out in order to evaluate the empirical and analytical

methods results. The rockmass behaviour was simulated through Drucker-Prager constitutive model. The tunnel was supported with shotcrete which was considered elastic. The load calculated from numerical analyses is a lower boundary of the final lining load since time dependent phenomena were not taken into account.

The numerical analyses were performed for 113 of the parameter combinations presented in Table 1 (H=100m, 200m and d=0.20m).

3 ANALYSES RESULTS

In Figure 3 is obvious that the final lining load estimated from all methods described afore for specific geometrical and geotechnical conditions has a great scatter. The characteristic value which was used for the evaluation was considered to be the vertical load for the empirical and analytical methods and the average value for the numerical analyses.

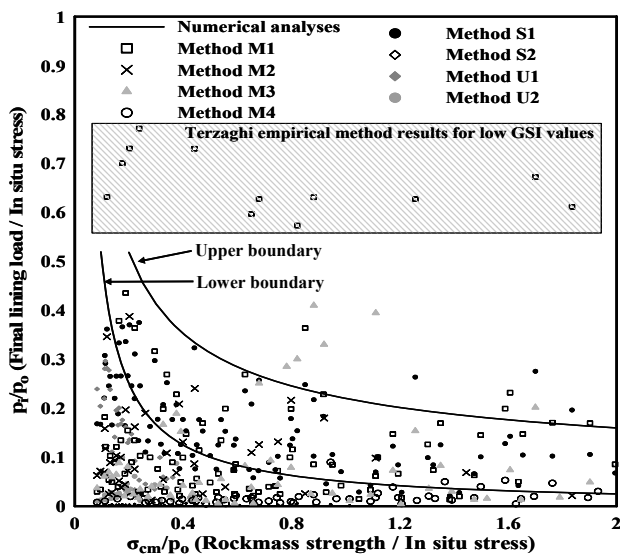


Figure 2. Normalised load estimation from empirical and analytical methods.

The main reason is that analytical and empirical methods are based on different assumptions and it is impossible to describe adequately the complex interaction problem created. Furthermore, only a small percentage lies between the boundaries of the loads estimated from the numerical analyses.

The low correlation coefficients (Table 2) of the load estimated from all the methods with the geotechnical parameters prove an inadequate simulation of the problem mechanism.

Table 2. Correlation coefficients (ρ) for final lining load and geotechnical parameters (GSI, σ_{cm}/p_0).

Method	GSI	σ_{cm}/p_0
M1	-0.37	0.34
M2	-0.70	-0.27
M3	-0.40	-0.05
M4	-0.28	0.45
S1	-0.96	-0.50
S2	-0.44	-0.50
U1	-0.54	-0.29
U2	-0.56	-0.24

Empirical and analytical methods estimations are evaluated through Figures 3 and 4 and factor R_N .

$$R_N = \sqrt{\frac{1}{n} \sum_{i=1}^n \left[\frac{(P_i/P_0)_{ABAQUS} - (P_i/P_0)_{method}}{(P_i/P_0)_{ABAQUS}} \right]^2} \quad (2)$$

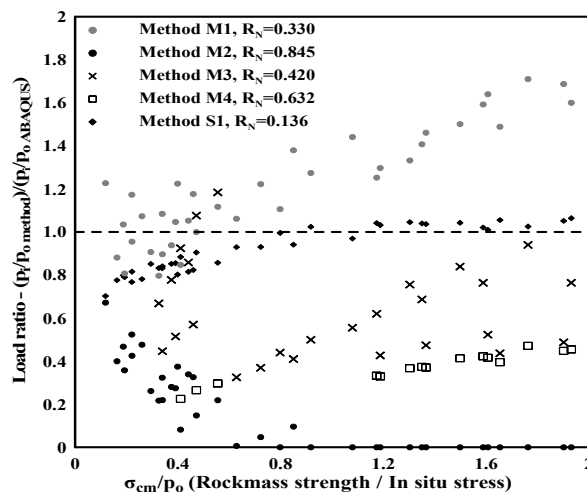


Figure 3. Normalised load ratios for overburden height H=100m.

It is noted that the parameter combinations which result to values of σ_{cm}/p_0 ratio greater than 2 have been omitted from Figures 3 and 4 since the final lining load in these cases is insignificant.

From Figures 3 and 4 becomes evident that most of the methods tend to underestimate the load on final lining. Only method S1 and method M1 for H=100m have satisfactory convergence with numerical analyses results for the whole breadth of geotechnical conditions examined. However method M1, since it depends only on rockmass classification, results in very low values for H=200m and it would be very conservative for overburden height less than 100m. Methods M3 and M4 result to low final lining loads and their convergence is improved for higher values of σ_{cm}/p_0 ratio and H=100m. Method M4, which also takes into account only rockmass classification, is also characterized by high values of R_N and unsatisfactory convergence.

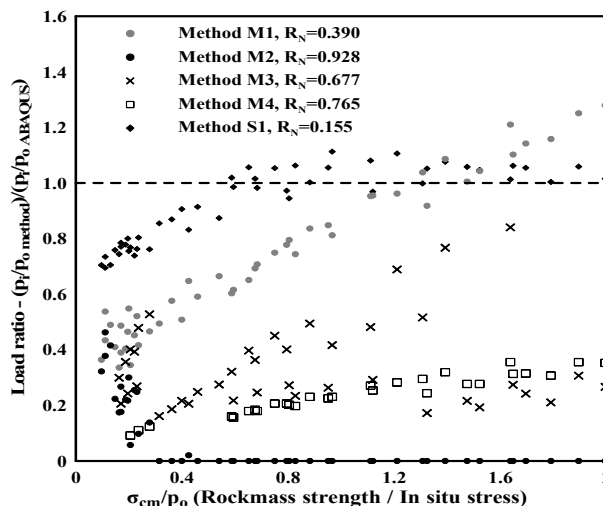


Figure 4. Normalised load ratios for overburden height H=200m.

Methods S2 and U2, frequently used in the tunnel designs studied, are based on wrong principles, because rockmass around a tunnel, even in plastic zone, does not behave as dead weight since it can be self-supported. Additionally decrease of the rockmass confinement, which can be achieved by forepolling or fiberglass in conventional excavation

method, which leads to an increase of the pressure on the lining, according to these methods results in a decrease of the load because of the decrease of plastic zone width. Consequently these methods were not taken into account in the comparisons and calculations presented.

It must be noted that the convergence of the loads (Figures 3 and 4) is reduced in case that the average of vertical and horizontal load is adopted as a characteristic value for the empirical and analytical methods.

4 CONCLUSIONS

Empirical and analytical methods, which have been a very useful tool for many years in tunnel engineering, are still widely used for final lining load estimation. They are based on simplified approaches to achieve solution for a very complex geotechnical problem. The loads estimated from these methods have a great scatter due to the different assumptions they are based on. The low correlation coefficients between tunnel final lining loads and geotechnical conditions prove an inadequate simulation of the phenomenon mechanism. Singh et al (1992) have compared loads estimated from empirical and analytical methods with in situ measurements and concluded the methods examined are unreliable in most cases.

"Empirical Terzaghi method" and "Unal method" are considered unreliable since they take into account only rockmass classification. Nevertheless the first one has a better understanding of the phenomenon mechanism since it is characterized by a decreasing rate of change as a function of GSI.

"Terzaghi analytical method" and "Protodyakonov method" which are based on similar principles can provide satisfactory results, only for tunnels under low overburden but they do not take into account the excavation procedure and the confinement taking place which differentiates the stress field around the tunnel.

Convergence-confinement methods S1 and U1 are probably the most reliable since the load is calculated based on the interaction of rockmass and support measures. However the most important disadvantage of these methods is that they refer to circular tunnel sections and hydrostatic earth pressure, assumptions which lead to favourable conditions. The reason that they are not sufficiently correlated with the geotechnical parameters examined is that a decrease of σ_{cm}/ρ_0 ratio leads to an increase of rockmass confinement before the support installation.

The "Plastic zone dead weight method" is based on wrong principles and is considered unreliable.

According to the calculations and comparisons presented empirical and analytical methods for tunnel final lining load estimation are not considered reliable in general and each one should be used only in specific and very limited cases of tunnel geometry and geotechnical conditions. Furthermore their reliability level would decrease even more in cases of a more complex tunnel geometry (horseshoe tunnel section, tunnel with two branches), complex support systems (anchors, steel sets, fiberglass nails etc) and tunnel excavation in rockmass with creep behaviour.

ACKNOWLEDGMENT

The author is grateful to Pr. M. Kavvadas for his advises and support in the current paper.

REFERENCES

Abaqus Inc. 2004. *Abaqus theory manual*.

Barton, N., Lien, R., & Lunde J. 1975. Estimation of Support requirements for underground excavations. *Proceedings of the 16th Symposium on Rock Mechanics*, University of Minnesota, Minneapolis, USA, pp. 163-177.

Bierbaumer, H. 1913. *Die Dimensionierung des Tunnelmauerwerks*. Engelmann, Leipzig.

Chern, J.C., Shiao, F.Y., & Yu, C.W. 1998. An empirical safety criterion for tunnel construction. *Proceedings of the Regional Symposium on Sedimentary Rock Engineering*, Taipei, Taiwan, pp. 222-227.

Fortsakis, P., Magkanas, K., & Kavvadas, M. 2006. Methodologies and loads for tunnel final lining design. Presentation of data from Egnatia Highway tunnels. *Proceedings of the 15th Hellenic Conference on Reinforced Concrete*, Alexandroupoli, Greece, Vol 4, pp. 117-128. Athens: Technical Chamber of Greece. (in Greek)

Hoek, E., Carranza-Torres, C., & Corkum, B. 2002. Hoek-Brown failure criterion-2002 Edition. *Proceedings of the 5th North American Rock Mechanics Symposium and the 17th Tunnelling Association of Canada: NARMS-TAC*, Toronto, Canada, Vol. 1, pp. 267-273.

Marinos, P., & Hoek, E. 2000. GSI: a geologically friendly tool for rock mass strength estimation. *Proceedings of the GeoEng2000 at the International Conference on Geotechnical and Geological Engineering*, Melbourne, Australia, pp. 1422-1446. Lancaster: Technomic publishers.

Marinos, V., Korkaris, K., Mirmiris, K., Petroutsatou, K., Koumoutsakos, D., Proutzopoulos, G., Romosiou, A., Fortsakis, P., Kiamos, K., Lazaridou, S., Pitsas, G., Rhgopoulou, M., Marinos, P., & Lampropoulos, S. 2006. The construction of a geotechnical tunnel data base for Egnatia Odos S.A. *Proceedings of the 5th Hellenic Conference on Geotechnical and Geoenvironmental Engineering*, Ksanthi, Greece, Vol. 3, pp. 525-531. Athens: Technical Chamber of Greece. (in Greek).

Protodyakonov M. 1960. *Klassifikacija Gorotworu*. In French T. at O.S. Paris, 1974.

Rabsewicz, L., & Golser, J. 1973. Principal of dimensioning the supporting system for the New Austrian Tunneling Method. *Water Power March*: 88-93.

Singh, B., Jethwa, J., Dube, A., & Singh, B. 1992. Correlation between observed support pressure and rockmass quality. *Tunnelling and Underground Space Technology*. Elsevier, Vol. 7, No. 1, pp. 59-74.

Terzaghi, K. 1946. Rock defects and loads on tunnel supports. In: *Proctor, R.V. & White, T.C. Rock tunnelling with steel supports*. Youngstown: Commercial shearing and stamping Co.

Unal, E. 1983. *Design guidelines and roof control standards for coal mine roofs*. PhD thesis. The Pennsylvania State University.

Wickham, G. 1972. Support determination based on geologic predictions. *Proceedings of Rapid Excavation and Tunneling Conference*, New York, USA.

Wickham, G., Tiedman H., & Skinner, E. 1974. Ground support prediction model. *Proceedings of North American Rapid Excavation and Tunneling Conference*, San Francisco, USA, Vol. 1, pp. 691-708.

Fragility curves for the seismic vulnerability assessment of waterfront structures

Courbes de fragilité pour l'évaluation de la vulnérabilité sismique des structures portuaires

K. Kakderi & K. Pitilakis

Department of Civil Engineering, Aristotle University of Thessaloniki, Greece

ABSTRACT

The aim of the study is to propose adequate fragility curves for waterfront/ retaining structures using available data from past earthquakes' damages in Europe and worldwide and numerical analysis of typical cases. Initially, existing fragility curves and damage states are evaluated and their shortcomings and/or limitations are assessed. In the second stage typical waterfront structures, with different foundation soil conditions and seismic excitations, are studied using appropriate numerical modelling. The corresponding damage levels are estimated in respect to the induced residual displacements and the seismic response of the soil-structure system. Considering aleatory uncertainties of the parameters involved, analytical fragility curves are then constructed for the different types of waterfront structures and foundation conditions. Finally the computed analytical fragility curves are compared with the validated empirical ones, in order to propose fragility functions and corresponding damage levels for waterfront/ retaining structures based on European distinctive features.

RÉSUMÉ

Le but de l'étude est l'estimation des courbes analytiques de fragilité sismique des murs de soutènement portuaires en utilisant des données expérimentales, des observations des dommages et des analyses numériques. Les limitations des courbes existantes sont discutées et validées. Ensuite on étudie numériquement plusieurs typologies des murs de soutènement portuaires afin d'estimer des courbes analytiques de fragilité pour différents niveaux de sollicitations sismiques. Les courbes de fragilité sont évaluées pour les différents types des murs et de sols de fondation, en tenant compte de l'interaction sol-structure à partir de l'estimation des déformations résiduelles. Les courbes analytiques, ainsi évaluées, sont comparées avec les courbes empiriques existantes. Le but final est de proposer des courbes de fragilité dans le contexte de l'Europe.

Keywords : Retaining walls, waterfront structures, fragility curves, vulnerability, damage states

1 INTRODUCTION

Most failures of waterfront structures are associated with outward sliding, deformation and tilting. There is a large number of references regarding seismic damage of port structures, mostly after earthquakes in the USA and Japan, while similar observations are quite limited in Europe. The aim of the present study is to propose adequate fragility curves for waterfront/ retaining structures using available empirical data and numerical analysis of typical cases.

2 EVALUATION OF EXISTING SEISMIC FRAGILITY CURVES

Empirical fragility curves describing earthquake induced damage to waterfront structures are proposed in HAZUS (NIBS 2004). They describe log-normal cumulative distributions which give the probability of reaching or exceeding certain damage states for a given degree of permanent ground displacement (PGD). In this case, no distinction between the different wall typologies and no specification of the type and source of ground displacement (deformation due to ground shaking or ground failure) are made.

Analytical methods have been also used for the vulnerability assessment of quay walls (Roth and Dawson 2003, Roth et al. 2003). The standard "structural-engineering approach" for wharf seismic design, relies on soil-structure interaction models; alternatively, a full dynamic analysis can be performed. This kind of analysis provides a useful insight of the seismic behavior of waterfront structures but cannot be easily applicable for a straightforward vulnerability assessment of different wall typologies and foundation conditions under different levels of seismic excitation. Ichii 2003 and 2004 proposed several analytical fragility curves for the assessment of direct earthquake-induced damage to gravity-type quay walls using simplified dynamic finite element analysis, considering also the occurrence of liquefaction phenomena. Different vulnerability curves are given in the form of log-normal probability distributions for different peak ground acceleration levels.

The type and the degree of seismic damages depend upon the typology of the waterfront structures, the local site conditions, the intensity of the seismic loading, the design factors of safety and the occurrence of liquefaction. The damage states on the other hand are defined based on the seismic response of the waterfront structure itself, the level of induced and allowable permanent displacements, the serviceability level and the retrofitting cost as a percentage of the replacement value.

In all cases, several uncertainties are involved related to the existence and accuracy of empirical data, the assumptions of the analysis, the definition of the damage states and the level and characteristics of induced seismic motion. To account for the various uncertainties, a probabilistic approach for the seismic vulnerability assessment of waterfront structures is usually adopted.

The validation of existing fragility curves has been made with the observed quay wall damages in the small ports in Lefkas island during the 2003 Lefkas Ms=6.4 earthquake (Kakderi et al. 2006). In the present paper we present the construction of analytical fragility curves for different typologies of gravity waterfront structures with different soil foundation conditions exclusively for ground shaking.

3 NUMERICAL MODELING OF TYPICAL CASES

In order to estimate the induced seismic behavior and consequently to assess the functionality of waterfront structures, several typical cases, with different foundation soil conditions and seismic excitations have been studied using 2D finite element analysis (Plaxis 2007). The foundation soils exclude the occurrence of liquefaction phenomena and all permanent displacements are due to ground shaking. First, the proposed procedure has been validated using the case of the slightly to moderately damaged quay walls in Lefkas, Greece during the strong 2003 earthquake (PGA=0.45g).

3.1 Seismic analysis of a typical quay wall during the Lefkas (2003) earthquake

Damage to waterfront structures has been recorded during the Lefkas (14/8/2003, Ms=6.4) earthquake in Greece. The newly constructed quay walls in the marina suffered minor to moderate damages with relative observed residual seaward displacements of the order of 12 cm to 15cm. There are some evidence that at least in one location a partial liquefaction of the foundation subsoil occurred (Margaris et al. 2003). Using an 1D elastoplastic back analysis (Cyclic1D, Elgamal et al. 2001), the computed ground displacements due to lateral spreading were of the order of the observed displacements; however the observed damages should be attributed in a certain degree to the increased total lateral seismic earth pressures behind the quay walls. The monolithic gravity structures of the marina quay walls were analyzed using 2D finite element analysis; the deconvoluted time history of the main earthquake record (PGA=0.45g) was used as input motion. Soil classification and dynamic properties of soil materi-

als were derived from the available geotechnical information (Pitilakis et al. 2005). Figure 1a presents the typical soil profile in the Marina district; Figure 1b illustrates the typical cross section of the studied quay wall and Figure 1c the deformed mesh with seaward displacements in accordance to the actual observations identifying the primary failure mode.

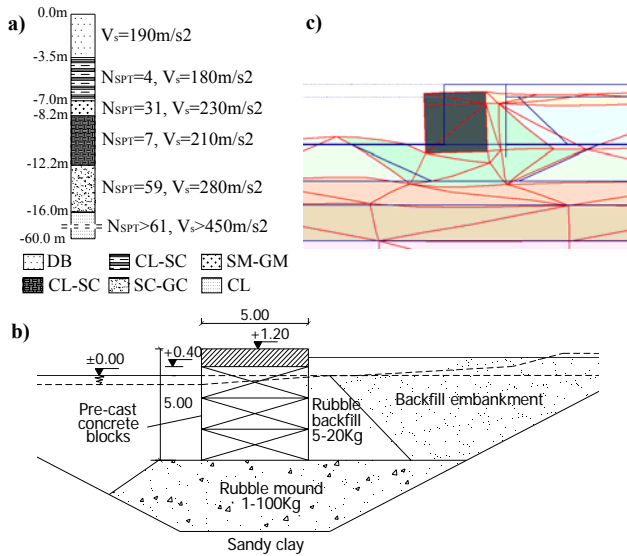


Figure 1. (a) Soil profile in the marina area, (b) Typical cross section of the quay wall and (c) Deformed mesh for the LeFKas quay wall analysis (displacements scaled up to 10 times).

The estimated residual horizontal displacements at the top of the wall were computed equal to 16 cm considering a quite low material damping. Thus a good agreement is achieved assuming that the final seismic response of the quay walls was a combined result of partial liquefaction and increased lateral earth pressures in the backfill.

3.2 Typical wall configurations and input data

In order to construct the analytical fragility curves, different types of quay wall typologies and foundation conditions were examined. A typical simplified profile is shown in Figure 2. Monolithic gravity structures having different heights ($H=8\text{m}$, 10m , 12m and 16m) and height to width ratios (W/H) equal to 0.7 and 0.9 , are examined (in total 8 wall section combinations). Plane strain conditions and appropriate boundary conditions were used in all analyses.

Four different ground soil types (soil B1-B4 in Figure 2) have been used corresponding to soil categories B (soil B2, B4) and C (soil B1, B3) of EC8; their material physical and dynamic properties along with the ones of the backfill (soil A) and the rubble mound are provide in Table 1. The bedrock is set equal to 30m . Parametric 2D numerical analyses have been performed in order to evaluate the expected 2D seismic motion in free field conditions with respect to 1D equivalent linear analysis in terms of frequency content and soil amplification.

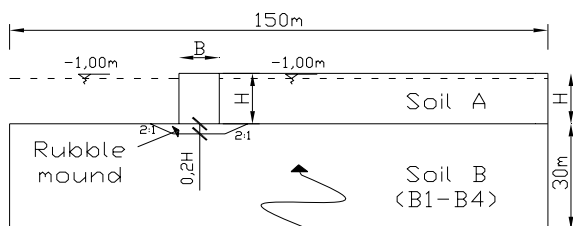


Figure 2. Typical wall and soil configuration

The soil is modeled with an elastoplastic Mohr-Coulomb model. Part of the backfill is considered fully saturated and

the wall is considered rigid. A limited capability of relative movement between the wall, the rubble mound and the backfill is assumed using appropriate interface elements.

Table 1. Soil properties

Properties	Rubble mound	Soil A (SG)	Soil B			
			B1 (SM)	B2 (SM-SG)	B3 (CL)	B4 (CL)
γ_d (KN/m ³)	18	20	18	19	18.5	19.5
γ_{sat} (KN/m ³)	20	21	19.5	21	20	21.5
V_s (m/sec)	450	280	250	500	250	500
ν Poisson	0.3	0.35	0.35	0.35	0.35	0.35
c	1	1	2	2	30	40
ϕ (o)	40	38	30	35	17	20
permeability k_x	1	0.05	0.05	0.1	10^{-5}	10^{-5}
permeability k_y	1	0.05	0.05	0.1	10^{-5}	10^{-5}

Five different earthquake records have been used as input motion: (i) Kozani (T), Greece, $M_w=6.6$, 1995, (ii) Athens (Kypseli-L), Greece, $M_w=5.9$, 1999, (iii) Montenegro-[TRA (EW)], former Yugoslavia, $M_w=6.9$, 1979, (iv) Palm Springs (wwt), USA, $M_w=6.0$, 1986, (v) Kocaeli (Gebze-NS), Turkey, $M_w=7.4$, 1999. They all refer to rock soil conditions (soil category A in EC8). They were scaled to five levels of peak ground acceleration ($PGA=0.1, 0.3, 0.5, 0.7$ and $0.9g$) in order to estimate the seismic response of the soil-structure system for different levels of induced seismic intensity. Since the earthquake is modeled by imposing a prescribed displacement at the mesh bottom boundary, the displacement time histories have been used for the parametric analysis performed (800 in total) after applying appropriate filtering and base line correction.

Material damping has been selected either zero or introduced by means of Rayleigh damping and for a damping coefficient $\xi=5\%$. The respective damping parameters are estimated based on the fundamental frequency of each earthquake record (ranging from 1.5 to 3.5 Hz). This assumption results in a possible over-damping of the system's dynamic behavior leading to reduced values of the estimated response parameters. This is taken into consideration for the construction of the analytical fragility curves (Section 4).

3.3 Wall-backfill –soil response

For the soil profiles B1 and B3 ($V_s=250\text{m/s}$) the fundamental period in free field conditions is equal to $T_p=0.55\text{s}$, while for the soil conditions B2 and B4 ($V_s=500\text{m/s}$) the corresponding value is $T_p=0.34\text{s}$.

The whole wall-backfill-soil system has fundamental periods ranging from 0.12sec to 0.45sec depending on (i) the soil conditions, (ii) the wall geometry and (iii) the predominant frequency of the input motion. Higher values are observed for the larger quay wall and for larger periods of input Ricker pulses. Higher amplification is observed in the quay wall compared to the backfill. Figure 3 illustrates an indicative example of the computed transfer functions between (a) the top and the bottom of the waterfront structure and (b) the backfill in free field conditions for the case of the largest quay wall (16m height and 14m width), soil type B2 ($V_s=500\text{m/s}$) and for a Ricker pulse with $T_p=0.2$ sec.

3.4 Results of parametric analysis

The seismic response of the soil-structure system is estimated in terms of soil deformation and stresses. The maximum and residual displacements of the waterfront structure are also computed, as they determine its serviceability. Typical seismic failure modes of gravity quay walls are observed, including tilting with seaward displacement and settlement of the backfill. Figure 4 illustrates the deformed mesh for one typical case of analysis referring to a quay wall of 10m height and 7m width analyzed for the 1999 Kocaeli earthquake scaled to $PGA=0.5g$. The maximum computed total and seis-

mic earth pressures are compared to the Mononobe-Okabe ones in Figure 5. The computed angle δ of the inclination of the effective earth pressures behind the wall is of the order of 1/3 of the friction angle. Figure 5 also illustrates the maximum computed shear stresses beneath the quay wall; there is an average 40% exceedance of the shear strength of the foundation soil producing the residual displacements of the structure.

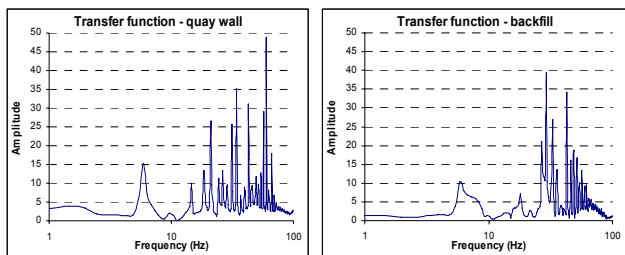


Figure 3. Transfer functions for the waterfront structure (left) and the backfill in free field conditions (right).

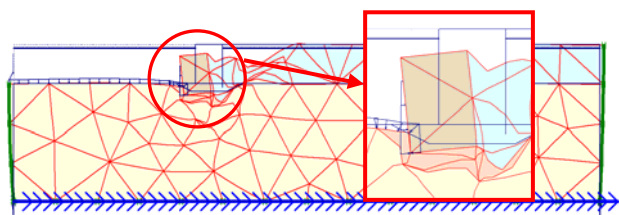


Figure 4. Example of the deformed mesh for a typical case of analysis (displacements scaled up to 50 times).

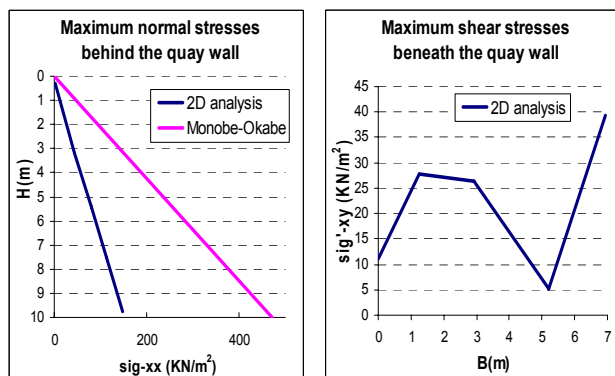


Figure 5. Computed total and dynamic earth pressures behind the wall and shear stress beneath the gravity wall.

The computed residual horizontal seaward displacements at the top of the quay walls, vary with the frequency content and duration characteristics of the input motion, the waterfront structure typologies and the type of the foundation soil. In general, higher values of permanent displacements are observed for lower frequencies, foundation soils with lower V_s values and smaller/ lighter walls. Also in higher walls we observe higher values of horizontal movements as a result of the tilting. The range of the computed residual seaward movements is given in Table 2 for all the waterfront structures' typologies examined.

Table 2. Residual seaward displacements at the top of the quay walls.

PGA	W/H = 0.7		W/H = 0.9	
	min u_x (cm)	max u_x (cm)	min u_x (cm)	max u_x (cm)
0.1g	1.1	13.3	0.3	16.5
0.3g	10.1	39.7	4.4	48.8
0.5g	14.7	68.7	9.0	82.1
0.7g	18.5	93.8	12.3	112.7
0.9g	22.0	115.1	15.2	145.0

Similar trends of the seismic response are observed for quay walls with height $H \leq 10m$ and height $H > 10m$ as well as for the foundation soil types B1, B3 ($V_s=250m/s$) and B2, B4 ($V_s=500m/s$). This facts is leading to four categories used in the construction of the analytical fragility curves.

4 ANALYTICAL FRAGILITY CURVES

Fragility curves are computed by cumulative distribution functions, giving the probability of reaching or exceeding different levels of damage. Usually they are represented as two-parameter (median and log-standard deviation) lognormal distribution functions.

To define the damage states, a damage index (DI) is introduced describing the ratio of the residual seaward displacement at the top of the quay wall (u_x) to the quay wall height (H). We establish a relationship between the damage index ($DI=u_x/H$) and the input motion intensity in terms of the PGA value for outcrop conditions. Considering the numerous uncertainties, the fragility curves are constructed using the mean values plus standard deviation of the damage index $DI=u_x/H$. According to the International Navigation Association (PIANC 2001), four damage levels are defined (Degree I-IV) based on the degree of the normalized residual horizontal displacement (u_x/H). The above thresholds for the damage index are also adopted herein for the definition of the four different damage states (minor, moderate, extensive and complete damages) as shown in Table 3.

The median values of peak ground acceleration that correspond to each damage state are defined as the values that correspond to the mean damage index based on the mean line of the damage index-PGA relationship. The standard deviation (β) describes the total variability associated with each fragility curve. Three primary sources contribute to the total variability for any given damage state (NIBS 2004), namely the variability associated with the discrete threshold of each damage state, the capacity and strength of each structural type and the earthquake ground motion. The uncertainty in the definition of damage state is assumed to be equal to 0.4 (similar to HAZUS for buildings). No variability on the structural capacity is taken into account, due to the assumption of a rigid structure. Finally, the uncertainty associated with seismic demand, is taken into consideration evaluating the variability in the calculated PGA values at the center of gravity of the waterfront structure. The total uncertainty is estimated as the root of the sum of the squares of the component dispersions.

Table 3. Definition of damage states for gravity walls (PIANC, 2001)

Level of damage	Normalized residual horizontal displacement (u_x/H)
Minor damages	Less than 1.5%
Moderate damages	1.5~5%
Extensive damages	5~10%
Complete damages	Larger than 10%

Figure 6 illustrates the derived fragility curves for minor and moderate damage states for the cases examined in the present work. The parameters of the proposed fragility curves are given in Table 4.

Table 4. Parameters of the proposed fragility curves

	Median PGA (g)		β
	Minor damages	Moderate damages	
$H \leq 10m, V_s=250m/sec$	0.11	0.37	0.54
$H \leq 10m, V_s=500m/sec$	0.07	0.34	0.58
$H > 10m, V_s=250m/sec$	0.14	0.44	0.49
$H > 10m, V_s=500m/sec$	0.10	0.4	0.57

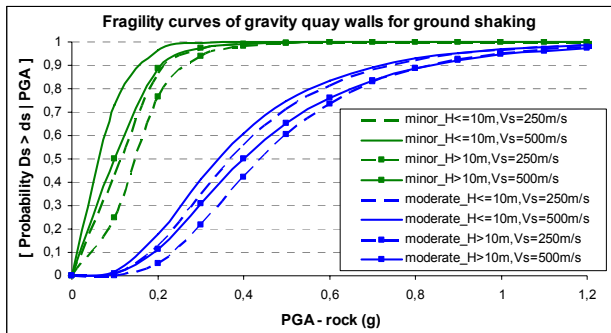


Figure 6. Proposed fragility curves for gravity waterfront structures due to ground shaking.

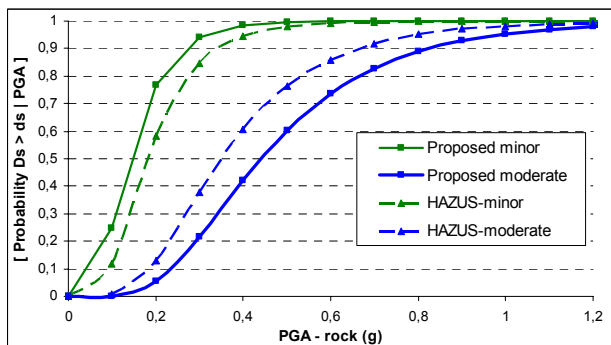


Figure 7. Comparison of the proposed fragility curves with the ones proposed in HAZUS for the case of height $H > 10m$ and $V_s = 250$ m/s.

The computed fragility curves are compared with the ones proposed by HAZUS and Ichii (2003). Since the empirical curves proposed in HAZUS are in terms of permanent ground displacements (PGD), the estimated damage index-PGA relationship is used for the conversion to PGA and for a mean wall height of 10m. In general, it is observed that the fragility curves proposed by Ichii (2003) differ from the proposed ones in this paper giving higher displacement values for the same level of intensity. The reason is that they are accounting for the occurrence of liquefaction phenomena. Comparing to the HAZUS fragility curves, the differences are rather small, but yet some diversity is observed according to the wall typology and soil foundation conditions which are not considered in HAZUS methodology. Figure 7 presents the comparison of the proposed fragility curves with the ones proposed in HAZUS for the case of wall height $H > 10m$ and $V_s = 250$ m/s.

5 CONCLUSIONS

We presented a set of analytical vulnerability functions for ordinary quay walls/ retaining structures' typologies commonly used in Europe, due to ground shaking. We are considering the distinctive features of the wall typology, the foundation soil type and the input ground motion characteristics. The proposed fragility curves for ground shaking are providing a more accurate estimation of the expected seismic performance of such structures for ordinary strong seismic excitations and foundation conditions. This is of major concern for coastal Mediterranean countries, exposed in high seismic risk, in order to enhance the seismic reliability and safety of port facilities.

REFERENCES

EC8, Part 5 2002. European Standard.
 Elgamal, A., Yang, Z., Parra, E., and Ragheb, A. 2001. CYCLIC 1D, UCSD.

Ichii, K. 2003. Application of Performance-Based Seismic Design Concept for Caisson-Type Quay Walls. Dissertation, Kyoto University.

Ichii, K. 2004. Fragility Curves for Gravity-Type Quay Walls Based on Effective Stress Analyses. Proceedings of 13th World Conference on Earthquake Engineering, Vancouver, BC Canada, August.

Kakderi, K., Raptakis, D., Argyroudis, S., Alexoudi, M. and Pitilakis K. 2006. Seismic Response and Vulnerability Assessment of Quaywalls. The Case of Lefkas. Proceedings of the 5th National Conference of Geotechnical and Environmental Engineering, Xanthi, Greece (in Greek).

Margaris, B., Papaioannou, Ch., Theodulidis, N., Savaidis, A., Anastasiadis, A., Klimis, N., Makra, K., Demosthenous, M., Karakostas, Ch., Lekidis, V., Makarios, T., Salonikiotis, T., Sous, I., Carydis, P., Lekkas, E., Lozios, S., Skourtsos, E. and Danamos, G. 2003. Preliminary Observations on the August 14, 2003, Lefkada Island (Western Greece) Earthquake. EERI Special Earthquake Report – November 2003, p.p.1-12, Joint report by Institute of Engineering Seismology and Earthquake Engineering, National Technical University of Athens and University of Athens, November.

National Institute of Building Sciences (NIBS) 2004. Earthquake loss estimation methodology. HAZUS'04. Technical manual, vol.1. Federal Emergency Management Agency, Washington, D.C.

PIANC 2001. Seismic Design Guidelines for Port Structures. International Navigation Association, Balkema, 474p.

Pitilakis, K., Alexoudi, M., Kakderi, K., Manou, D., Batum, E. and Raptakis, D. 2005. Vulnerability analysis of water supply systems in strong earthquakes. The case of Lefkas (Greece) and Duzce (Turkey). Proceedings of the International Symposium on the Geodynamics of Eastern Mediterranean, 15-18 June.

Plaxis 2007. Plaxis finite element code for soil and rock analyses. User's Manual, Version 8.6 Dynamic, The Netherlands.

Roth, W.H. and Dawson E.M. 2003. Analyzing the seismic performance of wharves, part 2: SSI analysis with non-linear, effective-stress soil models. Proceedings of the 6th U.S. Conference and Workshop on Lifeline Earthquake Engineering, TCLEE, Monograph No. 25, August.

Roth, W.H., Dawson, E.M., Mehrain, M. and Sayegh, A. 2003. Analyzing the seismic performance of wharves, part 1: Structural-engineering approach. Proceedings of the 6th U.S. Conference and Workshop on Lifeline Earthquake Engineering, TCLEE, Monograph No. 25, August.

ΑΡΘΡΑ ΜΕΛΩΝ ΕΕΕΕΓΜ ΣΤΟ 17TH ICSMGE

Groutability and effectiveness of microfine cement grouts Injectabilité et efficacité des injections des ciments très fins

D.N. Christodoulou & A.I. Droudakis
Democritus University of Thrace, Xanthi, Greece
I.A. Pantazopoulos
University of Patras, Patras, Greece
I.N. Markou
Democritus University of Thrace, Xanthi, Greece
D.K. Atmatzidis
University of Patras, Patras, Greece

ABSTRACT

A laboratory investigation was conducted in order to evaluate the properties, the groutability and the effectiveness of microfine cements. Four gradations from CEM II/B-M (according to EN 197-1) type of cement were used having nominal maximum grain sizes of 100 μm , 40 μm , 20 μm and 10 μm . The properties of suspensions, with water to cement ratios of 1:1, 2:1 and 3:1 by weight, were determined in terms of viscosity, bleeding, setting times and unconfined compression strength. Groutability and effectiveness were evaluated by conducting one-dimensional injections into five different, clean sands using three specially constructed devices. The effectiveness of cement suspensions was quantified by conducting unconfined compression, triaxial compression and permeability tests on grouted sand specimens. Groutability of cement suspensions increases with increasing cement fineness and water to cement ratio. Microfine cement suspensions with water to cement ratios of 2:1 and 3:1 can penetrate into medium to fine sands. Groutability predictions by conventional criteria are not always confirmed by laboratory injections. Sands grouted with microfine cements obtained unconfined compression strength values of up to 3 MPa and, in terms of the Mohr-Coulomb failure criterion, exhibited significant cohesion (up to 1360 kPa). The permeability coefficient of the sands was reduced by up to 5 orders of magnitude.

RÉSUMÉ

Une étude en laboratoire a été conduite pour évaluer les propriétés, l'injectabilité et l'efficacité des ciments très fins. Quatre différentes courbes de gradation de CEM II/B-M (selon EN 197-1), ont été utilisées avec des dimensions maximales des grains à 100, 40, 20 et 10 μm . Les propriétés des suspensions, avec un rapport de poids entre eau et ciment de l'ordre de: 1:1, 2:1 et 3:1, ont été déterminées en termes de viscosité, évapotranspiration, temps de solidification et compression simple. Injectabilité et efficacité ont été évaluées au moyen des injections unidimensionnelles, dans cinq différents sables purs, en utilisant trois dispositifs expérimentaux, spécialement fabriqués à ce propos. L'efficacité des suspensions de ciment a été quantifiée par des essais de compression simple, des essais de compression triaxiale et des essais de perméabilité, sur des échantillons de sable injecté. L'injectabilité des suspensions en ciment augmente avec leur finesse, aussi bien qu'avec le rapport eau - ciment. Les suspensions en ciment très fin ayant des rapports d'eau sur ciment de l'ordre de 2:1 et 3:1, peut pénétrer dans des sables fins ou moyennement fins. Les prédictions d'injectabilité par des critères conventionnels ne sont pas toujours confirmés par les essais d'injection en laboratoire. Des sables injectés par des ciments très fins ont obtenu des valeurs de compres-

sion simple 3 MPa au maximum, alors que, en termes du critère de rupture de Mohr-Coulomb, présentent des valeurs de cohésion significatives (jusqu'à 1360 kPa). Le coefficient de perméabilité des sables est réduit de 5 ordres de magnitude au maximum.

Keywords : grouting, suspensions, microfine cements, laboratory investigation, grouted sand, groutability, permeability, strength

1 INTRODUCTION

The safe construction and operation of many structures frequently requires improvement of the mechanical properties and behavior of soils by permeation grouting using either suspensions or chemical solutions. The former have lower cost and are harmless to the environment but can not be injected into soils with gradations finer than coarse sands. The latter can be injected in fine sands or coarse silts but are more expensive and, some of them pose a health and environmental hazard. Efforts have been made to extend the injectability range of suspension grouts by developing materials with very fine gradations. As a result, a number of fine-grained cements, called microfine or ultrafine cements, has been developed and manufactured. The behavior of microfine cements in permeation grouting is the objective of many ongoing research efforts.

Presented in this paper are preliminary results obtained and observations made during an extensive laboratory investigation conducted in order: (a) to develop a series of new microfine cements and (b) to investigate the behavior and performance of microfine cements in permeation grouting by documenting suspension properties and evaluating groutability of suspensions and effectiveness of grouting with these materials.

2 MATERIALS AND PROCEDURES

For the purposes of this investigation, a cement of type CEM II/B-M, according to EN 197-1, was used. The ordinary cement (designated as F0) was pulverized in order to produce three additional cements with nominal maximum grain sizes of 40 μm , 20 μm and 10 μm , which are designated as F1, F2 and F3, respectively. The grain size distributions of all cements are shown in Figure 1. All suspensions were prepared

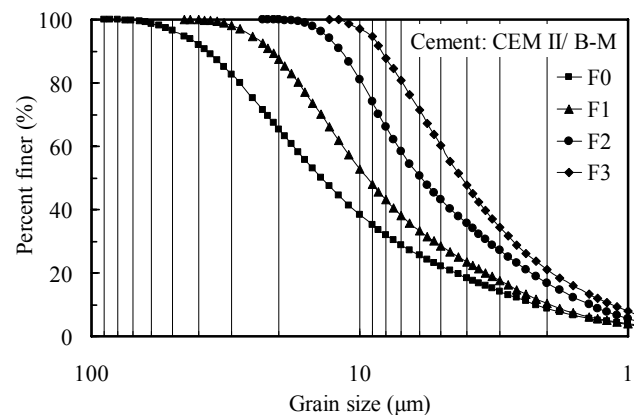


Figure 1. Grain size distributions of cements.

using potable water since it is considered appropriate for preparing cement-based grouts. A dosage of superplasticizer equal to 1.4% by weight of dry cement was added to F1, F2 and F3 cement suspensions for viscosity reduction. The water/cement (W/C) ratios of all suspensions used, was equal to 1:1, 2:1 and 3:1 by weight. The properties of suspensions were evaluated in terms of bleeding capacity, viscosity, setting times and strength. The values of suspension properties presented in Table 1 indicate that fine (F1) and microfine (F2 and F3) cement suspensions enhanced with superplasticizer can be used in permeation grouting for soil improvement.

Table 1. Cement suspension properties.

Cement	W/C ratio	Apparent viscosity, cP		Bleeding capacity, %	Setting times, hours		Unconfined compression strength, MPa	
		60 rpm*	3 rpm*		Initial	Final	7 days	28 days
F0	1:1	193	2123	16	9	14	4.4	9.0
	2:1	26	265	50	9	18	2.5	3.9
	3:1	10	23	64	10	37	1.4	2.7
F1	1:1	7	14	29	7	10	10.3	12.7
	2:1	2	2	47	7	11	1.9	3.3
	3:1	1.5	2	67	8	12	1.0	1.9
F2	1:1	30	416	2	5	8	6.9	10.6
	2:1	8	40	35	7	12	2.3	2.8
	3:1	2	4	49	8	19	1.1	1.6
F3	1:1	111	1885	2	4	6	8.3	9.7
	2:1	17	226	19	5	8	3.2	3.6
	3:1	3	15	38	6	8	1.3	1.5

* Viscometer rotation speed, Viscosity values obtained at t = 0 min

The grouted soils were clean, uniform sands with angular grains. Five different sand gradations were used with grain sizes limited between sieve sizes (ASTM E11) Nos. 5 and 10, 10 and 14, 14 and 25, 25 and 50, and 50 and 100, and designated as S1, S2, S3, S4 and S5, respectively. The sands were grouted in dense condition (mean value of relative density, D_r , $98 \pm 1\%$) and were dry prior to grouting. The angles of internal friction, ϕ , for all sands range from 44° to 45° , as obtained from UU triaxial compression tests in dense, dry specimens. The values of other properties of sands are presented in Table 2.

Table 2. Sand properties.

Sand	Specific gravity, Gs	Void ratios		Permeability coefficient, * k_{20} , cm/sec
		Minimum, e_{min}	Maximum, e_{max}	
S1	2.71	0.66	1.06	2.31
S2	2.72	0.68	1.03	0.80
S3	2.72	0.69	1.07	0.22
S4	2.70	0.70	1.06	0.04
S5	2.72	0.72	1.12	0.013

* Sands in dense condition

The groutability of suspensions was evaluated by performing injections into sand columns of a diameter equal to 7.5 cm and a length equal to 36.5 cm. The special device (Figure 2a) consisting of a pressurized feed tank with a stirring shaft, an air pressure regulator and a line to the PVC grouting column, was used. Injection was stopped when either the volume of the injected grout was equal to two void volumes of the sand in the column or when the injection pressure became equal to 200 kPa.

The special apparatus shown in Figure 2b was used for injecting sand columns with cement suspensions. It allows for adequate laboratory simulation of the injection process and investigation of the influence of the distance from injection point on the properties of grouted sand. The grouting column was made of PVC tube with an internal diameter of 7.5 cm and a height of 144 cm. Injection was stopped when either the volume of the injected grout was equal to two void volumes of the sand in the column or when the injection pressure became equal to 700 kPa. After curing for 28 days, the grouted columns were cut in alternating lengths of 16 cm and 9 cm. The resulting specimens with a length of 16 cm were tested in unconfined compression at an axial strain rate equal to 0.05 %/min. The specimens with a length of 9 cm were utilized for constant head permeability testing under water pressures ranging from 10 kPa to 200 kPa, using a specially constructed apparatus which allowed for testing of the grouted specimens in the PVC tube.

The laboratory equipment shown in Figure 3 was used to produce small-size grouted sand specimens, with a height of



(a) (b)

Figure 2. Laboratory equipment (a) for groutability evaluation and (b) for grouting sand columns.

11.2 cm and a diameter of 5.0 cm, ready for testing. This system consists of a pressurized feed tank with a stirring shaft, a pressure regulator and grouting manifolds with a line to each of four specimen molds. Unconsolidated – undrained triaxial compression tests were conducted on both grouted and ungrouted dense sand specimens at an axial strain rate equal to 0.2 %/min and confining pressures of 100, 200 and 400 kPa.



Figure 3. Laboratory equipment for producing small-size grouted sand specimens.

3 GROUTABILITY

For the purposes of the experimental investigation reported herein, groutability was evaluated by conducting injection tests with the apparatus shown in Figure 2a. Groutability was characterized as "satisfactory" when the predetermined quantity of grout (two void volumes of the sand column) could be injected, as "moderate" when the volume of injected grout was approximately equal to one void volume of the sand column, and as "impossible" when the quantity of the injected grout was very small. From the results of the injection tests presented in Table 3, it can be observed that groutability was "satisfactory" in S1 and S2 (Nos. 5-10 and 10-14) sands for all combinations of suspension composition. Groutability in S3 (Nos. 14-25) sand was "moderate" or "impossible" for F0 (ordinary) cement suspensions and "satisfactory" for the finer cement suspensions. The S4 (Nos. 25-50) sand was grouted "satisfactorily" only with microfine cement F2 suspensions having W/C ratio equal to 3:1 and microfine cement F3 suspensions having W/C ratios of 2:1 and 3:1. Groutability of all suspensions with W/C ratio equal to 1:1 was "impossible" in S4 sand. Penetration in S5 (Nos. 50-100) sand was negligible for any cement suspension used. Accordingly, it can be stated

that the increase of cement fineness and/or W/C ratio significantly improves the groutability of cement suspensions. On a quantitative basis, microfine cement suspensions with W/C ratios of 2:1 and 3:1 can be injected in medium to fine sands.

Table 3. Groutability predictions and experimental results

Cement	Sand	N ₁	N ₂	W/C ratio	N	Injection result *	
F0	S1	70	47	1:1-3:1	58	S	
	S2	46	32	1:1-3:1	39	S	
	S3		25	17	1:1	23	I
					2:1	23	M
					3:1	23	M
F1	S4	11	7	1:1-3:1	12	I	
	S5	5	3	1:1-3:1	7	I	
	S1	119	85	1:1-3:1	101	S	
	S2	78	57	1:1-3:1	68	S	
	S3	42	30	1:1-3:1	36	S	
F2	S4	19	13	1:1	19	I	
	S5		9	6	2:1	19	I
					3:1	20	I
					1:1-3:1	10	I
	S1	210	161	1:1-3:1	183	S	
S2	138	108	1:1-3:1	123	S		
F3	S3	75	58	1:1-3:1	66	S	
	S4	34	25	1:1	32	I	
	S5		15	12	2:1	32	M
					3:1	31	S
					1:1-3:1	16	I
S1	297	236	1:1-3:1	260	S		
S2	195	159	1:1-3:1	175	S		
S3	106	85	1:1-3:1	93	S		
S4	47	37	1:1	44	I		
S5		22	18	2:1	43	S	
				3:1	43	S	
				1:1-3:1	23	I	

* S: satisfactory, M: moderate, I: impossible

A preliminary evaluation of groutability can be made using available criteria, such as the "groutability ratios" (Mitchell 1981; Verfel 1989) which are defined as $N_1 = (D_{15})_{soil} : (D_{85})_{grout}$ and $N_2 = (D_{10})_{soil} : (D_{95})_{grout}$. D_{10} , D_{15} , D_{85} , and D_{95} are characteristic grain sizes of soil and grout. Grouting is considered possible for $N_1 > 25$ or $N_2 > 11$ and not possible for $N_1 < 11$ or $N_2 < 6$. $N_1 > 20$ is considered the minimum condition necessary for penetration and, if $N_1 \geq 50$, satisfactory permeation should be achieved. Values of N_1 and N_2 for the materials used in this investigation are presented in Table 3. A comparison between predictions and laboratory observations indicates that conventional criteria, such as the groutability ratios, may yield relatively optimistic predictions which are not always confirmed experimentally. This is attributed to the fact that groutability ratios are based solely on characteristic grain sizes of grout and soil and do not take into consideration factors, such as W/C ratio, which have an effect on groutability. The inadequacy of groutability ratios to predict correctly the groutability of cement based suspensions has also been verified by others (Zebovitz et al. 1989; De Paoli et al. 1992; Akbulut & Saglamer 2002).

Groutability can also be estimated using the empirical formula presented by Akbulut & Saglamer (2002):

$$N = \frac{D_{10}(soil)}{d_{90}(grout)} + k_1 \frac{w/c}{FC} + k_2 \frac{P}{D_r} \quad (1)$$

where N is groutability (if $N > 28$ soil can be grouted sufficiently by cement-based grouts), D_{10} and d_{90} are characteristic grain sizes of soil and grout, w/c is water to cement ratio of grout, FC is the finer content of soil passing through a 0.6 mm sieve, P is the grouting pressure, D_r is relative density of soil and k_1 , k_2 are constants. Although the values used, were not always between the limits given by Akbulut & Saglamer (2002), groutability N was computed by applying Equation 1

for the injection tests conducted in this investigation and the results obtained, are shown in Table 3. It can be observed that, predictions of groutability using Equation 1 are closer to the experimental results than the predictions based on groutability ratios, due to the fact that a larger number of factors affecting groutability is taken into consideration in this Equation.

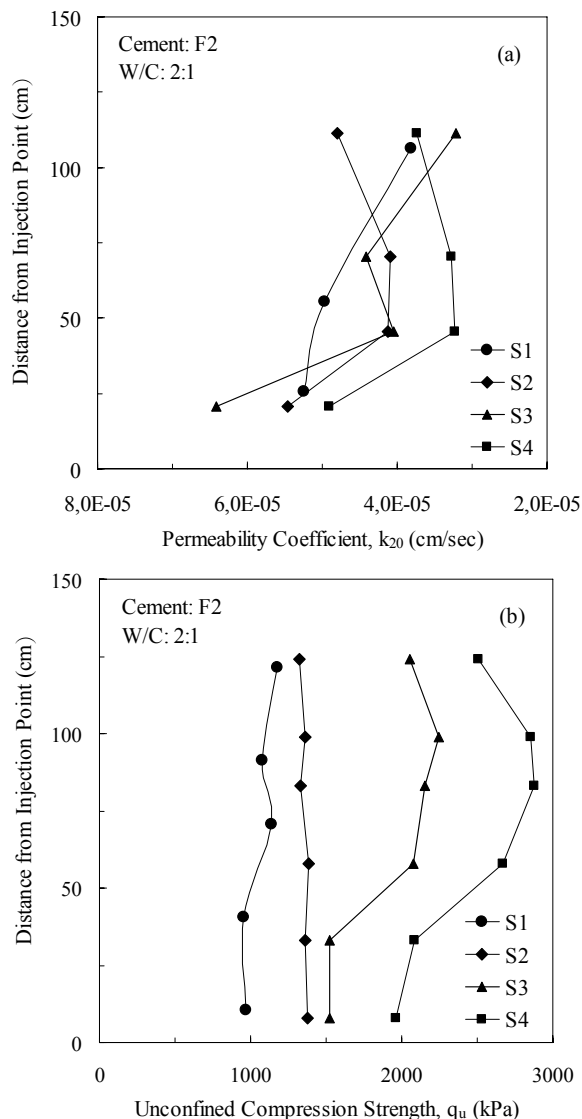


Figure 4. Permeability (a) and unconfined compression strength (b) of specimens from grouted sand columns.

4 EFFECTIVENESS

Results of permeability and unconfined compression tests conducted on specimens obtained from microfine cement grouted sand columns, after curing for 28 days, are presented in Figure 4. The permeability of the grouted sand specimens (Figure 4a) ranged from $3.2 \cdot 10^{-5}$ cm/sec to $6.4 \cdot 10^{-5}$ cm/sec indicating an improvement (reduction) of sand permeability by 3 to 5 orders of magnitude and the unconfined compression strength of the grouted sand specimens (Figure 4b) ranged from 1 MPa to 3 MPa. Permeability reduction increases with increasing grain size of the sand and is not substantially affected (remains significant) by the distance from injection point. On the contrary, unconfined compression strength increases with decreasing sand grain size due to the increase of the number of grain-to-grain contact points as the grain size of sand decreases (Zebovitz et al. 1989) and, either is unaffected by the distance from injection point (S1 and S2 sands), or is lower near the injection point (S3 and S4 sands), observation that needs further documentation. Sands

with permeability ranging between $2 \cdot 10^{-2}$ and $2 \cdot 10^{-3}$ cm/sec have been grouted with various microfine cements (Legendre et al. 1987; Zebovitz et al. 1989; De Paoli et al. 1992) and the permeability of the grouted sands had values ranging from 10^{-3} cm/sec to 10^{-7} cm/sec (a reduction of sand permeability by 1 to 5 orders of magnitude). Accordingly, the end effect of grouting with the suspensions used in this investigation on sand permeability is comparable to that obtained by grouting with other microfine cement suspensions.

The results obtained from all triaxial compression tests indicate a significant strength increase due to grouting which can be quantified in terms of the strength ratio, defined as the ratio of the deviatoric stress at failure of grouted and ungrouted sand specimens, tested under the same confining stress. The effects of confining stress, cement gradation and grout water to cement ratio are shown in Figure 5 for specimens prepared with S3 sand. It can be observed that the strength ratio values decrease with increasing confining stresses and with increasing water to cement ratio of the grouts, while they increase with increasing cement fineness. The effect of sand grain size on strength ratio values is shown in Figure 6 for specimens grouted with very fine cement (F3) at water to cement ratio of 2:1. It can be observed that the strength ratio values decrease with increasing sand grain size and this effect is more pronounced at low confining stresses.

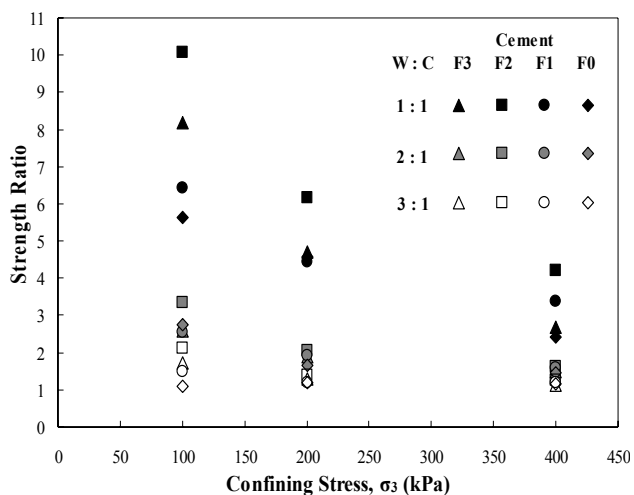


Figure 5. Effect of confining stress and grout composition on strength ratio values.

Strength parameter values were also obtained by applying the Mohr-Coulomb failure criterion. The observed significant strength increase (as quantified by the strength ratio values) is attributed primarily to the development of cohesion in the grouted sands, rather than to an increase of the angle of internal friction. A wide range of values was obtained for cohesion, indicating a significant effect of grout composition and sand grain size. Cohesion values ranged between 70 and 260 kPa, 290 to 490 kPa and 620 to 1360 kPa for grout with water to cement ratio of 3:1, 2:1 and 1:1, respectively, increasing with increasing cement fineness. Cohesion values increased with decreasing sand grain size and ranged between 325 to 600 kPa, when the sand gradation was varied from limiting sieves Nos. 5–10 to 25–50. The values obtained for the angle of internal friction did not exhibit a consistent trend. Although, a small increase (up to 3° over the value for ungrouted sand) was usually obtained, in some cases the effect of grouting was negligible and even slightly detrimental to the value of the internal friction angle.

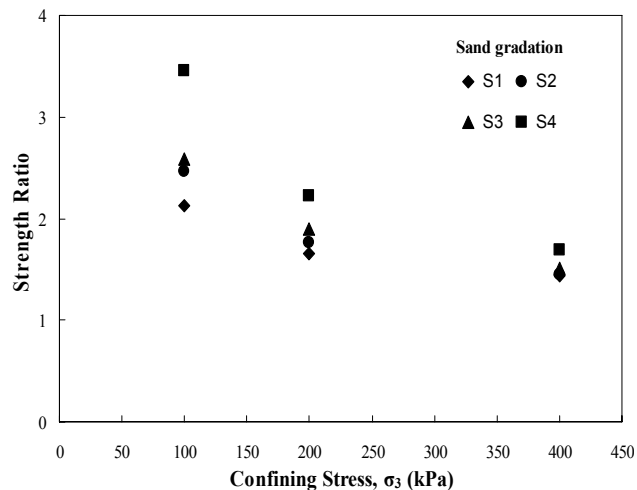


Figure 6. Effect of sand grain size on strength ratio values.

5 CONCLUSIONS

Based on the results obtained and the observations made during this investigation, the following conclusions may be advanced:

1. The increase of cement fineness improves the groutability of cement suspensions rendering them effective for grouting of medium to fine sands. Predictions of groutability by groutability ratios are often optimistic, while predictions by an empirical formula were found to be closer to the experimental results.
2. A satisfactory reduction (3 to 5 orders of magnitude) of the permeability of sands can be obtained by grouting with microfine cement suspensions. Permeability reduction increases with increasing grain size of the sand.
3. In terms of strength improvement, grouting with micro- or ultra-fine cements, produced by grinding of common cements, offers a significant advantage over the coarser cements with the same chemical composition.

ACKNOWLEDGEMENTS

The research effort reported herein is part of the research project (PENED) which is co-financed by E.U. – European Social Fund (80%) and the Greek Ministry of Development – GSRT (20%).

REFERENCES

- Akbulut, S. & Saglamer, A. 2002. Estimating the groutability of granular soils: a new approach. *Tunnelling and Underground Space Technology* 17: 371-380.
- De Paoli, B., Bosco, B., Granata, R. & Bruce, D. 1992. Fundamental observations on cement based grouts (2): microfine cements and Cemill[®] process. *Proc., Conf. on Grouting, Soil Improvement & Geosynthetics*, New Orleans, ASCE, 1: 486-499.
- Legendre, Y., Hery, Ph. & Vattement, H. 1987. Microsol grouting, a method for grouting fine alluvium. *Proc., Sixth Int. Offshore Mech. and Arctic Engrg. Symposium*, Houston, ASME, 1: 433-440.
- Mitchell, J.K. 1981. Soil improvement – state of the art report. *Proc., 10th ICSMFE*, Stockholm, A.A. Balkema, 4: 509-565.
- Verfel, J. 1989. *Rock grouting and diaphragm wall construction*. Amsterdam: Elsevier Science Publishers.
- Zebovitz, S., Krizek, R. & Atmatzidis, D. 1989. Injection of fine sands with very fine cement grout. *J. Geotech. Engrg.* 115: 1717-1733.

Tunnel Stability Factor – A new controlling parameter for the face stability conditions of shallow tunnels in weak rock environment

Facteur de stabilité de tunnel : Une paramètre nouveau qui contrôle les conditions de stabilité des fronts d'excavation pour les tunnels peu profonds dans un environnement des roches tendres

I. Mihalís

Geotechnical Consultant, MSc, DIC, ikmihalís@tellas.gr

S. Konstantís

Geotechnical Engineer, PGSD, MSc, COWI A/S

A. Anagnostópoulos

Professor Emeritus, NTUA, Greece

G. Vlavianós

Head of Geotechnical Division, Ministry of Public Works, Greece

G. Doulís

Geotechnical Engineer, EDAFOMICHANIKI S.A.

ABSTRACT

The present paper justifies, on the basis of a significant number of parametric analyses, the use of Tunnel Stability Factor (TSF) in the preliminary assessment of tunnel's face stability conditions for low overburden heights in weak rocks.

The Tunnel Stability Factor is determined mathematically according to the following relationship:

$$TSF = \sigma_{cm} / \gamma H^a D^{1-a}$$

where : σ_{cm} & γ is the strength and the specific unit weight of the in-situ rockmass surrounding the tunnel,

$\sigma_{cm} = 2c / \tan(45^\circ + \phi/2)$, c is the cohesion and ϕ the angle of internal friction of the rockmass, respectively,

H is the height of overburden soil,

D is the equivalent diameter of the underground opening.

The execution of all parametric analyses has been based on the use of 3-D wedge limit equilibrium model. The examined tunnel cases included circular tunnel cross - sections with diameter $D=4\text{m} - 10\text{m}$ and overburden heights $H=10\text{m} - 20\text{m}$. The weak rock conditions were characterized by the following shear strength parameters: $c=5\text{KPa}-20\text{KPa}$, $\phi=25^\circ-30^\circ$. Groundwater conditions have been also included in the parametric analyses as an independent variable.

RÉSUMÉ

La présente communication, basée sur un nombre important d'analyses paramétriques, justifie l'emploi d'un Facteur de Stabilité du Tunnel (TSF) pour la détermination préliminaire des conditions de stabilité du front d'excavation, dans un environnement des roches tendres de petit recouvrement. Le Facteur de Stabilité du Tunnel est défini mathématiquement selon la formule :

$$TSF = \sigma_{cm} / \gamma H^a D^{1-a}$$

avec : σ_{cm} et γ : La portance et le poids volumique de la masse rocheuse autour du tunnel,

$\sigma_{cm} = 2c / \tan(45^\circ + \phi/2)$, c étant la cohésion et ϕ l'angle de frottement interne de la masse rocheuse,

H : l' hauteur du sol de recouvrement,

D : le diamètre équivalent d'excavation.

Toutes les analyses paramétriques ont été basées sur l'utilisation d'un modèle eu dièdre tridimensionnel en équilibre limite. Les cas des tunnels examinés concernent des sections circulaires avec diamètre $D=4\text{m}-10\text{m}$ et hauteur de recouvrement $H=10\text{m}-20\text{m}$.

Les conditions des roches tendres ont été caractérisées par les paramètres de cisaillement suivants : $c=5\text{ KPa}-20\text{KPa}$, $\phi=25^\circ-30^\circ$.

La présence de la nape souterraine a été aussi prise en compte dans les analyses paramétriques comme une variable indépendante.

Keywords : tunnel, face stability, support pressure, weak rocks, tunnel stability factor

1 INTRODUCTION

During the excavation works for the construction of shallow tunnels in weak rocks, instability phenomena on the area of the tunnel face are often observed. In these cases, the favourable arch effect either does not take place due to geometrical constraints or its temporary duration is so small that does not contribute to the stability of the tunnel face.

This potential instability dictates the necessity for application of adequate support pressure on the tunnel face, active in the case of use of TBM or passive (for instance with fibre glass nails) in the case of NATM.

Absence of this necessary support pressure may result in excessive face extrusion. This may initiate the potential for partial or total failure of the tunnel face with the form of the chimney failure and in some cases a crater, that reaches the ground surface introducing adverse effects on the structures located in the area.

The causes that lead to a potential instability and failure of the tunnel face are associated with the geometrical characteristics of the tunnel cross-section, the strength and deformability characteristics of the rockmass surrounding the tunnel, the in situ stress state in the area of excavation as well as the presence of underground water table above the tunnel crown.

2 FACE STABILITY

2.1 Limit equilibrium model with side friction

The face stability in homogenous soil can be assessed by considering the simple collapse mechanism presented in figure 1. This 3-D model, which was originally proposed by (Horn 1961), is based on the Silo theory from (Janssen 1895).

The circular cross section of the tunnel is approached by a square with side length the diameter D of the tunnel. The collapse mechanism comprises a wedge and a prism that extends from the tunnel crown to the ground surface. The soil/rockmass is considered to behave as elastic- perfectly plastic material according to the Mohr-Coulomb failure criterion, with shear strength characteristics the cohesion c and the angle of internal friction ϕ . Hence, at every point along the slide surfaces, the shear strength is given by the following expression (1):

$$\tau = \frac{c}{F} + \sigma \frac{\tan \phi}{F} \quad (1)$$

where σ and F are the normal stress and the safety factor, respectively.

The wedge of the collapse mechanism is subjected to the following actions: (a) the self weight, (b) the resulting normal and shear forces along the failure surfaces ADE, BCF and

ABFE, (c) the support force applied on the tunnel face and (d) the vertical force due to the weight of the overlying prism in the interface DEFC.

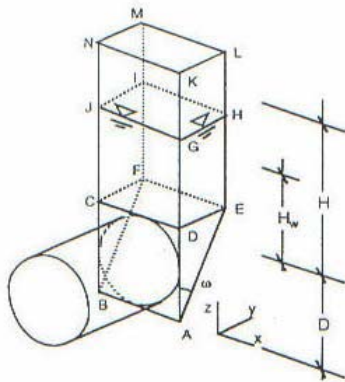


Figure 1 Collapse mechanism (after Horn, 1961)

The support pressure for a given failure mechanism characterised by a specific slope ω of the slide surface ABFE is derived through the solution of the limit equilibrium equations for the wedge. The critical slope ω_{cr} is determined through an iterative procedure until the maximisation of the necessary support pressure for a given safety factor or until the minimisation of the safety factor for a given support pressure.

In case of presence of underground water table above the tunnel crown, all the calculations are performed on the basis of effective stresses while it is considered that the distribution of the water pressures along the slide surfaces has a hydrostatic pattern.

The shear stresses depend essentially on the horizontal stresses that act perpendicular to the vertical slide surfaces. However, the horizontal stresses can not be determined without consideration of the deformability characteristics of the ground. Following the silo theory of (Janssen 1895), a constant coefficient λ of the horizontal to the vertical stresses is adopted. (Terzaghi and Jelinek 1954) suggested the use of $\lambda=1$. In the present work, the value $\lambda=0,8$ was adopted based on the experiments conducted by (Gudehus and Melix 1986) and (Melix 1987).

The vertical force on the interface CDEF is determined through the application of the silo theory of Janssen first on the part of the prism above the ground water table and then on the remaining part between the ground water level and the tunnel crown, in order to take into account the different specific unit weights of the soil above and below the ground water table.

The mean effective vertical stress σ' on the surface CDEF is given by the following expression (2):

$$\sigma_v = \frac{\gamma' r - c}{\lambda \tan \phi} \left(1 - e^{-\lambda \tan \phi H_w / r} \right) + \frac{\gamma_d r - c}{\lambda \tan \phi} \left(e^{-\lambda \tan \phi H_w / r} - e^{-\lambda \tan \phi H / r} \right) \quad (2)$$

where H , H_w , γ_d and γ' are the height of the overburden soil, the height of the ground water table above the tunnel crown (see figure 1), the dry unit weight and the effective unit weight under buoyancy of the soil, respectively. The parameter r denotes the ratio of the volume to the periphery of the prism and is defined as:

$$r = 0,5D \tan \omega / (1 + \tan \omega) \quad (3)$$

Equation (2) is valid for safety factor F equal to 1. Other values of the safety factor may be considered by replacing the cohesion c and $\tan \phi$ through c/F and $\tan \phi/F$, respectively as shown in equation (1).

Regarding the distribution of stresses σ on the slide surfaces ADE and BCF of the wedge the linear approach suggested in (DIN 4126 1986) is adopted, as depicted in figure 2. Consequently, the vertical stress σ_z increases linearly with depth due to the weight of the soil, while the contribution of the interface stress σ_v decreases.

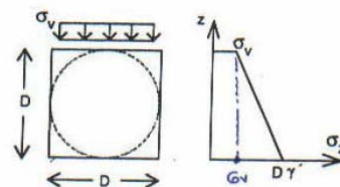


Figure 2 Distribution of vertical stresses on the slide surfaces of the wedge

Hence, the mean friction resistance τ_ϕ is calculated through the integration of the term $\lambda \sigma_z \tan \phi$ on the slide surfaces ADE and BCF:

$$\tau_\phi = \lambda \left(\frac{1}{3} \gamma' D + \frac{2}{3} \sigma_v \right) \frac{\tan \phi}{F} \quad (4)$$

(Anagnostou and Kovari 1994) performed numerical analysis in order to examine and verify the accuracy of the approach presented in figure 2. In these analysis, the equilibrium of the wedge was analysed according to the silo theory and the wedge was divided in horizontal slices. The analysis showed that the approach proposed in DIN 4126 overestimates the vertical stress σ_z and hence the shear resistance. However, the uncertainties associated with the linear approach of figure 2 can be eliminated by choosing a lower value of λ in equation (4). In the present work, the value $\lambda=0,4$ was adopted, namely half of the value that was adopted for the part above the tunnel.

3 TUNNEL STABILITY FACTOR

As it has already been mentioned, the general stability of the tunnel face depends on the in situ strength of the soil/rockmass surrounding the tunnel, the geometrical characteristics and the excavation depth of the tunnel.

(Mihalís et al. 2001) have proposed the use of the Tunnel Stability Factor (TSF) for the assessment of the behaviour of underground openings in weak rock conditions, which combines all the above influence factors and can be considered as an important parameter for the initial assessment of the overall behaviour of tunnel cross sections.

The Tunnel Stability Factor (TSF) is defined through the following mathematical expression:

$$TSF = \frac{\sigma_{cm}}{\gamma H^a D^{1-a}} \quad (5)$$

where:

σ_{cm} & γ are the strength and the specific unit weight of the in-situ rockmass surrounding the tunnel, respectively

$\sigma_{cm} = 2c / \tan(45^\circ + \phi/2)$ with c the cohesion and ϕ the angle of internal friction of the rockmass, respectively

H is the height of overburden soil and

D is the equivalent diameter of the underground opening

The exponent a is a parameter that depends on the type of tunnel behaviour assessment under consideration, such as assessment of tunnel stability in relation to radial convergence and potential squeezing problems, assessment of tunnel face stability etc.

4 PARAMETRIC ANALYSIS

4.1 Variable parameters

In the framework of the parametric analysis of the present work, the following case combinations were examined:

- Circular cross section with diameters D=4, 6, 8 and 10m
- Overburden height H=10, 12.5, 15, 17.5 and 20m
- Weak rock with cohesion c=5, 10, 15 and 20 KPa and angle of internal friction $\phi=25^\circ$ and 30°
- Height of ground water column $H_w=H/2, H/4$ and 0m.

4.2 Safety factor considerations

In the parametric analysis, the support pressure P that must be applied on the tunnel face of a shallow tunnel for the achievement of a given factor of safety was determined. Support pressures P were calculated for safety factors of SF=1, 1.1, 1.2, 1.3 and 1.4.

It was considered that when the support pressure is such that a safety factor of 1 and 1.1 can be achieved, the face has a high failure probability, also due to the various inherent uncertainties associated with the estimation of the geomechanical properties of the surrounding rockmass and the simplifying assumptions adopted in the failure model. When the applied support pressure on the face results in safety factors of 1.2 and 1.3, it can be considered that the face is temporarily safe, under the geotechnical notion of the term. When the safety factor is in the order of 1.4, it can be considered that the support pressure applied on the tunnel face is sufficient to achieve permanent stability. The terms temporary and permanent stability are more appropriate for the case where the tunnel is conventionally excavated and the face support takes place for instance with the use of fibreglass anchors. When the tunnel is excavated with a TBM these terms denote in a way the escalation of the safety factor, except for the case of interventions.

5 RESULTS

5.1 Definition of TSF

According to the results of the parametric analysis, the analytical form of the Tunnel Stability Factor was defined as:

$$TSF = \frac{\sigma_{cm}}{\gamma H^{0,35} D^{0,65}} \quad (6)$$

(Mihalis et al. 2001) have proposed the value 0,75 for the exponent a, for the case where the TSF is used for the assessment of tunnel stability in weak rocks in relation to the radial convergence of the tunnel walls, the evolution of plastic zone around the excavation and the potential for evolution of squeezing problems. In this case, the relative contribution of the overburden height H is higher in comparison to the tunnel diameter, since the potential for evolution of squeezing problems is in direct conjunction with the ratio of the in situ strength of the rockmass to the overburden pressure (Hoek 1999).

On the other hand, in the assessment of tunnel face stability in weak rock with low overburden height, where the evolution and activation of the arch effect is questionable, the predominant contribution comes from the tunnel diameter, namely the area where the tunnel face extrusion shall evolve. The bigger the diameter of the tunnel, the higher the radial

pre-convergence and axial face extrusion and higher the potential for evolution of failure mechanisms on the face.

5.2 Support pressure on the tunnel face

For each safety factor, a diagram was produced (see diagrams 3 to 7) that correlates the dimensionless parameters P/c and TSF for various values of the groundwater table level H_w . In addition, the associated mathematical expressions with the highest correlation of the results of the parametric analysis were derived.

5.2.1 Dimensionless diagrams

(1) Safety factor 1.0

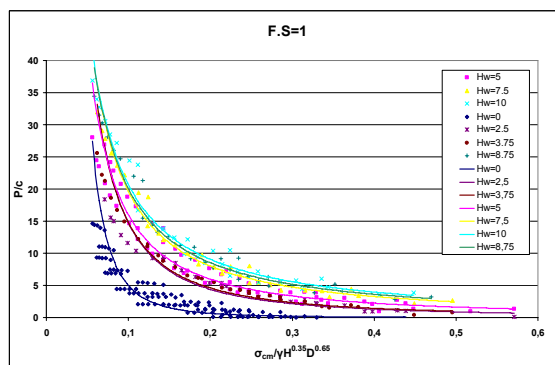


Figure 3 Support pressure on the tunnel face for limit equilibrium

(2) Safety factor 1.1

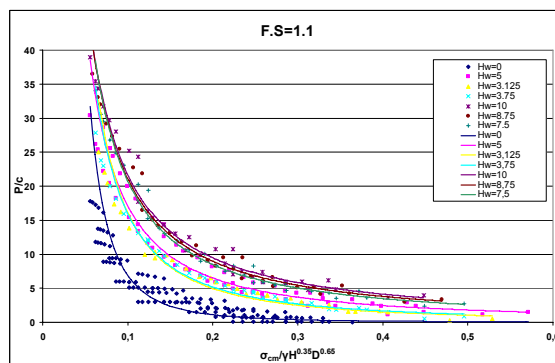


Figure 4 Support pressure on the tunnel face for safety factor 1.1

(3) Safety factor 1.2

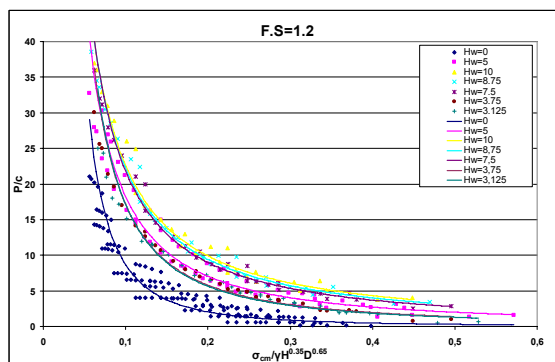


Figure 5 Support pressure on the tunnel face for safety factor 1.2

(4) Safety factor 1.3

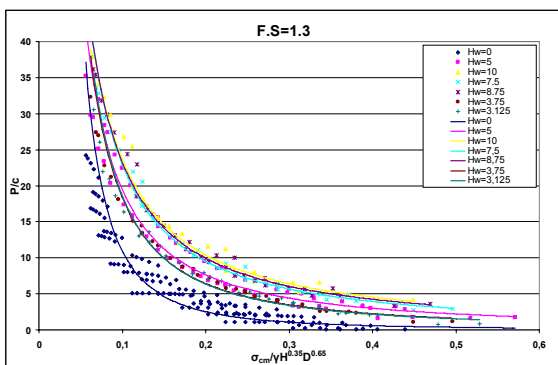


Figure 6 Support pressure on the tunnel face for safety factor 1.3

(5) Safety factor 1.4

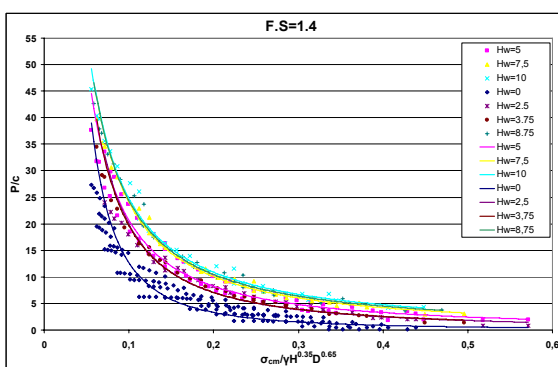


Figure 7 Support pressure on the tunnel face for safety factor 1.4

5.2.2. Mathematical expressions

All the above trend lines can be summarised in the following mathematical expression, with the values of A and B given in table 1:

$$P/c = A \left(\sigma_{cm} / (\gamma H^{0.35} D^{0.65}) \right)^{-B} \quad (7)$$

Table 1 Values of A and B for mathematical expression (7)

	SF=1	SF=1.1	SF=1.2	SF=1.3	SF=1.4
A_ Hw=0	0,0058	0,0161	0,0724	0,0846	0,1456
A_ Hw≥2,5m	a)	c)	e)	g)	i)
B_ Hw=0	2,9344	2,6322	2,0797	2,1108	1,9394
B_ Hw≥2,5m	b)	d)	f)	h)	j)

- a) $0,1514H_w - 0,1688, R^2=0,99$
- b) $2,3536H_w^{-0,2956}, R^2=0,97$
- c) $0,1587H_w - 0,1625, R^2=0,99$
- d) $2,3775H_w^{-0,3039}, R^2=0,98$
- e) $0,1544H_w - 0,0523, R^2=0,99$
- f) $2,1529H_w^{-0,2591}, R^2=0,98$
- g) $0,1514H_w + 0,055, R^2=0,99$
- h) $2,0156H_w^{-0,2308}, R^2=0,98$
- i) $0,14H_w + 0,2374, R^2=0,98$
- j) $1,7964H_w^{-0,1782}, R^2=0,96$

6 CONCLUSIONS

On the basis of the results taken from the performed parametrical analyses, a number of practical design charts with the associated mathematical expressions have been produced. These charts essentially provide an assessment of the support pressure P that needs to be applied on the tunnel face for the assurance of stability conditions (characterised by a certain value of safety factor) in conjunction to TSF values.

It is noted that, although the wide range of all the examined cases (in terms of ground, groundwater and tunnelling conditions), the aforesaid design charts provide a well determined trend of behaviour, due to the small degree of scattering of the calculation results. As a consequence of this, all the presented in this paper design charts and mathematical expressions could be safely used for preliminary design purposes, by providing the necessary face support measures of shallow tunnels in weak rock conditions.

REFERENCES

Anagnostou, G. & Kovari, K. 1994. Stability Analysis for tunnelling with slurry and EPB shields. Proc. Gallerie in condizioni difficili, Torino, 29.11-1.12.1994

DIN 4126, 1986. Ortbeton-Schlitzwände. Konstruktion und Ausführung (in German)

Gudehus, G. & Melix, P. 1986. Standsicherheitsnachweise für Bauzustände von Tunneln in schwach kohäsiven Gebirge. STUVA, Forschung + Praxis 30, 145-152 (in German)

Hoek, E. 1999. Tunnel support in weak rock. Notes of Lecture presented at the National Technical University of Athens

Horn, M. 1961. Horizontaler Erddruck auf senkrechte Abschlussflaechen von Tunneln. In Landeskonferenz der ungarischen Tiefbauindustrie, Budapest (German translation, STUVA, Duesseldorf)

Janssen H. A. 1895. Versuche über Getreidedruck in Silozellen. Zeitschrift des Vereins deutscher Ingenieure, Band XXXIX, No. 35, 1045-1049 (in German)

Konstantis, S. 2003. Examination of underground opening face stability conditions in urban areas. Post Graduate Master Thesis, National Technical University of Athens

Melix, P. 1987. Modellversuche und Berechnungen zur Standsicherheit oberflächennaher Tunnel. Veröff. des Inst. für Boden und Felsmechanik der Univ. Fridericiana in Karlsruhe, 103 (in German)

Mihalis, I.K., Kavvadas, M.J. & Anagnostopoulos A.G. 2001. Tunnel Stability Factor – A new parameter for weak rock tunnelling. Proceedings, 15th Int. Conference on Soil Mechanics and Geotechnical Engineering, Istanbul, Vol. 2, pp. 1403 – 1406

Terzaghi, K. & Jelinek, R. 1954. Theoretische Bodenmechanik, 505 Berlin: Springer-Verlag (in German)

Installation damage of nonwoven polypropylene geotextiles

Endommagement pendant l'installation de géotextiles on tissés en polypropylène

D.K. Atmatzidis, D.A. Chrysikos & I.M. Papaefstathiou
University of Patras, Greece

ABSTRACT

European standard ENV ISO 10722-1 specifies a test for comparative evaluation of the installation damage of geosynthetics. Tests were conducted according to ENV ISO 10722-1 on 32 nonwoven, polypropylene geotextiles with mass per unit area from 100 to 2200 g/m² and tensile strength from 8 to 125kN/m. The effects of number of loading cycles and aggregate hardness were also investigated. A very good correlation ($R^2 \approx 0.90$) was obtained between installation damage index values and mass per unit area of the geotextiles. The damage index values obtained for geotextiles with mass over 500g/m² ranged between 85% and 95% indicating very limited installation damage. The damage index values of geotextiles with mass less than 500g/m² ranged between 43% and 85% indicating a very strong effect of geotextile mass on installation damage. Aggregate hardness by itself may not be a good indicator of damage potential. Increasing load cycles results in increased damage potential.

RÉSUMÉ

La norme Européenne ENV ISO 10722-1 spécifie la procédure d'un essai d'évaluation comparative de l'endommagement des géosynthétiques pendant leur installation. Suivant cette norme, on a effectué des essais sur 32 géotextiles non tissés en polypropylène dont la masse varie entre 100 et 2200 g/m² et la résistance en traction varie entre 8 et 125kN/m. On a de plus étudié les effets d'un nombre de cycles de chargement et de la dureté des agrégats. On a trouvé une très bonne corrélation ($R^2 \approx 0.90$) entre l'indice d'endommagement pendant l'installation et la masse par unité de surface des géotextiles. L'indice d'endommagement des géotextiles ayant une masse supérieure à 500g/m² varie entre 85% et 95%, ce qui démontre un endommagement limité pendant leur installation. L'indice d'endommagement des géotextiles ayant une masse inférieure à 500g/m² varie entre 43% et 85%, ce qui démontre un effet important de la masse du géotextile sur l'endommagement dû à la procédure de l'installation. La dureté de l'agrégat par elle-même n'est pas nécessairement un bon indicateur du potentiel d'endommagement. L'accroissement des cycles de chargement conduit à une augmentation du potentiel d'endommagement.

Keywords : geotextiles, nonwoven, installation damage, laboratory testing

1 INTRODUCTION

It is generally recognized that geotextile property values, obtained by standardized laboratory testing procedures, should not be used directly in design but should be suitably reduced to account for in situ conditions. Accordingly, reduction factors are applied on the laboratory generated property values to obtain corresponding allowable values. In strength-related problems, reduction factors are introduced to account for installation damage, long-term creep effects and chemical or biological degradation. Installation damage of geotextiles has been investigated both by field and by laboratory testing. A comprehensive review of field test results by Hufenus et al. (2005) indicates that the installation damage of geotextiles depends on geotextile type, aggregate gradation and grain shape, aggregate lift thickness, compaction energy and type of compaction equipment. Due to the large number of variables affecting the results of field tests, mostly qualitative evaluations of the available information can be obtained.

European Standard ENV ISO 10722-1 specifies a test for comparative evaluation of the installation damage of geosynthetics and yields a damage index value as the ratio of a reference property value of damaged to undamaged specimens. A geosynthetic specimen is placed between two layers of synthetic aggregate (sintered aluminium oxide) each 75mm thick, with grain sizes between 5mm and 10mm and Los Angeles coefficient (abrasion resistance) of not less than 1.9. Loading is applied through a 100mm by 200mm stiff plate. Cyclic loading between 5kPa and 900kPa at a frequency of 1Hz for 200 loading cycles is applied. Information from laboratory investigations based on standard procedures (i.e. Naughton and Kempton 2002, Paula et al. 2004) is limited primarily due to the small number of geosynthetics tested per reported investigation and provides no correlations between installation damage and geosynthetic physical and/or mechanical properties.

The observations stated above, provided the impetus for the laboratory investigation reported herein. Scope of this investigation is to provide a quantitative evaluation of installation damage of nonwoven polypropylene geotextiles based on results obtained for a relatively large number of samples tested according to standard procedures. Correlations with physical and mechanical properties were attempted. The effect of aggregate hardness and number of loading cycles was evaluated.

2 MATERIALS AND PROCEDURES

An overall view of the laboratory equipment used for conducting the installation damage tests reported herein is shown in Figure 1. This loading frame was constructed in-house and allows control of the maximum pressure of the applied cyclic load as well as the frequency and the number of loading cycles. As specified by ENV ISO 10722-1, the test container was made of stainless steel, with 300mm by 300mm internal dimensions in plan, and consisted of two parts each 75mm deep. The lower part was filled with two layers of aggregate each compacted to a pressure of 200kPa for 60s.

After placement of the geotextile specimen, the upper part of the container was loosely filled with aggregate. The assembled container is also, shown in Figure 1. The protruding portion of the geotextile specimen is used to obtain the reference property value for undamaged material.

For the purposes of the investigation reported herein, geotextile specimens were taken from large size samples obtained from six different manufacturers. The size of the samples ranged from 6m² to 10m² with a width equal to the standard production roll width of each manufacturer. All geotextiles were nonwoven, polypropylene, needle-punched and were made of staple fibers. One geotextile series was thermally post-treated on both surfaces. The physical and mechanical properties of the geotextiles tested covered a wide range of values. Mass per unit area (EN ISO 9864) ranged from 96.7g/m² to 2205g/m². Thickness (EN ISO 9863) ranged from 1.17mm to 11.10mm. Tensile strength (EN ISO 10319) ranged from 7.9kN/m to 75.1kN/m in the machine direction and from 7.4kN/m to 148.2kN/m in the cross-machine direction. To avoid the use of commercial names, a generic notation is used (i.e. M1) to identify manufacturer and geotextile series.

All geotextiles were tested according to the standard procedures specified by ENV ISO 10722-1. Furthermore, five geotextiles were selected as representative of the whole group and tests were conducted in order to investigate the effect of the number of loading cycles and the hardness of the aggregate. Toward this end, tests were conducted (a) with 100 and 400 loading cycles, that is with half and double the number of standard loading cycles and (b) with two more aggregates other than the standard.



Figure 1. Laboratory equipment (ENV ISO 10722-1).

The aggregate used for conducting standard tests according to ENV ISO 10722-1 was a commercially produced aluminium oxide (corundum) with angular grains and grain sizes between 5mm and 10mm. The Los Angeles coefficient of this aggregate had a value equal to 11 according to EN 1097.02. The second aggregate used was commercially produced using electric arc furnace slag and the third aggregate was crushed limestone (marble). Both had angular grains with a gradation as specified by the standard and Los Angeles coefficient equal to 16 and 26, respectively.

3 RESULTS AND OBSERVATIONS

After each test, the geotextile specimen was carefully recovered and visually inspected for damage in the form of perforations. A hole count was made and recorded. As an example of this type of damage, shown in Figure 2 is a geotextile specimen at an intermediate stage of wide-width tensile testing. In general, the number of holes decreased with increasing geotextile mass per unit area but no holes or other discontinuities were observed for geotextile specimens with mass per unit area over 300g/m². For light weight geotextiles with mass per unit area between 100 and 150g/m², a significant number of holes was observed ranging between 10 and 20 per specimen (500 to 1000 per m²) while for geotextiles with mass per unit area between 150g/m² and 300g/m² the hole count ranged between 5 and 10 per specimen (250 to 500 per m²).

Installation damage was quantified on the basis of results obtained from wide-width tensile tests conducted, according to standard EN ISO 10319, on the damaged and undamaged specimens of all geotextile samples. The percent retained tensile strength and failure deformation were computed and the results are shown in Figure 3. It can be observed that geotextiles with mass per unit area of about 500g/m² or higher, retain a significant percentage of their tensile strength and failure deformation which ranged between 85%



Figure 2. Damage observed as holes on geotextile specimen during tensile testing.

and 96% and between 75% and 90%, respectively. For geotextiles with mass per unit area of about 500g/m² or less the retained tensile strength and failure deformation decrease significantly with decreasing mass per unit area. For these geotextiles, a linear correlation between mass per unit area and retained tensile strength and failure deformation was obtained, as a first order approximation. When the damage index is expressed in terms of retained tensile strength, the correlation is very good and yields a correlation coefficient value of R²=0,934. However, damage index values expressed in terms of failure deformation exhibit a significant scatter and are not well correlated to mass per unit area (R²=0,662). These general observations were substantiated by considering separately each of the geotextile series tested. Presented in Figure 4 are typical results, obtained for one of the geotextile series tested, indicating that the damage of geotextile samples with mass per unit area higher than 400 to 500g/m² is relatively small and yields a reduction of the reference test value of not more than 10% to 20%.

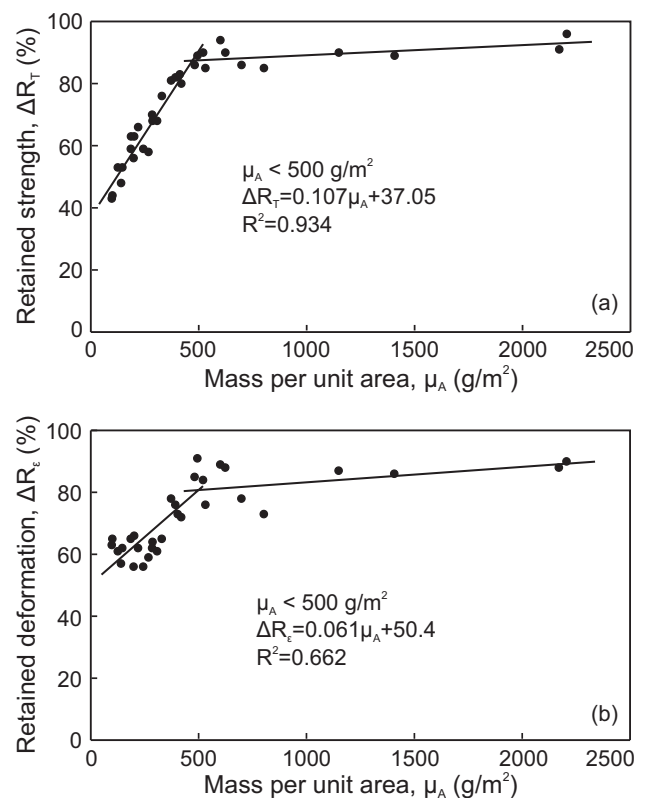


Figure 3. Correlation between geotextile mass per unit area and retained (a) tensile strength, (b) failure deformation.

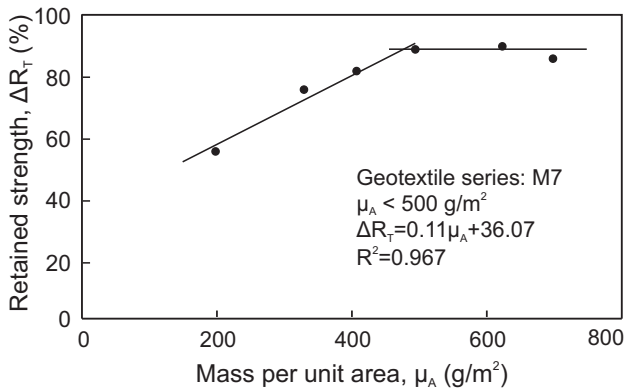


Figure 4. Typical results per geotextile series.

Five geotextiles, representative of the whole group, were further tested in order to evaluate the effect of the number of load cycles and aggregate hardness on the induced damage. As shown in Figure 5, in terms of retained strength, the induced damage increases by increasing the number of load cycles. However, when half (100 cycles) of double (400 cycles) the standard number of load cycles (200) is applied, the effect on damage index values is not proportional. On the average, an increase of the damage index by 4% and a decrease by 7% was obtained when 100 and 400 cycles, respectively, were applied. Accordingly, the specification of 200 load cycles appears to be reasonable.

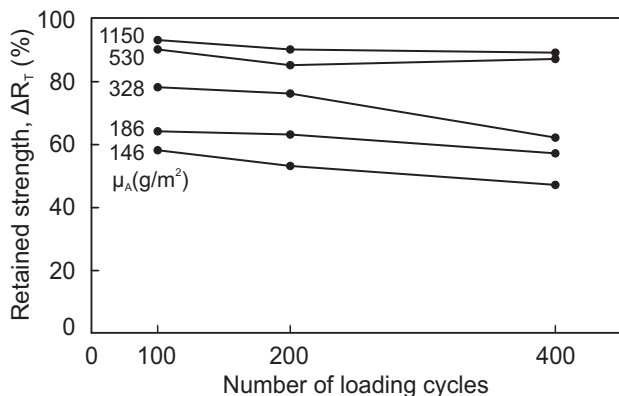


Figure 5. Effect of number of loading cycles on retained tensile strength.

Shown in Figure 6 are the results obtained when the five representative geotextile samples were tested with aggregates having different hardness values, as expressed by the Los Angeles abrasion coefficient. It can be generally observed that decreasing aggregate hardness results in increasing percentage of the retained reference properly value (reduced damage). However, it should be noticed that while the Los Angeles coefficient was increased from 11 to 16 and 26 (45% and 136% increase respectively) the resulting improvement of the damage index was, on the average, only 8% and 9%, respectively. This observation indicates that aggregate hardness by itself is not a good indicator of damage potential.

4 REDUCTION FACTORS

Installation damage strength reduction factors are recommended by Koerner (2005) for eleven different areas of application. The minimum recommended value is equal to 1.1 (1.5 for filtration/separation in railroads) and refers to applications with relatively short service lifetimes and/or cases where creep is not critical to overall performance. The maximum values recommended by Koerner (2005) range between 1.5 and 2.5 (3.0 for railroads). The FHWA (Elias 2001) recommends a range of installation reduction factors between 1.4 and 2.5 when aggregate with $d_{max} < 102\text{mm}$ and $d_{50} \approx 30\text{mm}$ is used, while for finer aggregate ($d_{max} < 20\text{mm}$ and

$d_{50} \approx 0.7\text{mm}$) the recommended values range between 1.1 and 1.4. Based on results of field tests on 83 nonwoven geotextiles, Hufenus et al. (2005) recommend values ranging from a minimum of 1.1 to 1.2 to a maximum of 1.8 to 2.1 depending on aggregate and compaction equipment characteristics.

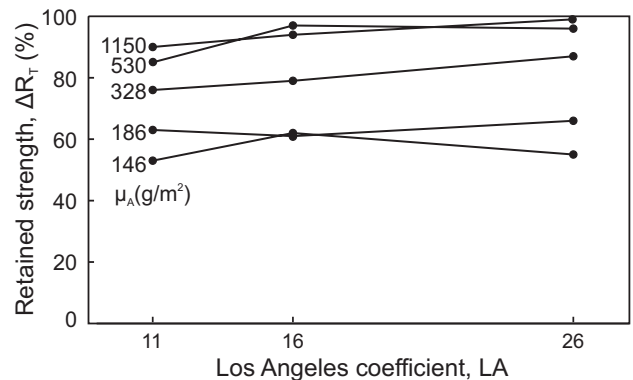


Figure 6. Effect of aggregate hardness on retained tensile strength.

The damage index values obtained for all geotextiles tested during this investigation, were used to compute the corresponding reduction factors, for damage during installation (inverse of damage index when expressed as a decimal number). For geotextiles with mass per unit area over 500g/m^2 , the reduction factor values range between 1.05 and 1.20 while for geotextiles with lower mass per unit area they range between 1.20 and 2.10. It can be observed that the results obtained from the investigation reported herein are in very good agreement with the recommended values. It should be noted, however, that available recommendations do not classify or evaluate geotextiles according to their physical and/or mechanical properties and this may result in the application of similar values for the reduction factor for either light or heavy geotextiles.

5 CONCLUSIONS

Based on the results obtained and the observations made during this investigation, the following conclusions may be advanced for the installation damage of nonwoven polypropylene geotextiles:

1. The mass per unit area of the geotextiles can be used as an indicator of installation damage potential.
2. Damage index values obtained in terms of retained wide-width tensile strength are well correlated with the mass per unit area of the geotextiles.
3. The effect of installation damage is not significant for geotextiles with mass per unit area over 500g/m^2 .
4. The number of load cycles specified by standard ENV ISO 10722-1 is reasonable and there is no reason for significant deviations from this number.
5. The Los Angeles coefficient value of the aggregate used to conduct the standard test is not, by itself, a good indicator of potential damage.
6. Existing recommendations provide a realistic range for installation damage reduction factors but specific values should be selected taking into account geotextile physical or mechanical properties.

ACKNOWLEDGEMENTS

The contribution of Mr. A. Parasyris and Mr. E. Polyviou in conducting some of the laboratory tests is acknowledged. The following manufacturers provided large size samples:

Fibertex, Geofabrics, Bonar, Thrace Plastics, Synthetic Industries, Naue Fasertechnik.

REFERENCES

Elias, V. 2001. Corrosion/degradation of soil reinforcements for mechanically stabilized earth walls and reinforced soil slopes, FHWA-NHI-00-044, Federal Highway Administration, Washington, USA.

Hufenus, R., Ruegger, R., Flum, D. & Sterba, I. 2005. Strength reduction factors due to installation damage of reinforcing geosynthetics, *Geotextiles and Geomembranes*, Vol. 23, pp.401-424.

Koerner, R.M. 2005. *Designing with Geosynthetics*, Pearson Prentice Hall, New Jersey, U.S.A.

Naughton, P.J. & Kempton, G.T. 2002. In service performance of geotextile separators, Proceedings of the 7th International Conference on Geosynthetics, Nice, France, 22-27 September, Vol. 4, pp. 1505-1508.

Paula, A.M., Pinho-Lopes, M. & Lopes, M. 2004. Damage during installation laboratory test. Influence of the type of granular material, Proceedings of the 3rd European Geosynthetics Conference, Munich, Germany, 1-3 March, Vol. II, pp. 603-606.

Geotechnical investigation and seismic analysis of underground monuments in Alexandria, Egypt

Investigations géotechniques et analyses séismiques des monuments souterraines en Alexandrie, Egypte

K. Pitilakis & S. Bandis

Department of Civil of Engineering, Aristotle University of Thessaloniki, Greece.

S. Hameda

Faculty of Archaeology, Cairo University, Giza, Egypt

ABSTRACT

Modern underground structures (i.e. tunnels) are less vulnerable to seismic actions than above ground structures. However underground monuments like tombs and catacombs, present certain construction and geometrical particularities that make them quite vulnerable, both in long term static and especially under seismic conditions. The analysis of the stability of these complex monuments under static and strong seismic loading, together with other factors affecting material strength (rising water level, aging and weathering), are the key factors for the efficient restoration and retrofitting of these underground monumental structures. The paper presents the geotechnical, geophysical investigations and the numerical static and seismic analysis of selected underground monuments in Alexandria, Egypt i.e. the Catacombs of Kom El-Shoqafa, El-Shatbi Necropolis and the Necropolis of Mustafa Kamil.

RÉSUMÉ

Les structures souterraines (tunnels etc.) sont généralement moins vulnérables aux séismes que les bâtiments. Catacombes et autres monuments souterraines sont au contraire assez vulnérables, due aux particularités géométriques, et structurales des ces constructions antiques. L'analyse fiable de la stabilité statique et séismique, avec quelque autres facteurs qui influent la résistance en long terme des matériaux formant la structure des catacombes, sont les éléments clés pour tous travaux de restauration. L'article présente les résultats principaux des études géotechniques, géophysiques et des analyses numériques faites sur quelques catacombes en Alexandrie de l'ère Hellénistique et Romaine, afin d'estimer leur pathologie sous conditions statiques et séismiques en vue d'évaluer la stratégie appropriée de restauration.

Keywords: underground monuments, geotechnical investigation, 2D-3D static analysis, seismic analysis, microtremors

1 INTRODUCTION

Ancient monuments and archaeological sites need special protection particularly in seismic-prone regions like the Mediterranean basin, with very active seismotectonic regime and complex geological, geotechnical conditions.

The Greek-Roman catacombs in Alexandria and in other places in this region meet these geo-environmental conditions. The geological formations where most catacombs were excavated is a soft rock, which forms the basic construction material of these monumental exceptional structures.

In the present paper, we present in a first phase a comprehensive geotechnical survey undertaken in the three archaeological sites, comprising geophysical ambient noise measurements (microtremors), as well as field and long-term laboratory experiments and tests, in order to define the physical, mechanical and dynamic properties of the soils and soft rock materials. In the second stage, we present the main results of the detailed static and seismic numerical analysis of these underground monumental structures (catacombs). The aim of the paper is to evaluate the pathology of these structures in view of their future restoration processes.

The seismic analysis is performed considering adequate seismic scenarios corresponding to the seismotectonic features of Alexandria. Advanced soil-rock elastoplastic modeling has been used through out the different phases of the numerical finite element analysis.

The particular aim of the study and the analysis is twofold: (a) to investigate the safety margins of the existing monuments, under their present conditions, against environmental (i.e. weathering, aging, rise water level, lack of preservation and maintenance) and extreme seismic loads and (b) to investigate the potential improvement of their global behavior applying specific retrofitting techniques.

The work presented herein may be considered as a preliminary pilot study to assess the pathology of underground monumental structures, like catacombs, in a particularly unfavorable environment, exposed to considerable weathering, aging, human and seismic activity. An efficient restoration and retrofitting of these historical monuments must be based on a well documented and constrained assessment of the pathology.



El-Shatbi Necropolis

Catacombs of Kom El-Shoqafa

Figure 1. Some underground monuments in Alexandria, (present state).

2 GEOTECHNICAL SURVEYS AND TESTS (FIELD AND LABORATORY TESTS)

The results from geotechnical surveys comprising sampling and SPT measurements indicated that the Catacombs of Kom El-Shoqafa and Amod El-Sawari sites which in the centre of the city, 2.5 kilometres from the sea shoreline, are excavated in oolitic sandy limestone (calcareous cemented sand); it is yellowish white massive, fine to medium grained cross-bedded sandstone cemented with calcareous cement and intersected conjugated joints filled with very fine friable sand saturated with water in the lower parts. This unit is underlined by loose calcareous sandstone. It is a brownish medium to fine grained calcareous limestone over saturated with ground water. It overlies the El Hagif formation (Pliocene) or the older Miocene (El-Fouly, 2000). Surface quaternary deposits obscure actual contact. The other two archaeological sites, which are close to the shoreline of Alexandria (El-Shatbi Necropolis, Mustafa Kamil Necropolis) are excavated in oolitic intraclastic or calcarenitic limestone (coastal ridge) (yellowish white upwards becoming brownish yellow downwards).

Measured uniaxial compressive strength (UCS= 2-3 Mpa) suggest that according to the classification adopted by the Geological Society of London (1970), which based on unconfined compression strength, and the classification proposed by (ISRM, 1981), these calcarenitic rocks of the underground monuments, are classified as weak to very weak soft rocks, with high deformability. Also the (RQD) rock quality designation system for these soft rock is RR=18 and RQD=15 -20 % with a very poor quality range from 0 to 25. In addition, the results of the static deformability tests conclude that the rocks types under investigation are characterized of high deformability.

Three stages in creep behaviour have been recognized from the uniaxial and triaxial creep tests; in the first one, denominated by primary creep, strain occurs at decreasing rate. Under certain conditions, the primary creep curve approximates a steady rate of strain, called secondary creep.

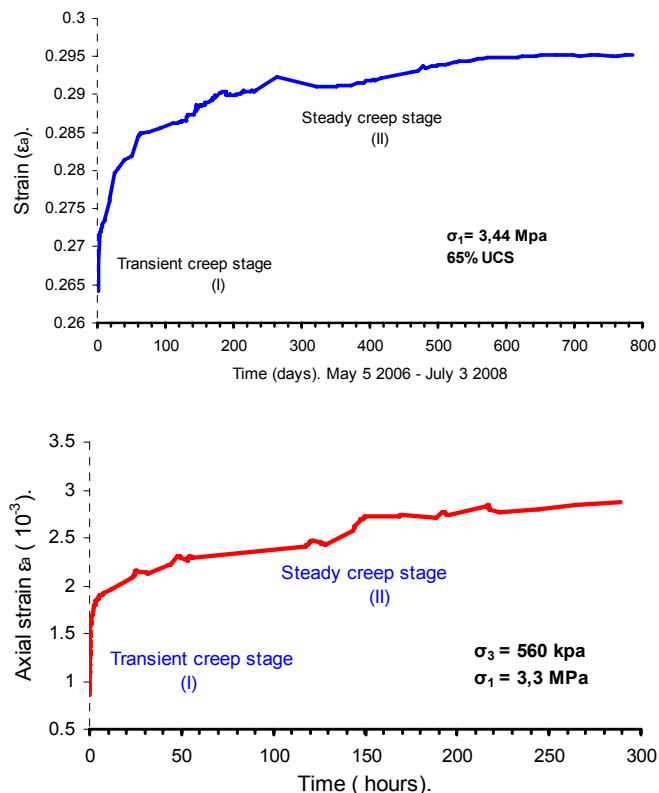


Figure 2. El-Shatbi Necropolis: Strain-versus-time uniaxial and triaxial creep tests.

3 GEOPHYSICAL TESTS - AMBIENT NOISE MEASUREMENTS

Array microtremor measurements have been carried out to define the shear velocity profile at the three archaeological sites. The ReMi method (Louie, 2001) has been used and the estimated Vs profile is given in Figure (3), (Hemeda, 2008).

The obtained shear wave seismic velocities show a relatively high shear wave velocities ranging between 200 m/s to 1600 m/s. (Figure.3) It is clear that the ground conditions were the underground monuments in Alexandria are excavated cannot be classified as real rock at least close to the surface (<6m) where the weathering is very important.

4 DURABILITY ASPECTS OF ANCIENT CONSTRUCTION MATERIALS OF THE ARCHAEOLOGICAL SITES

Different tests have been made to assess the durability aspects and the weathering impact on the bulk structure of the rock mass used as construction materials. The following set of mineralogical analyses has been performed for the soft rock and other construction materials.

- X-ray diffraction
- Thermal analyses DTA&TGA
- X-ray Fluorescence analysis
- Chemical analyses (for plaster and painting layers collected samples)

Site-3: Vs Model

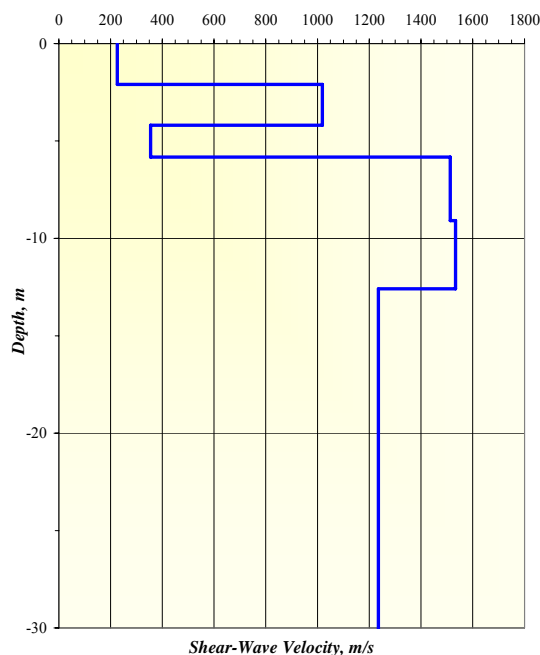


Figure 3. Vs model in El-Shatbi archaeological site.

- Transmitted plane polarized light (for the collected rock samples).
- Scanning electron microscopy (SEM), attached with EDX Microprobe (energy dispersive X-ray) microanalyses.
- Porous media characterization for weathered and sound rock samples.
- Pore size measurement and Specific surface area by nitrogen BET-TPV.
- Determination of the specific surface area (SSA).
- Grain size characteristics of the weathered (salt contaminated) rock samples.
- Saturation coefficient, S.
- Capillary water uptake measurements.

The soft rock where the subterranean monuments in Alexandria have been excavated (oolitic intraclastic, calcarenitic and oolitic sandy limestone), have an important intrinsic sensitivity to weathering factors especially the underground water and salt weathering effects. The infiltration of the underground water through the porous rock is one of the main problems of the underground monuments in Alexandria. The weathering process is linked to the textural characteristics, like poor geotechnical properties, chemical carbonated composition, and presence of soluble salts in the porous system, marine climate with characteristic humidity and marine spray, and underground water. The durability of the rock is moderate to low due to its high free silica content. The durability of the calcarenitic and sandy oolitic limestone is found to be low (Hemeda et al, 2007).

5 PRELIMINARY 2D- STATIC NUMERICAL ANALYSIS

The results from the 2D static analysis (using PLAXIS) of a typical cross section, of the catacombs of Kom El-Shoqafa, (Hemeda, 2008), indicated (Fig, 4) that the maximum ground displacements above the catacombs were small (of the order of $1.13 \cdot 10^{-3}$ m), but some rock columns and piers are under relatively high vertical compression stresses. The peak vertical effective compressive stresses on the most critical rock pier are equal to $-1.42 \cdot 10^3$ KN/m².

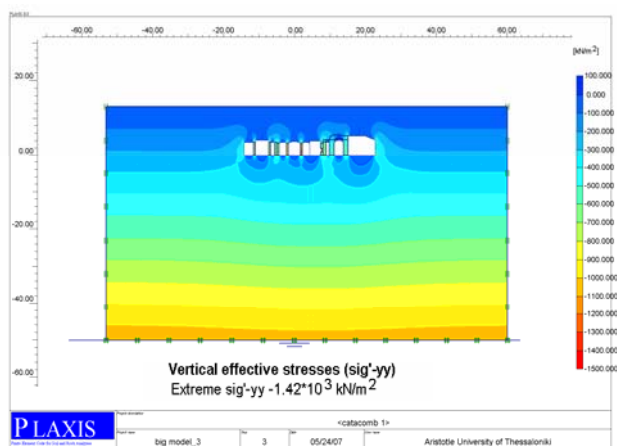


Figure 4. Typical 2D Static numerical analysis of Catacombs of Kom El-Shoqafa (use of PLAXIS).

The static analysis of a typical cross section in Mustafa Kamil tomb 1, indicated that the ground displacements were of the order of $135 \cdot 10^{-6}$ m, and the peak horizontal displacements $U_x = 52 \cdot 10^{-3}$ m. However, some rock columns and piers are under relatively high vertical compression stresses (i.e. -416 KN/m^2).

In the Mustafa Kamil tomb 2, the ground displacements were of the order of $703 \cdot 10^{-6}$ m, while some rock columns and piers are under relatively high compression stresses. The peak vertical effective compressive stresses is equal to $-1 \cdot 10^3 \text{ KN/m}^2$.

In the Eastern side of El-Shatbi Necropolis the ground displacements were very small (of the order of $86 \cdot 10^{-6}$ m), but the ceiling and the sidewalls of the entrance are under relatively high compression stresses. The peak vertical effective compressive stresses = -613 KN/m^2 .

In the Western side of El-Shatbi Necropolis, the ground displacements were very small (of the order of $626 \cdot 10^{-6}$ m), but the ceiling and the sidewalls of entrance are under relatively high compression stresses. The peak vertical effective principal compressive stresses = -614 KN/m^2 .

6 3D STATIC NUMERICAL ANALYSIS

The results from the detailed 3D static analysis indicated that the vertical ground displacements above the rotunda of the Kom El Shoqafa catacomb were small (maximum vertical displacements of the order of 2.6 mm to 3 mm in the whole domain); the peak horizontal displacements are calculated equal to 1.0 mm. Some rock piers were found under relatively high

Compression stresses (Figure 5). The calculated peak effective principal vertical compressive stresses on supporting rock pillars is $-1.74 \cdot 10^3 \text{ KN/m}^2$ and the calculated peak effective principal tensile stress is 200 KN/m^2 . The factor of safety of the most critical rock pillar is 1.47, where the acceptable safety factor should be higher than 1.6. Also the overstress state is beyond the elastic regime.

7 SEISMIC ANALYSIS OF SELECTED UNDERGROUND MONUMENTS IN ALEXANDRIA

The under study underground monuments in Alexandria are essentially 2D/3D structures, which has to be modeled accordingly. In the present study, we have modeled the complex catacombs and other tombs in 2D, assuming an equivalent plane strain approach and applying the PLAXIS b.v. 8 with different seismic scenarios, corresponding to the seismotectonic features of Alexandria. Advanced soil-rock elastoplastic modeling has been used. Extensive time domain parametric analysis were performed in order to examine the

response of the Catacombs subjected to seismic motions with different amplitudes of ground motion and different frequency content. (Kalamata, Greece, 1986, Erzincan, Turkey, 1992, Aqaba, Egypt, 1995). The analysis takes into account the complex behavior of the structure with the aim to determine the threshold PGA and the corresponding developed stresses, which should remain lower than the actual strength of different elements composing the catacombs.

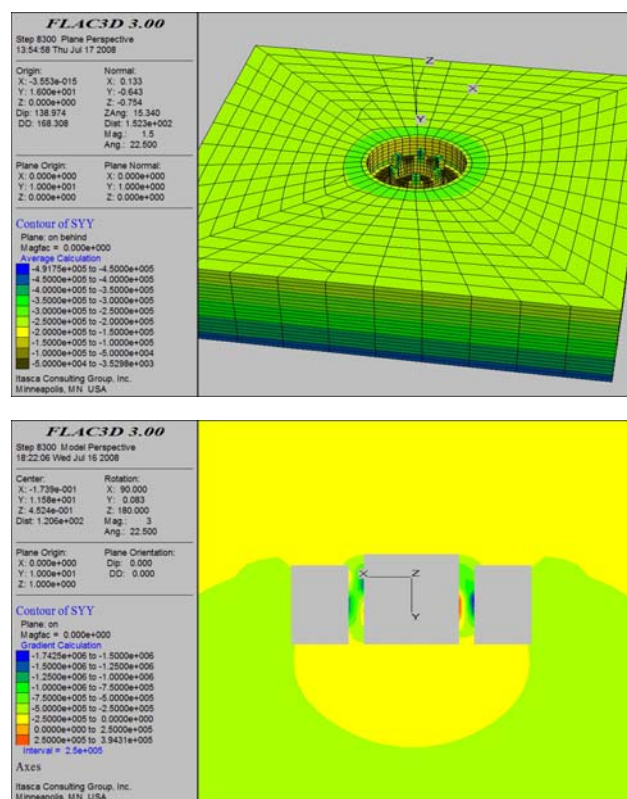


Figure 5. 3D Static numerical analysis of Catacombs of Kom El-Shoqafa. (FLAC 3D).

Figure 7 presents the calculated shear stresses for the three seismic scenarios and different input time histories in the most critical pier of the Catacombs of Kom El-Shoqafa. Considering the available strength of the rock pier the numerical analysis proved that the this critical pier is safe for PGA values lower than 0.10g, which is low for the actual seismic activity and the past seismic history of the city. Retrofitting and strengthening is hence necessary.

The seismic analysis of Mustafa Kamil Necropolis, Tomb number 1, proved that the rock piers, which are the most vulnerable parts of the whole complex, present a sufficient safety margin for PGA values lower than 0.24g in case of the Kalamata and Erzincan earthquakes and $\text{PGA} = 0.14 \text{ g}$ for the Aqaba seismic scenario. For the tomb number 2 the most critical piers are safe for PGA values lower than 0.24g in case of the Erzincan earthquake and $\text{PGA} = 0.16 \text{ g}$ for the Kalamata seismic scenario. In addition, PGA values lower than 0.08g in the case of Aqaba earthquake.

Finally the seismic analysis of El-Shatbi Necropolis proved that the ceiling and sidewalls of the excavations, which are the most vulnerable parts, have a sufficient safety factor for PGA values lower 0.24g in case of the Erzincan earthquake, 0.16g in the case of Kalamata earthquake, and 0.15g in the case of Aqaba earthquake scenarios. In another cross section no.2 proved that the ceiling and sidewalls of the excavations, which are the most vulnerable parts, are rather safe until PGA values 0.24g in case of the Kalamata, Erzincan and 0.16g in the case of Aqaba earthquake scenarios.

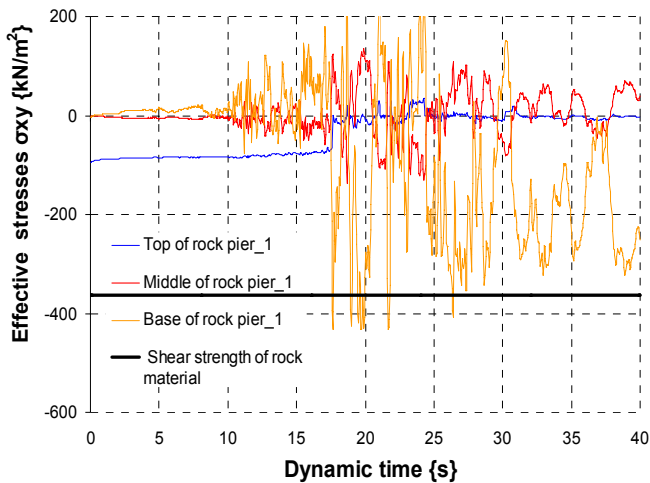


Figure 6. Effective shear stresses σ_{xy} - time histories for the most critical rock Pier_1, Catacombs, Aqaba RQ. The PGA value = 0.24g.

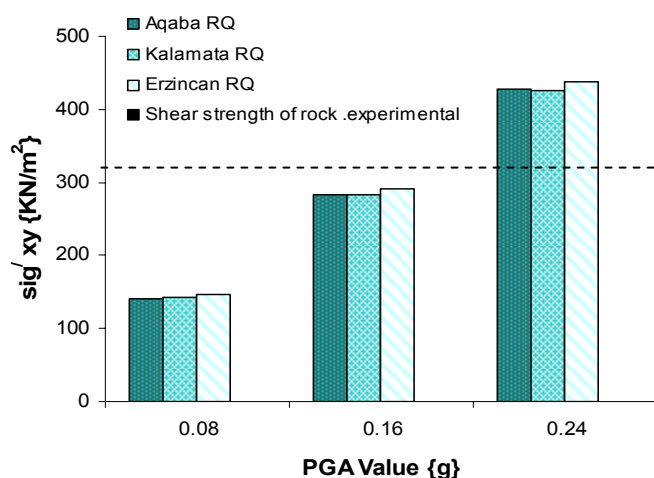


Figure 7. Maximum effective shear stresses σ_{xy} on the base of rock pier_1, for Aqaba, Erzincan, and Kalamata earthquakes, scaled to several values of PGA.

According to the Global Seismic Hazard Assessment Program, 1999 the seismic hazard analysis in Egypt gives in Alexandria a PGA of the order of 0.16g with 475 years mean return period. Considering this fact, the seismic analysis of the three above mentioned underground monuments in Alexandria, proved that for the expected PGA values in Alexandria,, some critical parts of these vulnerable underground monuments (rock piers), present low safety factors and they cannot sustain the induced seismic loading without appropriate strengthening.

8 CONCLUSIONS

A short overview of the static and seismic safety of three underground archaeological sites and underground monuments in Alexandria, Egypt is presented.

Laboratory and field measurements proved that the strength of the calcarenitic and sandy limestone, where the underground monumental structures are excavated, is low; it is also measured that the RR=18 and RQD=15 -20 % while quality ranges from 0 to 25 which is very poor. In addition, the results of the static deformability tests suggest that the rocks types under investigation are characterized with high deformability and low durability.

The shear wave seismic velocities calculated in the three sites with array microtremor measurements show a range of shear wave velocities varying between 200m/s to 1600 m/s indicat-

ing a rather high rock weathering at least close to the surface.

Considering all other affecting factors and the specific geometry of the catacombs this low rock strength affects seriously the safety of these catacombs both under static and seismic loading conditions.

The results from the 2D and 3D static analysis indicate that the horizontal and vertical ground displacements above the rotunda (Catacombs) are small (1.0 to 3.0mm). Some rock piers are under relatively high compression stresses. The calculated peak effective principal vertical compressive stress is equal to $-1.74 \cdot 10^3$ KN/m². The calculated peak effective principal tensile stress is 200 KN/m² and the factor of safety of the most critical rock pillar is $1.47 < 1.6$ which is considered an acceptable safety factor. Also the overstress state is beyond the elastic regime.

The seismic analysis of these underground monumental structures for three seismic scenarios of different PGA values, proved that for $PGA > 0.10g$, which is rather low considering the seismic activity and the past seismic history of the city, there are some critical supporting parts of these catacombs structures (i.e. rock piers and columns) that are not safe, and in general, the catacombs need considerable strengthening.

In conclusion the detailed analysis of the catacombs in Alexandria proved that these important underground monuments present low safety factors for both static and seismic loading and consequently a well focused strengthening and retrofitting program is deemed necessary.

ACKNOWLEDGMENT

The authors are grateful to Dr E. Bakasis., Dr D. Pitilakis for their helps and fruitful remarks.

REFERENCES

- El-Fouly, A.A. 2000. Voids Investigation at Gabbari Tombs, Alexandria, Egypt using Ground Penetrating Radar Techniques. ICEHM2000, Cairo University, Egypt. pp 84.
- Hemeda, S., Pitilakis, K., Bandis, S., Papayianni, I., and Gamal M. 2007. The Underground monuments (Catacombs) in Alexandria, Egypt. Proceedings of the 4th International Conference on Earthquake Geotechnical Engineering", Thessaloniki, Greece, 25-27 June. pp. 715- 738.
- Hemeda, S. 2008. An integrated approach for the pathology assessment and protection of underground monuments in seismic regions. Application on some Greek-Roman monuments in Alexandria, Egypt. Ph D thesis, Aristotle University of Thessaloniki, Greece.
- Louie, J.N. 2001. Faster, better: "Shear-wave velocity to 100 meters depth from refraction microtremors arrays". BSSA, 91, pp 347-364.

Experiences from the installation of geotechnical instruments in dams

Expériences par l'installation des instruments géotechniques dans des barrages

Z.R. Papachatzaki
National Technical University of Athens, Greece
K.Anastasopoulos, C.Oikonomidis & S.Siachou
Public Power Corporation, Athens, Greece
G. Dounias
Edafos S.A., Athens, Greece

ABSTRACT

The paper presents experience gained with geotechnical instruments installed in several Greek dams that were built during the last few decades. The encountered problems and the applied practices are addressed. A list of many issues faced during installation and operation, according to the instrument type, is presented. Proposals are made in order to improve instrumentation practice.

RESUME

Ce papier présente les expériences obtenues par l'installation des instruments géotechniques dans plusieurs barrages grecs, construits pendant les dernières décennies. Les problèmes rencontrés et les pratiques appliquées se sont rapportés. Une liste des plusieurs cas affrontés pendant l'installation et l'opération est présentée, selon le type des instruments. Des propositions sont faites pour améliorer la pratique d'instrumentation.

Keywords: geotechnical instruments, dams

1 INTRODUCTION

Dam engineers are aware of problems associated with malfunctions of geotechnical instruments installed in dams, which have in some cases led to false alarms, or, even worse, failed to provide early warnings about developing instabilities. Most of these problems could have been avoided if the whole procedure (design, installation and monitoring) did keep in line with guidelines provided by the manufacturer, as well as by the technical literature available [Dunicliff, 1993; USBR, 1987; ICOLD bulletins].

This paper presents in brief some of the problems concerning instrumentation, encountered in several earth and rockfill dams that were erected recently in Greece. The current practice is discussed, and, where appropriate, proposals are made on how to improve current practice.

2 PROBLEMS AND PROPOSALS

Table 1 presents important issues to be addressed for various measuring devices. A reference code is being assigned to each case that is commonly a source of problems, with the first letter referring to the relevant project phase (i.e. design, installation or operation).

2.1 Design Phase (D)

Most of the problems encountered could have been avoided by careful consideration, during the design, of every aspect of instrument installation and operation. The following present some broad guidelines on the design of dam instrumentation:

- Instruments should be placed in order to measure parameters critical for dam safety at places of specific interest, taking into account the size and importance of the project and the ground conditions. Instrumentation should be oriented towards providing answers to specific questions concerning dam safety, and not just proving the validity of well-established geotechnical theories (Peck, 2001).

- Instrument placement is often a nuisance during construction. The instrumentation layout has to be simple and robust. When possible, instruments that obstruct construction should be avoided.

- The number and type of instruments placed should conform to the human resources (number and training of the personnel) available on site during construction and operation.

The aforementioned principles may apply into the design practice as follows:

Specifying the instrument type necessitates the estimation of the minimum and maximum values to be recorded (pore pressure, deformation, settlement etc). The measuring range usually also dictates the accuracy/sensitivity (**D1**). The range of interest during construction may differ from that during dam operation. At Papadia dam (67m high rockfill dam), a 35m deep cut-off diaphragm wall (D/W) was constructed under the dam core in pleio-pleistocene deposits down to the sound bedrock. Numerous vibrating wire piezometers were installed in order to monitor pore pressures developing in the foundation during reservoir filling and project operation. However, pumping tests were performed in order to test the water tightness of the D/W, before fill placement. During these tests a significant number of the instruments provided erratic data (Fig. 1), necessitating cross-checking of their records by installing several new standpipe piezometers and repeating the pumping tests.

The erratic measurements were mainly attributed to the fact that the pore pressure values were close to the sensitivity of the vibrating wire piezometers, since their measuring range and sensitivity was selected to conform to the high head conditions established in the foundation after reservoir filling. A better choice would have been to provide two groups of vibrating wire piezometers: one with a low range to assess the effectiveness of the D/W, and another with a high range to provide information during first filling and operation.

Selection of the suitable piezometer type is also a matter of debate (**D2**). Vibrating wire piezometers tend to be more and more popular, but their use is not always justified.

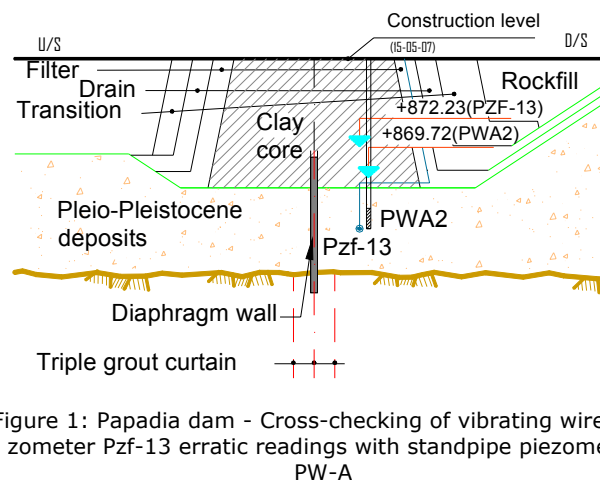


Figure 1: Papadia dam - Cross-checking of vibrating wire piezometer Pzf-13 erratic readings with standpipe piezometer PW-A

In the case of the 21m high Aghia Barbara earthfill dam on a permeable foundation, the design provided for a number of vibrating wire piezometers, in the foundation. As variations of the water table after construction were anticipated to be rather small, and having in mind the Papadia experience, it was decided during construction to replace vibrating wire by standpipe piezometers. The performance of these piezometers was proved to be very successful, adequately recording water table fluctuations during reservoir first filling and operation and providing useful information for the effectiveness of the cement-bentonite diaphragm wall in the foundation.

Table 2: Important issues to be addressed for various measuring devices

	Flow measuring weir	Vibrating wire piezometers	Open standpipe piezometers	IDEL instruments	Inclinometers	Strong motion recorders	Settlement Gauges	Extensometers	Surface monuments	Load Cells
Instrument range and sensitivity (D1)		•		•		•	•	•		•
Selection of instrument to measure pore pressures (D2)		•	•							
Selection of Measuring settlements in the dam core (D3)				•			•			
Grouting for stabilisation (D4)			•		•	•		•		
Grouting for water sealing (D5)		•	•							
Avoiding cable couplings (D6)		•					•			
Stable anchoring (D7)						•			•	
Safe access and protection (D8 a & b)	•	•	•	•	•	•	•	•	•	•
Succession of construction works (D9)		•	•	•	•		•	•	•	•
Selecting instrument material (D10)			•	•	•					
Protective ARMCO type pipes (D11)		•				•				
UPS provision (D12)						•				
Anti-lightning protection (D13)		•				•				•
Use of telescopic couplings (D14)				•						
Protecting casings in rockfill (D15)				•						
Scheduling measurements (D16)	•	•	•	•	•	•	•	•	•	•
Installation record, labelling and signalling (I1)		•	•	•	•	•	•	•	•	•
Verticality of installation (I2)				•						
Referencing instrument to a stable point (I3)				•						
Ensuring water tightness (I4)		•	•							
Avoiding reading errors (Om1)	•	•	•	•	•	•	•	•	•	•
Attributing measurements to the correct instrument (Om2)		•					•	•		•
Avoiding errors in piezometer measurements (Om3)		•								
Avoiding effects of traffic on measurements (Oa1)									•	
Provision of assessment software (Oa2)				•	•					
Assessment assumptions (Oa3)				•						

Seepage is probably the most critical parameter concerning dam safety and operation and the simplest and most reliable way to measure it is by means of collector pipes and measuring weirs (Peck, 2001). These devices can provide very important information (such as the exact quantity of seepage through the dam and foundation, the clarity of the seeping water etc.) and should be installed in every dam. In Smokovo (rockfill dam, 109m high), a measuring weir was not provided by design. The embankment was built 5 years before first filling, and skepticism was expressed concerning dam safety, mainly due to inadequate construction records available. A seepage measuring weir was deemed necessary and was constructed right before reservoir filling, providing confidence during first filling.

When measurement of vertical settlements in the core is considered of paramount importance (D3), settlement gauges (hydraulic or other type) might be a safer, although more expensive, solution than combined inclinometer – settlement gauges (referred to herewith as IDEL instruments). At Ilarion (a 130 m. high earthfill – rockfill dam), where both types of instruments (IDEL - hydraulic settlement gauges) were placed close to each other, settlements recorded were quite similar. Leakage paths may form along the IDEL casings, due to inadequate compaction around them (Peck, 2001; Dunicliff, 1993). If such instruments are damaged and inoperable, it is better to fully plug them with suitable grout before filling the reservoir.

Drawings and specifications should include details and instructions to ensure correct installation. Efficient

grouting around instruments installed in boreholes is essential; otherwise gaps may permit ravelling or collapse of the borehole walls, resulting in deformations and false records (D4). Unreliable records of movements in inclinometers, of the zigzag pattern depicted in Figure 2, are quite often (here from the abutments of Thissavros, a 172m high rock-fill dam). When installing these instruments in highly disturbed rock, pre-grouting the hole, re-drilling and water testing should be the recommended practice.

For nested piezometers (multiple piezometers installed in one borehole), insufficient grouting means insufficient sealing of each piezometer tip, leading to identical readings (D5).

In order to avoid this, each instrument can either be placed in a separate hole or, for diaphragm type piezometers, the fully-grouted method (Dunicliff, 2008) can be applied. The effectiveness of the traditional method of sealing with bentonite pellets above the sand-pack is lately disputed especially in jointed rockmasses, due to the tendency of the bentonite pellets to arch part-way down the borehole.

To avoid couplings in electrical piezometers cables and hydraulic settlement gauges tubes and minimise bends, cable and tube routes and the total length for each individual instrument should be clear in the drawings (D6).

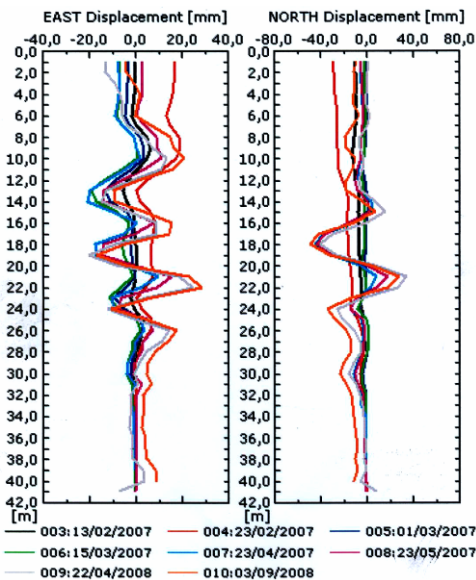


Figure 2: Typical inclinometer deformation pattern indicating inadequate grouting around the casing

In order to give reliable measurements, surface monuments and in particular strong motion recorders need a stable foundation, preferably anchored (**D7**).

Access roads and facilities for the measuring crew (as well as to a buggy, if necessary) must be ensured in the design (**D8a**). On the other hand, instruments should be, as far as possible, not easily detected or accessible by unauthorized people, in order to be protected against vandalism. Moreover, the location of the instruments should be safe against natural hazards (rockfalls, slides etc - **D8b**).

The time of installation must also be clearly specified particularly in relation to works that might harm them (**D9**). At Papadia dam, the additional grouting that had to be done close to installed vibrating wire piezometers, resulted in destroying some of them.

Instrument materials may also be critical and should be specified in the design (**D10**). Plastic tubes and casings were found generally preferable to metallic ones, since they are more durable, lighter, more flexible and easier to install or remove (if re-drilling of the hole is needed). They have, though, to be protected against rodents attack. Aluminium inclinometer casings were subject to corrosion attack problems, either by groundwater or by cement grout. At This-savros dam, corrosion of aluminium casings close to the water table occurred a few years after instrument installation. At Smokovo dam, the aluminium casings were destroyed so quickly that no measurements were ever taken.

Vertical instrument cables must be placed in segmental corrugated pipes (ARMCO type), preferably coming in nestable half sections (**D11**). The diameter of these riser pipes depends partly on the number of cables, but should be large enough to be filled with sand and to resist excessive deformations.

Strong motion recorders should be provided with UPS, as the memory of the recorder fills up in case of successive power supply interruptions (**D12**). All electrical instruments have to be protected against lightning during construction and operation of the project. A number of malfunctions in vibrating wire piezometers (Loutros, a 50m high rockfill and Papadia dams) have been attributed to that reason (**D13**).

For IDEL instruments telescopic couplings are preferable, since they provide better guidance for the wheels of the measuring probe in the slots and allow higher settlements without casing breakage (**D14**). Settlement collars should

be placed right below the couplings, allowing free sliding, compatible with the settlements of the fill. Malfunctions due to inadequate available sliding margins have been recorded in Messochora (a 150m high CFRD dam) and Evinos (a 126m high earthfill dam). In the latter case, all casings in the core broke at almost the same elevation, probably under the same strain conditions.

The casings of IDEL instruments placed in rockfill have to be well protected by enveloping the casing with several co-centric filter layers, with gradually increasing particle sizes (**D15**), a difficult task as it has to be done by hand. Moreover, metallic cross-arms of a significant length must be attached to the settlement collars, well embedded in the fill, so that the settlements measured should be that of the embankment and not of the filter column surrounding the casing.

The frequency of measurements should be defined by the design, as well as by the alert-alarm limits for every instrument (**D16**). The frequency of measurements should be adjusted so that production of big volumes of data, and the consequent demand for assessment, is avoided. The decision on the provision of an automated data acquisition system must be made by considering, among other factors, the human resources available and the number and importance of instruments to be monitored. These systems are still very sensitive and set false alarms, but their advantages with respect to continuous time-histories, real time monitoring and low operational cost, will render them common practice in the near future.

2.2 Installation phase (I)

The installation of instruments should be done according to the design and the instructions of the manufacturer, under close supervision and in cooperation with the design team. Where practicable, the manufacturer should train the personnel and supervise installation. Instruments installed in the dam body, and in particular in the core of embankment dams, should be placed with great care, since their restoration or even replacement in case of malfunction is much more difficult and in some cases not possible.

A detailed installation record should be kept for each instrument. Immediately after installation, instruments should be named for future reference (this holds especially for extra instruments, not provided by the original design), be properly labelled, marked and protected, in order to avoid damages by the construction plant (**I1**).

IDEL instrument casings, which are raised with the fill, should be kept as vertical as possible during installation (**I2**), in order to prevent bending due to the unavoidable deformations that occur during fill construction. In the case of Ilarion dam, the significant deviation from verticality rendered them, very soon, impossible to measure. Moreover, the precise coordinates (x,y,z) of each new settlement collar should be recorded immediately after installation, with reference to a stable positioning monument, well outside of the dam body. This helps greatly if the IDEL instrument casing is sheared or obstructed at some intermediate point, making the lowest magnetic plate (which is usually taken as a reference point) not accessible (**I3**). Malfunctions of this type were recorded in several dams (i.e. Messochora, This-savros, Gradini, and, more recently, Ilarion and Papadia).

It is essential to stop precipitation and surficial water from entering the piezometer tube in standpipe piezometers (**I4**). This is the case if the instrument head is not well isolated (not embedded in concrete or when the casing is not protruding adequately out of the soil). Careful filling of the annulus between the borehole and the casing with cement mortar or grout, up to the very top is also essential.

2.3 Operation phase(O)

2.3.1 Measurements (Om)

Erroneous readings are a common problem. If recording "manually", measurements should be double-checked and compared to the latest ones, when on site. Usually, readings are not expected to greatly vary without good reason, this being more so after dam completion. The recording crew should check carefully such cases and the information should be immediately passed on for data assessment (**Om1**).

A common error is the recording of the wrong instruments (**Om2**). When allowed by the advances in technology and the budget of the project, a data logger system helps to avoid these errors. However, during construction, many cables or tubes tend to end up in the same place, usually bearing just a small non - waterproof, hand-written label with the instruments name. This label can be easily damaged and be possibly re-placed erroneously. A request should be addressed to the manufacturers in order to provide these instruments with a digital signature so that they can be accurately detected.

For standpipe piezometers (**Om3**), it is quite common to get erroneous measurements due to moisture that is present on the walls of the casing or on the measuring device, so producing a wrong signal. Another problem, commonly observed, is getting erroneous readings due to using measuring tapes that were cut and subsequently clumsily restored, missing some centimetres or even meters that the measuring crew was unaware of.

If instruments heads are left uncapped, some peculiar problems may arise. This was the case at Thissavros dam, where insects (wasps) had entered uncapped extensometer slots, constructing nests in them, so affecting measurements.

2.3.2 Data assessment (Oa)

Data assessment demands the participation of experienced and trained personnel that will consider all the conditions applying during the measurement and investigate all possibilities to avoid wrong conclusions. The data assessment team should be in contact with the design team and be aware of the concepts of the design. For example, if an instrument stops functioning they should be able to judge whether the information it provides is significant and if has to be replaced.

Data assessment should start right after instrument installation, so that the reliability of the instrument is assessed as soon as possible and false alarms by problematic instruments are avoided during operation. Even the cause of the failure or the malfunction of an instrument should be assessed because it may give valuable information. For example, vibrating wire piezometers readings may drift off when their cables are sheared (if they are not given enough slack) when passing from intensely deforming zones.

Surface monuments placed close to roads are commonly influenced by pavement construction works and heavy traffic (case reported in Pramoritza dam). This problem can be solved by taking measurements right before and after the works (**Oa1**).

For inclinometers and IDEL instruments, where the measuring points are numerous, the manufacturer should supply an appropriate presentation and evaluation software (**Oa2**), compatible with the commercially available ones (spreadsheets etc).

For IDEL instruments placed in a compressible foundation (weak rocks should also be considered as such), the elevation of the lowest settlement collar should not be considered to be fixed (especially if under a high embankment like Ilarion dam), unless the embedment depth in the underlying sound bedrock is significant (**Oa3**). In order to overcome this problem, as far as possible, settlements should be double checked with reference to the elevation of the upper settlement collar (taken by surveying methods).

Finally it should be noted that contrary to experience from other dams, load cells installed in Greek dams (Thissavros and Evinos) appear to work well, providing reasonable measurements.

3 CONCLUSIONS

Facing numerous incidents concerning instrumentation problems in Greek dams provided the experiences outlined. The manufacturers should note that the dam instrumentation will benefit a lot from:

- Provision of a way to identify each electrical instrument, e.g. a unique signal response
- Automated data loggers for all instruments
- Development of instruments that will minimise obstruction to construction activities (wireless signals?)

4 ACKNOWLEDGMENTS

The authors would like to thank Mr. P. Xistris, G. Hatzigianelis and D. Kottidis for providing useful information by sharing their long experience in dam instrumentation.

5 REFERENCES

- Dunicliff, J., 1993, *Geotechnical instrumentation for monitoring field performance*, John Wiley & Sons
- Dunicliff, J., 2008, Geotechnical instrumentation news episode 55, *Geotechnical News*, 29-40
- ICOLD, 1988, *Bulletin 060: Dam monitoring-General considerations*
- ICOLD, 1989, *Bulletin 68: Monitoring of Dams and Hydro Foundation*
- ICOLD, 1992, *Bulletin 087: Improvement in existing Dam monitoring -Recommendations and case histories*
- ICOLD, 2000 *Bulletin 118: Automated dam monitoring systems - guidelines and case histories.*
- Peck R.B., 2001, Embankment dams, Instrumentation versus monitoring, *Geotechnical News*, 29-30 (www.bitech.ca)
- USBR, 1987, *Embankment dam instrumentation manual*

Student understanding of the concept of soil structure guides instructional interventions

La compréhension du concept de la structure du sol de la part des étudiants guide les interventions d'enseignement

M. Pantazidou
National Technical University of Athens, Greece

ABSTRACT

This paper presents a methodology instructors can use in class to elucidate concept understanding in order to design appropriate interventions. The methodology consists of (i) phrasing qualitative questions on fundamental course concepts and (ii) identifying in the answers the main categories that describe the variation of the students' thinking. The application of the methodology is demonstrated for the concept of "soil structure" in an environmental geotechnics course. The results reveal the students' misconceptions related to soil porosity and permeability. To address these misconceptions, alternative in-class activities are discussed.

RÉSUMÉ

Cet article présente une méthodologie que les enseignants peuvent utiliser en classe pour élucider la compréhension de divers concepts afin d'élaborer des interventions appropriées. La méthodologie consiste à (i) formuler des questions qualitatives sur des concepts fondamentaux du cours et à (ii) identifier dans les réponses les catégories principales qui décrivent la variation dans le mode de penser des étudiants. La démonstration faite ici concerne l'application de cette méthodologie au concept "structure du sol" dans un cours de géotechnique environnementale. Les résultats révèlent les idées fausses des étudiants par rapport à la porosité et la perméabilité du sol. Pour remédier à ces idées fausses, on discute ici certaines activités alternatives en classe.

Keywords: geotechnical instruction, soil structure, clays, concept, conceptual knowledge, misconception, conceptual change

1 INTRODUCTION

At some point in their careers instructors invariably experience bafflement at some of the errors made by students. Most experienced teachers with time develop strategies to minimize the frequency of these errors. Few instructors, however, can enunciate a systematic methodology for determining the misconceptions underlying the errors and, ideally, making suitable instruction modifications. This paper aims at proposing such a methodology and demonstrating how it can be incorporated in regular instruction (i.e. not necessarily in a research project on engineering education).

Instruction, in general, targets two major categories of knowledge: declarative knowledge ("know that") and procedural knowledge ("know how"). Engineering instruction in particular focuses more on procedural knowledge, especially during the later years of an undergraduate engineering curriculum. Conceptual knowledge, on the other hand, can be thought of as a subset of declarative knowledge and refers to the building elements of a domain and their interconnections. These are constructed over time by the learner and used, knowingly or not, to provide some structure to the subject domain. In engineering schools, declarative knowledge is often assessed with theory-related questions (e.g. asking students to perform derivations, or to choose among multiple factual affirmations), whereas procedural knowledge is assessed with problems involving calculations. Few learning experiences and assessment exercises target specifically conceptual knowledge, which is tested indirectly, since it feeds both into declarative and

procedural knowledge. This hypothesized relationship is logical, but not well understood nor demonstrated (Strevler et al. 2008). As a result, unless constructing and using specially-phrased diagnostic questions, it will be difficult to attribute recurring errors in problem solutions to either a conceptual or a procedural mix-up.

Asking questions about the building blocks of knowledge, as well as how these are deployed by the learners when faced with a cognitive task, yields a view of the learning process that is closer to the learner's than the teacher's perspective. Building on traditions in Instructional Psychology, Educational Research has developed tools that make possible to obtain answers to the questions just mentioned. One such technique consists of (i) accounting exhaustively for the procedural constituent elements of archetypical problems students confront in a domain and (ii) compiling short multiple-choice questions targeting each of these elements, which, in turn, are underpinned by a relatively small number of concepts. The outcome of the exercise is the collection of the questions, known as concept inventory, which after validation can be used either diagnostically or for assessment. The concept inventory approach was used by Steif (2004) in statics, a fundamental course in civil and mechanical engineering. According to Steif (2004), a representative statics problem is decomposed to (i) parsing of the system, (ii) reasoning about forces connecting parts, (iii) isolating bodies to impose equilibrium conditions and (iv) applying the equilibrium principle to selected bodies. For a common statics problem with blocks and ropes, a typical multiple-choice concept question would address the forces present in the free body diagram of a subset of blocks and cords (Steif and Hansen 2007).

Decomposition techniques such as the one described above are best suited to identify exactly where students make errors (i.e. they do not see that the forces that are equal and of opposite directions are exerted on different bodies), rather than why (a question that will have to unravel the understanding of force). Answering the "why questions" requires a probing of a different kind, offered by an approach known as phenomenography, which seeks to unveil students' mental models of concepts. Among its proponents, Bowden and Marton (1998) discuss a number of studies that have developed qualitative questions to diagnose "pre-conceptions" (what students bring to instruction), monitor understanding and assess impact of instruction. In fact, Bowden and Marton consider formulating suitable qualitative questions as the key undertaking in finding out what is learned by students. Within this tradition falls the work presented in this paper.

2 PROBING PERCEPTIONS OF SOIL STRUCTURE IN THE CONTEXT OF A GEOTECHNICAL CURRICULUM

In selecting topics and phrasing suitable qualitative questions, the guidelines given by Bowden and Marton (1998) become useful. The questions have to be open to different perspectives so that students decide on their own the relevant aspects of the problem that need to be addressed. They should preferably be stated without using standard technical jargon, because "specific facts and procedures usually rest on taken-for-granted ways of seeing, which are not put to the test". Finally, these questions should focus on fundamental concepts in the field that are central in the development of key skills.

The benefits resulting from the answers to these questions are manifold. They help the instructor (i) determine the "initial conditions" of the students (in other words, the pre-existing ideas from physics, mechanics and even from direct experience students bring to an engineering course); (ii) become familiar with the less technical language that comes naturally to novices; and (iii) diagnose any misconceptions. The non-technical nature of questions makes them suitable for use both before and after instruction, thus

incorporating seamlessly assessment in instruction. In addition, they provide a repertoire of explanations the instructor can re-introduce in the classroom and invite students to critique.

The concept explored herein is soil structure. Soil structure refers to the arrangement of soil particles relative to each other and to what holds them together. By implication, soil structure also refers to the pore space created among the particles.

Soil structure is a generative concept, in the sense that beliefs on pore space characteristics will play a role on predictions of crucial aspects of soil behavior, such as compressibility and permeability. However, since soil mechanics treats soil as a continuous material by practical necessity, students have few opportunities to question their beliefs on soil structure. Hence, not only is soil structure a key concept, but also has many chances to escape unexamined because it is not directly useful for problem solving.

In most civil engineering curricula, students take one or two courses on soil mechanics, where they are introduced to the concepts of soil structure, permeability and compressibility. In the beginning of their first course, students may be introduced to a qualitative description of the geometric arrangement of soil particles and the fundamental differences between sands and clays, the particles of which are held together with gravity forces and electrical forces, respectively. These introductory lectures commonly include a reference to the electrically charged surfaces of clays that attract water. The presence of this water makes clay moldable and solid-looking. The clay-water interaction phenomena and the huge surface area of the tiny, plate-like clay particles explain the ability of clays to hold large amounts of water, distributed in a very large number of tiny pores. Large amounts of water means large volume of pores.

Soil structure issues will seldom recur during topics discussed later in the curriculum in soil mechanics or geotechnical engineering courses. Instead, students deal routinely with the two aggregate measures of pore volume that are necessary for calculations: porosity (pore volume/total sample volume) and void ratio (pore volume/volume of solids).

The concept of soil structure was investigated in an environmental geotechnics course, a specialized geotechnical course often offered as an elective in the last year of a civil engineering curriculum. The environmental issues addressed in such a course make the topic of soil structure pertinent. This is because the structure of clays depends on the properties of the pore fluids: certain contaminants will affect the structure and hence the behavior of clays in undesirable ways (e.g. increase their permeability). The specific environmental geotechnics course is an advanced undergraduate course taught at the fifth year of the civil engineering program at the National Technical University of Athens (NTUA), Greece. In terms of prior instruction, students have already completed courses on soil mechanics, experimental soil mechanics and hydraulics.

The qualitative question formulated to test the conceptual understanding of soil structure reads as follows:

"In your opinion, in which soil type may we encounter higher porosity, in a sand or a clay? How do you justify your opinion?"

Students are further advised to support their answer mainly with personal observations (e.g. from everyday-life experiences with soil/dirt, such as playing with beach sand, or from an activity in the soil mechanics laboratory) rather than by what they can recall from instruction.

The question was initially asked during a mid-term exam. It was explained to students that the exam was mainly diag-

nostic and hence contributed only slightly to the final grade. In addition, it was clarified that the particular question would be graded for the richness of the justification of the opinion and not for the correctness of the answer. Although such measures seem to put most students at ease to give an answer that makes sense to them, it cannot stop those who recall instruction on clay structure to give the "right" answer.

3 PERCEPTIONS OF SOIL STRUCTURE AND IMPLICATIONS

The students' answers were an overwhelming "vote" for sand. More specifically, 28 students answered that they expect larger porosity in sands, whereas only 11 expect larger porosity in clays. (In addition, there were four students who answered "it depends", probably exhibiting the characteristic sense of discomfort many engineering students experience when faced with open-ended questions without clear-cut answers.) The explanations offered are summarized in Table 1. It should be noted that the number of explanations is larger than the number of the answers since many students provided more than one justification for their answer.

Table 1. Summary of justifications for porosity trends

Frequency	Answer and supportive arguments
28	Sand can have higher porosity because...
14	...sand has higher permeability
10	...sand has larger pores
10	...sand flows, whereas clay is dense, hard
3	...sand can be compacted more easily
2	...sand dries more easily (probable implication: sand has higher permeability)
1	...forces keep clay particles closer together
11	Clay can have higher porosity because...
3	...clay has open structure
3	...clay can absorb a lot of water
1	...clay is more difficult to dry (probable implication: clay holds more water)
1	...clay has more cracks and hence more voids

It is instructive to identify the categories of the arguments used by the students. Most students give explanations based on observations related either to the large size of sand pores, or to a few physical characteristics of soils (e.g. sands flow), including a measure of the easiness of water flowing through soils (i.e. permeability). A few students, however, contrary to the instructions, provide arguments originating from textbooks (e.g. clay has an open structure). It may be relevant to note that from a total of four textbook-type arguments, three are employed to support the answer that clay can have larger porosity.

A striking difference between the two sets of justifications is that the number of the arguments for sands is higher than the number of the respective answers. This indicates that the students are pretty confident about their "sand vote" since they can support it with more than one explanation (an average of about 1.5 explanations corresponds to each of the "sand votes", twice as much compared to the "clay votes"). On the contrary, the arguments for clay are fewer than the answers and are less well phrased, implying that students recalled the correct answer and then groped for explanations. In fact, one is tempted to posit that students follow the same procedure for arriving at either one of the two answers: they hold a mostly unexamined belief (either

through everyday-life experiences, or through instruction) and then search for arguments to support it, rather than the other way round. It is characteristic that the exact same argument is used to support both answers: the fact that sand dries more easily than clay is used as an argument both for sand (apparently focusing on higher permeability and, supposedly, higher porosity) and for clay (apparently interpreting the difficulty as an indication of clay holding more water and hence having higher porosity).

The belief that sands can have higher porosities than clays has also been found to be prevalent in an undergraduate soil mechanics class in another institution (Pantazidou 2001). There the question was asked in the format of "split task" assessment: the students were asked both about the "right" answer and whether their experience confirmed that answer. Some students answering correctly that clays can have larger porosity, specifically noted that experience told them otherwise.

4 INSTRUCTIONAL INTERVENTIONS

The answers of the students point to two kinds of misconceptions the instructor must address. The apparent one is reversing the belief that sands can have larger porosity, whereas the opposite is true. It should be noted here that students do have resources available that tell them otherwise. These include classic soil mechanics reference books, such as the one by Lambe and Whitman (1969), which includes a table with values of porosity for sands (with a maximum of 0.55), as well as a discussion later in the text on the possibility of soft clays to have much higher porosity. The same is true for the two soil mechanics textbooks available to NTUA students (Gazetas 2001; Kavvas 2002). However, it is doubtful whether students pay much attention to information in textbooks about typical values expected for key parameters, having become accustomed to an assessment practice whereby any numbers needed are always given to them and hence understandably concluding that "the quantification of their personal experience is unnecessary and irrelevant" (Redish and Smith 2008).

It seems that students need something more memorable than tables with numbers to appreciate the potential of clays to have large pore volume, perhaps a model of a physical process. Such a learning tool would simulate soil deposition by introducing soil particles at the top of a container full of water and let them settle at the bottom, attaining a configuration determined by the forces exerted among particles. A comparison between two deposition sequences starting with clay and sand particles with the same volume of solid material would show that a clay deposit can end up being "taller". The ideal software would magnify the invisible-to-the-naked-eye clay particles (making the correspondingly magnified particles of a fine sand the size of marble balls) and allow for interactive modification of the pore-water properties.

Unfortunately, although it is doable to simulate deposition of sand particles, our knowledge of the behavior of clays is not adequate to simulate deposition of clay particles at the scale of the pore level. Luckily, we can demonstrate these effects physically by letting a clay-water mixture and a sand-water mixture (with the same volume of solids) settle in volumetric tubes and observe the final volume/height of the soil. This is an extension of similar demonstrations used to show the effect of pore-water properties on the final volume of a clay sample and, indirectly, on the arrangement of the clay particles (Lambe and Whitman 1969). The corresponding laboratory demonstration is shown in Figure 1. If such a demonstration is incorporated in instruction, it may be possible to provide for some students a reminder more memorable than numbers; its power to enable conceptual change obviously remains to be investigated. Compared to the software described above, it is too static, since it does

not allow manipulation of the properties of the soil and the pore fluid, nor permit any kind of prediction.

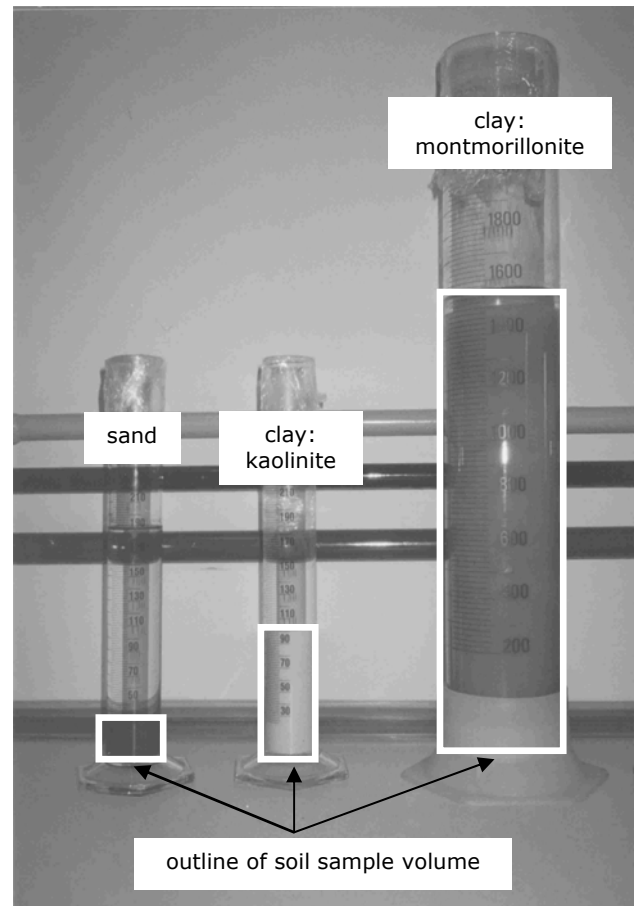


Figure 1. Soil samples produced through settlement of 40 grams of: sand, kaolinite and montmorillonite, with porosity values equal to 0.44, 0.85 and 0.99, respectively.

In addition to addressing the clay-sand misconception, the instructor has to deal with two persistent underlying misconceptions, namely that larger pores is equivalent to higher porosity and that higher permeability entails higher porosity. The first misconception can be partly a logical oversight: many small pores can win over fewer larger ones. However, the author's experience with students' answers suggests that the main culprit is paying more attention to the logical conclusion that larger particles create larger pores among them and less to the proportion of the pore/total (or pore/solid) space. A simple numerical calculation of porosity of two model porous materials created by a simple cubic packing of spheres, such as those shown in Figure 2, can demonstrate that porosity (n) in such geometrically regular particle arrangements is independent of particle size and, therefore, of pore size.

The second persistent underlying misconception is more related to hydraulics than soil mechanics, as the easiness with which water flows is related to the square of the radius of the pore through which water flows and not to the total pore volume. Model porous materials can again be employed to dispel this misconception. By modeling the pore space of two soil columns (A) and (B) with a bunch of cylindrical tubes of unequal radius (R), the cross sections of which are shown in Figure 3, it is easy to show that two soils of the same porosity (n) can have different values of permeability (k).

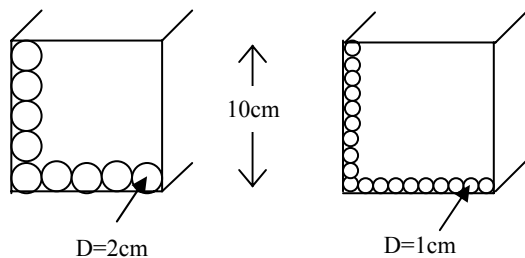


Figure 2. Cubic arrangements of spheres of unequal diameter (D) with the same porosity ($n=0.48$).

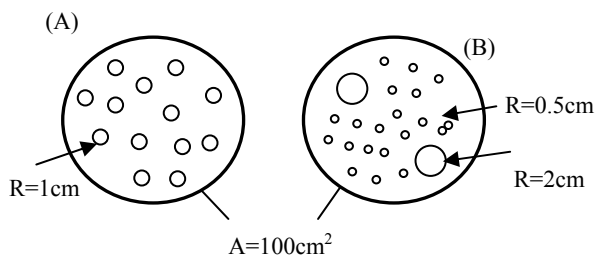


Figure 3. Models of soil columns with equal porosity ($n_A=n_B=0.41$) and unequal permeability ($k_B=2.6 \times k_A$).

It should be stressed that the author has assigned as homework in various classes the calculations of porosity (Figure 2) and permeability (Figure 3) with no significant effect on the answers of students to the clay-sand question. This observation is in line with literature showing that students' knowledge is not applied consistently in different contexts (Streveler et al. 2008). A more promising approach appears to be inviting students to critique answers such as those summarized in Table 1, in lieu of expecting the question asked to mobilize seemingly dormant pieces of knowledge. Whereas students are reticent in commenting on statements made by the instructor, they become uninhibited when asked to comment on statements made by students like them. The contents in Table 1 were able to create a very lively discussion in class, when students were prompted to say with which argument they agreed or disagreed more. In fact, some students were able to make the connection between the assignment depicted in Figure 3 (which was given earlier in the semester) and the fallacy of the statement that higher permeability entails higher porosity. However, systematic research is needed to evaluate the potential of each intervention to promote conceptual change.

5 CONCLUDING REMARKS

Instructors traditionally learn about the learning experience of their students indirectly, through the students' performance. To this tradition this paper adds the systematic instructor learning that results from analysis of answers to suitable qualitative questions, formulated to probe how students understand fundamental engineering concepts.

Investigation of the concept of soil structure demonstrated that students overlook the potential of clays to have very large pore space. This has significant practical implications, as large pore space also entails a high compressibility and deformation potential, which by association students may also overlook. Hence, interventions such as the ones proposed herein are necessary.

This article was written partly with the aim of serving as a "call for action" for the geotechnical community, in order to collectively produce qualitative questions suitable for probing students' understanding of key concepts. These questions will identify students' difficulties and these difficulties will become a guide for producing new instructional techniques and tools, from class debates to laboratory demonstrations. In fact, many existing demonstrations (Elton

2001) would be more effective with a tighter connection to specific identified misconceptions, whereas a few laboratory activities have already been developed to address specific conceptual difficulties (Burland 2008).

ACKNOWLEDGMENTS

The author thanks the students at NTUA for their open-mindedness and lively participation in the environmental geotechnics course and Mr. George Pirgiotis for setting up the soil columns in Figure 1.

REFERENCES

- Bowden, J. and Marton, F. 1998. *The university of learning: Beyond quality and competence in higher education*, Kogan Page Ltd., London, UK.
- Burland, J.B. 2008. Personal reflections on the teaching of soil mechanics, *1st Int. Conf. on Education and Training in the Geo-Engineering Sciences*, Constanza, Romania, June 2-4.
- Elton, D.J. 2001. *Soils Magic*, ASCE Geotechnical Special Publication No. 114, ASCE Publications, Reston, VA.
- Gazetas, G. 2001. *Soil Mechanics*, Edition 2.4, NTUA Publications, Athens, Greece (in Greek).
- Kavvasdas, M. 2002. *Soil Mechanics*, NTUA Publications (in Greek).
- Lambe, T.W. and Whitman, R.V. 1969. *Soil Mechanics*, John Wiley, New York, NY.
- Pantazidou, M. 2001. Instructional theory, engineering education and geotechnical engineering: Common links, *4th Hellenic Conference on Geotechnical and Geoenvironmental Engineering*, Athens, May 30-June 1, pp. 25-30 (in Greek).
- Redish, E.F. and Smith, K.A. 2008. Looking beyond content: Skill development for engineers, *J. of Engineering Education*, Vol. 97, No. 3, pp. 295-307.
- Steif, P.S. 2004. An articulation of the concepts and skills which underlie engineering statics, *34th ASEE/IEEE Frontiers in Education Conference*, Savannah, GA, Oct. 20-23, Paper No. T1A-1.
- Steif, P.S. and Hansen, M.A. 2007. New practices for administering and analyzing the results of concept inventories, *J. of Engineering Education*, Vol. 96, No. 3, pp. 205-212.
- Streveler, R.A., Litzinger, T.A., Miller, R.L. and Steif, P.S. 2008. Learning conceptual knowledge in the engineering sciences: Overview and future research directions, *J. of Engineering Education*, Vol. 97, No. 3, pp. 279-294.

Design charts for single piles under lateral spreading of liquefied soil

Concevez les diagrammes pour les piles simples sous la propagation latérale du sol liquéfié

Alexandros Valsamis
Dr Civil Engineer, Civil Engineering School, National
Technical University of Athens

George Bouckovalas
Professor, Civil Engineering School, National Technical
University of Athens

Emmanouil Drakopoulos
Civil Engineer Msc, National Technical University of Athens

ABSTRACT

When soil liquefaction occurs in slightly sloping ground or near free-face topographic irregularities large horizontal displacements may occur due to the lateral spreading of the liquefied ground. This kind of ground failure may cause extensive damage to pile-supported structures as witnessed in several recent earthquakes (Chi-Chi 1999, Kobe 1995, etc). A systematic analysis of the detrimental effect of lateral spreading requires a sophisticated 3-D numerical analysis. Still, there is need for preliminary estimation of the re-sponse of deep foundations based on readily available data, such as the geometric and the mechanical characteristics of the foundation and the maximum anticipated displacement at the ground surface. For this purpose, a set of over 200 parametric numerical analyses were performed, with the pseudo static P-y method, in order to analyze the basic parameters affecting the pile behavior. The results of the parametric analysis have been consequently combined into design charts for the computation of the maximum developed pile head displacement and moment.

RÉSUMÉ

Quand la liquéfaction de sol se produit en inclinant légèrement des irrégularités topographiques de libre-visage moulu ou proche les grands déplacements horizontaux peuvent se produire en raison de la propagation latérale de la terre liquéfiée. Ce genre d'échec au sol peut causer des dommages importants aux structures pile-soutenues comme été témoin dans plusieurs tremblements de terre récents (1999 Chi-Chi, Kobe 1995, etc.). Une analyse systématique de l'effet néfaste de la propagation latérale exige une analyse numérique à trois dimensions sophistiquée. Toujours, il y a besoin d'évaluation préliminaire de la réponse des bases profondes basées sur des données facilement disponibles, telles que les caractéristiques géométriques et mécaniques de la base et du déplacement prévu maximum sur la surface au sol. À cette fin, un ensemble de plus de 200 analyses numériques paramétriques ont été exécutés, avec la pseudo méthode du PY de charge statique, afin d'analyser les paramètres de base affectant le comportement de pile. Les résultats de l'analyse paramétrique ont été par conséquent combinés dans des diagrammes de conception pour le calcul du déplacement et du moment développés maximum de tête de pile

Keywords : liquefaction, lateral spreading, single piles, numerical investigation

1 INTRODUCTION

One of the most damaging effects of earthquake-induced soil liquefaction is the lateral spreading of soils, where large areas of ground move laterally to lengths ranging from some centimeters to a few meters. This phenomenon may occur in the case of even small surface inclination (e.g. 2÷4%) or small topographic irregularities (e.g. 2÷3m) such as those near river and lake banks.

In such cases, the kinematic interaction of single piles and pile groups with the lateral spreading ground may induce significant additional residual horizontal loads and bending moments to the pile, which cannot be predicted by common design methods for superstructure loading.

2 PSEUDO-STATIC PREDICTION METHODS

The detailed analysis of piles against lateral spreading is a rather complicated soil-structure interaction problem which, strictly speaking, requires a sophisticated numerical simulation, well beyond the limits of common applications. Thus, for simplified computations, a number of pseudo-static methodologies have been developed, where the loads or displacements applied by the laterally spreading ground are being estimated independently and subsequently applied as external loads to the pile. Existing pseudo-static methodologies may be divided in two categories:

- The **P-y method**, which relies upon the substitution of the ground with "Winkler type" springs that are governed by a non-linear load-displacement (P-y) law. According to this methodology an independent estimation of the ground displacement is made and the resulting displacements are applied to the base of the springs in order to evaluate the pile deflection and the corresponding shear forces and moments (e.g. Tokimatsu 1999, Boulanger et al 2003).
- The **limit equilibrium method**, which is based on a pseudo-static estimation of the ultimate pressure that the laterally spreading ground applies to the pile. Pile displacements and bending moments can be consequently evaluated (e.g. JRA 1996, Dobry et al 2003) from beam theory.

Recently, Ashford & Juirnarongrit (2004) concluded that the P-y method is the most reliable, after comparing the two most commonly used limit equilibrium methods (JRA, 1996 and Dobry et al., 2003) with a simple P-y method that used the curves proposed from Reese et al. (1974) for sands, degraded with a factor $\beta = 0.1$ in order to take into account the soil liquefaction. Bhattacharya et al. (2003) also concluded that the limit equilibrium method of JRA (1996) is systematically non-conservative. Thus, on the ground of these independent findings, the P-y method has been chosen to derive the design charts in this paper.

More specifically, the method proposed by Branderberg (2002) has been selected, according to which the P-y curves of API (1995) for the non-liquefied sands should be used, after being degraded with a loading factor β . This factor represents the effect of liquefaction on the mechanical characteristics (soil strength and deformation) of the natural soil and can be computed according to Table 1, in terms of the corrected blow count of the Standard Penetration Test ($(N_1)_{60-CS}$).

The aforementioned methodology has been chosen among seven (7) compatible methodologies (Ishihara & Cubrinovski, 1998, Cubrinovski et al., 2006, Rollins et al., 2005 & 2007, Tokimatsu, 1999, High Pressure Gas Safety Institute of Japan, 2000, Railway Technical Research Institute of Japan, 1999, and Matlock, 1970) following an extensive evaluation through comparison to three centrifuge experiments (Abdoun 1998) and one large shaking table experiment (Cubrinovski et al. 2004).

Table 1. Proposed degradation factors β after Branderberg (2000)

$(N_1)_{60-CS}$	β
<8	0 to 0.1
8-16	0.1 to 0.2
16-24	0.2 to 0.3
>24	0.3 to 0.5

3 PARAMETRIC ANALYSES

The numerical analyses have been performed with the help of the finite elements program NASTRAN (MacNeal-Schwendler Corp. 1994). Simulation of the liquefied soil layers was based on the P-y methodology outlined in the previous paragraph. The non-liquefied soil layers have been simulated with the P-y curves proposed by API (1995, 2002) without the use of a degradation factor. It should be mentioned that, as long as the non-liquefiable base layer does not fail, the exact P-y curve used for its simulation does not affect significantly the results, as its stiffness is almost 100 times larger than that of the liquefied soil above it.

Based on a previous study of the lateral spreading phenomenon (Valsamis et al., 2007), the variation with depth of the lateral displacements of the liquefied soil was assumed as a quarter sine, with the maximum displacement developing near the top of the layer and zero displacement at the bottom of the layer. On the other hand, the displacement of the non-liquefied soil layers was assumed to remain constant with the depth.

In total, 162 such parametric analyses have been performed, which refer in three basic combinations of pile and soil profiles (Figure 1):

- "2-layered geometry", where a single pile with free head conditions rests inside a uniform liquefied soil layer that overlies a non-liquefiable soil stratum.
- "3-layered geometry", that differs from the previous case due to the existence of a non-liquefiable soil crust
- "Fixed pile head" case, which differs from the 2-layered case due to the restraining of the pile head movement, in accordance with real cases where the existence of a superstructure prevents the pile head movement.

This categorization is justified on the grounds that any possible constraints on the free pile head displacement and rotation, either due to the non-liquefiable soil crust or a superstructure, proved to be among the the most important factors controlling the pile response. Note that, Ishihara & Cubrinovski (1998), Brandenburg (2002), Rollins et al. (2005) have also reached similar conclusions for the effect of the pile head constraint enforced by a non-liquefiable soil crust.

Sixty six (66) parametric analyses have been performed for the 2-layerd case and the following pile & soil input parameters:

- degradation factor $\beta = 0.05$ to 0.4
- soil friction angle $\phi = 32$ to 42° ($D_r = 35\sim 90\%$)
- thickness of liquefied soil layer $H_{liq} = 6$ to 10m
- Pile Elastic modulus $E = 30$ to 210 GPa
- Pile diameter $D = 0.15\text{m}$ to 0.6m ,
- Pile stiffness $EI = 16$ to $1336\text{ MN}\cdot\text{m}^2$, and
- Maximum ground surface displacement $D_h = 0.125\text{m}$ to 1.20m .

Fifty (50) more parametric analyses have been performed for the 3-layered case, with the thickness of the non-liquefied soil crust ranging from 1 to 4m and the previously mentioned range of the remaining input parameters. Finally, another forty six (46) parametric analyses were performed for the fixed pile head case and the above mentioned range of parameters.

4 DESIGN CHARTS

Pile design against lateral spreading must assure that, following the seismic excitation:

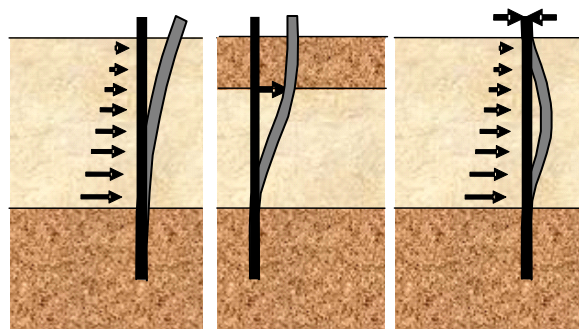


Figure 1. Static models for the (a) 2-layered, (b) 3-layered and (c) fixed pile head cases

- no structural failure of the pile has occurred (no development of plastic hinges at any depth), and
- no performance failure of the superstructure should be encountered due to excessive superstructure displacements.

To check against these criteria, both the maximum developing moment and the maximum displacement of the pile head are needed.

The depth of the maximum bending moment is in general variable. For the cases considered in this article (Figure 1), it is known before-hand that maximum moments develop at the interface between the liquefied soil layer and the non-liquefied base layer. Similarly, it is known before hand that the maximum pile displacement develop at the pile head, for the 2- and the 3- layered cases, and near the mid-depth of the liquefiable soil layer for the fixed pile head case. For these reasons, the statistical analysis of the parametric analyses results has been focused upon the magnitude of those two design parameters and not upon the respective location along the pile.

It should also be mentioned that the statistical processing was not "blind", e.g. based only on some algorithm that minimizes the error of the empirical predictions. On the contrary, a general form of the prediction relations was initially obtained based on analytical solutions of the static models presented in Figures 1a, 1b and 1c and subsequently the statistical processing was used to calibrate the general relations against the results of the parametric analyses.

Figures 2a and 2b present the proposed design charts for the maximum pile displacement and the associated bending moment for the 2-layered soil profile. Alternatively, the pile head displacement $D_{pile}(m)$ may be computed from Figure 2a and the respective maximum bending moment $M_{max}(kN/m)$ may be subsequently estimated as:

$$M_{max} = 2.2 \frac{EID_{pile}}{H_{liq}^2} \quad (1)$$

where $H_{liq}(m)$ is the liquefied soil layer thickness and $EI(kN/m^2)$ is the pile stiffness.

Observe that the relation in Figure 2a is strongly non-linear. This is due to the fact that the Winkler springs representing the soil are elasto-plastic and thus, after a certain soil displacement, the loads due to the lateral movement of the soil remain constant. This elastoplastic response of the soil springs is the main reason why the derivation of a simple analytical expression for the pile displacement was not possible. Moreover, note that the correlations of Figure 2a are not dimensionless and thus they should always be used in conjunction with the international system unit SI (kN, m).

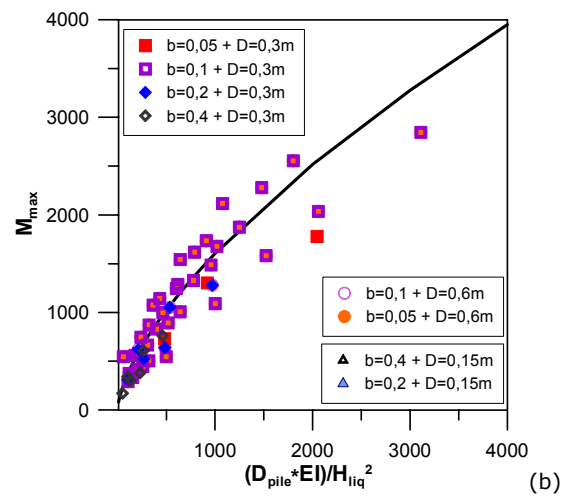
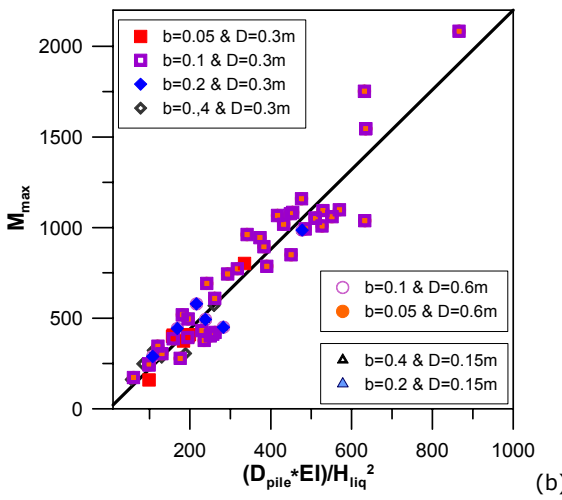
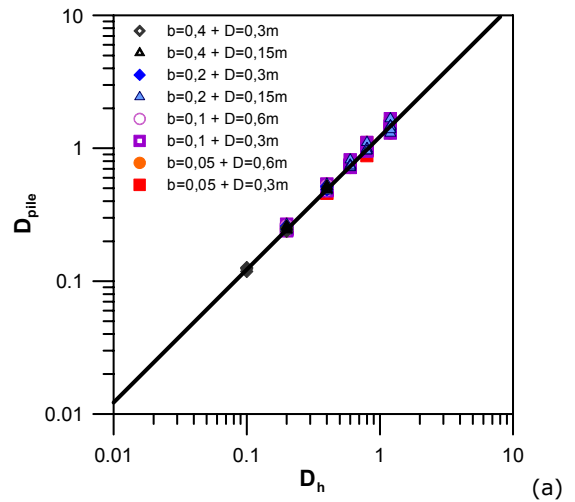
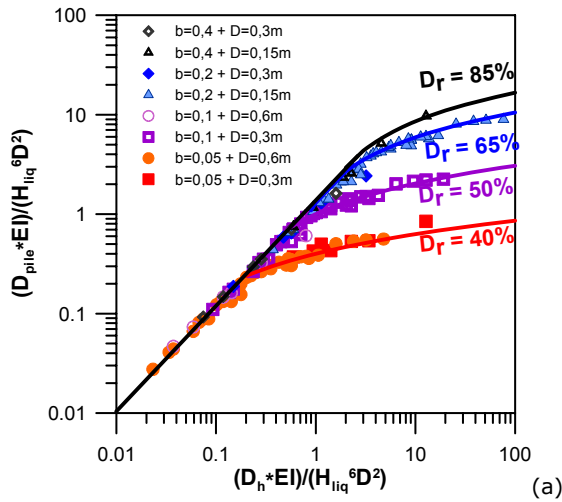


Figure 2. Design charts (a) for the maximum pile displacement and (b) for the maximum developing bending moment of the pile, for the 2-layered soil profile

Figure 3. Design charts (a) for the maximum pile displacement and (b) for the maximum developing bending moment on the pile, for the 3-layered soil profile

The design charts for the 3-layered soil profiles are shown in Figures 3a and 3b. Observe that the pile head displacement follows systematically the non-liquefied soil crust displacement. This observation has been also confirmed from centrifuge experiments (Abdoun, 1999) which show that pile head displacements are only slightly larger than soil surface displacements. In this case, it was possible to develop simplified analytical relations, both for the pile head displacement and the developing bending moments, namely:

$$D_{pile} = 1.22 \cdot D_h \quad (2)$$

$$M_{max} = 18 \left(\frac{EID_{pile}}{H_{liq}^2} \right)^{0.65} \quad (3)$$

Finally, Figures 4a and 4b present the design charts for the maximum pile displacement and bending moment respectively, in the case of the fixed pile head. In this case also, it was possible to establish simple to use analytical relations for the estimation of the above mentioned design parameters, namely:

$$D_{pile} = H_{liq}^{12} D_h^{0.3} \frac{\beta^2 D^2}{(EI)^2} \quad (4)$$

$$M_{max} = 18 \frac{EID_{pile}}{H_{liq}^2} \quad (5)$$

where β is the degradation factor for the soil strength due to the liquefaction which can be taken from Table 1.

5 CONCLUDING REMARKS

In the previous paragraphs, diagrams and relations were presented for the approximate evaluation of the maximum displacement and bending moment of the pile due to liquefaction-induced lateral spreading. The charts concern three different combinations of pile and ground conditions, often encountered in practice. The proposed design charts and relations should be used with the following limitations:

(a) They were derived pseudo-statically, taking only into account the final displacement of the ground, at the end of shaking. Any effects of the superstructure inertia are ignored.

(b) The expected free-field maximum ground surface displacement should be computed independently, based on the (many) available empirical relations which are published in the literature (e.g. Hamada, 1999, Youd et al, 2002).

(c) All the above mentioned charts and relations, and more specifically those concerning the 2-layered soil profile case, should be applied only when the soil has the capability to "flow" freely around the pile under investigation. In all other cases (e.g. small distance between the piles, sheet-pile wall, etc) they may lead to non-conservative predictions of the pile displacement and bending moment.

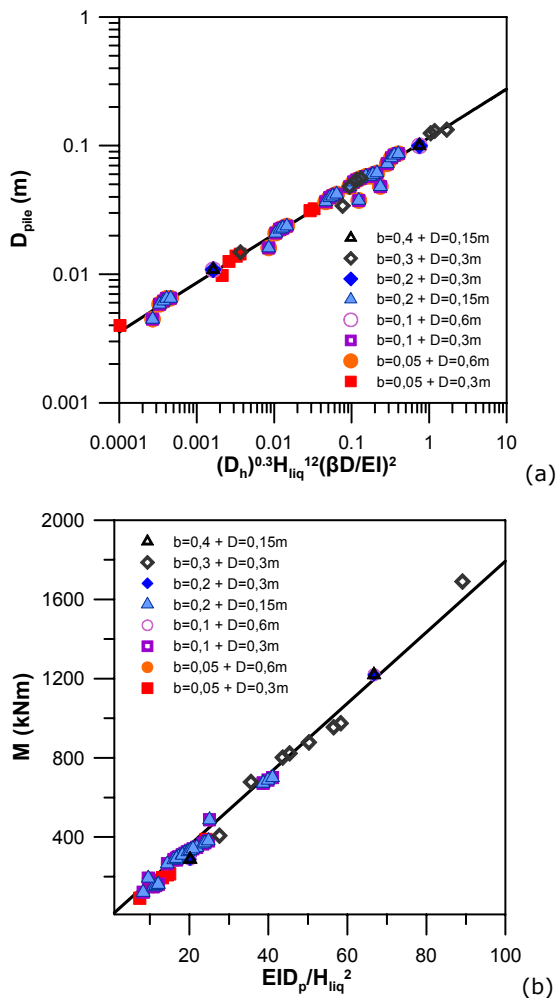


Figure 4. Design charts for the (a) maximum developed pile displacement and (b) the maximum developing bending moment on the pile, for the fixed pile head case

(d) It has been assumed that the pile has been adequately embedded to the non-liquefiable base soil layer so as to guarantee fixed bottom conditions during lateral ground spreading. When the pile has not been driven adequately to the bottom (non-liquefiable) soil layer, there is the possibility of pile extortion or significant pile base rotation which results to larger displacements for the pile head and smaller developing moments.

Finally, note that the results presented herein have been also evaluated against numerical 2-D and 3-D numerical analyses, where the coupled pile-laterally spreading ground response has been simulated with the aid an effective stress elastoplastic analyses (Valsamis 2009). These comparisons, not shown here due to length limitations, show that for the 3-layered geometry and the 2-layered geometry with fixed pile head the simplified P-y methodology gives accurate results. However, for the 2-layered geometry where the pile head can move freely, the P-y methodology slightly overpredicts the expected pile head displacements and thus the maximum developed moments which are calculated from them.

6 REFERENCES

Abdoun T. H. (1999) "Modeling of seismically induced lateral spreading of multi-layered soil and its effect on pile foundations", PHD Thesis, Rensselaer Polytechnic Institute, Troy, New York.

API (1995), "Recommended practice for planning, designing and constructing fixed offshore platform", Washington, DC: American Petroleum Institute.

API (2002), "Recommended practice for planning, designing and constructing fixed offshore platform", Washington, DC: American Petroleum Institute.

Ashford S. A. & Juirnarongrit T. (2004), "Evaluation of force based and displacement based analyses for responses of single piles to lateral spreading", 11th International conference on Soil dynamics & earthquake engineering, 3rd International conference on earthquake geotechnical engineering, 7-9 January 2004, Berkeley

Bhattacharya S. (2003), "Pile instability during earthquake liquefaction", PHD Thesis, University of Cambridge, UK.

Boulanger R.W., Kutter B.L., Brandenburg S.J., Singh P. and Chang D. (2003), "Pile foundations in liquefied and laterally spreading ground during earthquakes: Centrifuge experiments and analyses" Report No. UCD/CGM-03/01, University of California at Davis.

Brandenburg S.J. (2002), "Behavior of Pile Foundations in Liquefied and Laterally Spreading Ground", PHD Thesis, University of California, Davis

Cubrinovski M, Kokusho T. & Ishihara K. (2004), "Interpretation from Large-Scale Shake Table Tests on Piles subjected to Spreading of Liquefied Soils", 11th International conference on Soil dynamics & earthquake engineering, 3rd International conference on earthquake geotechnical engineering, 7-9 January 2004, Berkeley

Cubrinovski M. , T. Kokusho and K. Ishihara (2006), " Interpretation from large scale shake table tests on piles undergoing lateral spreading in liquefied soils" Soil Dynamics and Earthquake engineering, vol.26

Dobry, R., Abdoun, T., O' Rourke T.D., Goh S.H. (2003), "Single piles in lateral spreads: Field Bending Moment Evaluation", ASCE Journal of Geotechnical and Geoenvironmental Engineering, Vol. 129, No. 10, October, pp. 879-889

Hamada M. (1999), "Similitude law for liquefied-ground flow", Proceedings of the 7th U.S.-Japan Workshop on Earthquake Resistant design of lifeline facilities and countermeasures against soil liquefaction, pp. 191-205.

High Pressure Gas Safety Institute of Japan (2000), "Design method of foundation for Level 2 earthquake motion", (In Japanese)

Ishihara K. & Cubrinovski M. (1998), "Soil-pile interaction in liquefied deposits undergoing lateral spreading", XI Danube-European Conference, Croatia, May 1998

Itasca (2005), "FLAC version 5.0: Fast Lagrangian Analysis of Continua", Itasca Consulting Group, Minneapolis, Minnesota.

Itasca (1997), "FLAC3D version 2.0: Fast Lagrangian Analysis of Continua in 3 Dimensions", Itasca Consulting Group, Minneapolis, Minnesota.

Japan Road Association (1996), "Specifications for highway bridges", Part V Seismic Design

Karamitros D. (2008), PHD Thesis, work in progress

The MacNeal-Schwendler Corporation (1994), "MSC/NASTRAN for Windows: Reference Manual"

Matlock, H. (1970). "Correlations of design of laterally loaded piles in soft clay." Proc. Offshore Technology Conference, Houston, TX, Vol 1, No.1204, pp. 577-594.

- Railway Technical Research Institute (1999), "Earthquake resistant design code for railway structures", Maruzen Co. (in Japanese)
- Reese L.C. and Van Impe W. F. (2001), "Single piles and pile groups under lateral loading", A.A. Balkema/Rotterdam/Brookfield, Book p.p.463.
- Rollins K.M, Gerber T.M., Lane J.D. and Ashford S.A. (2005), "Lateral resistance of a full-scale pile group in liquefied sand", ASCE Journal of Geotechnical and Geoenvironmental Engineering, Vol 131, No. 1, January, pp. 115-125.
- Rollins K.M., Bowles S., Brown D. & Ashford S. (2007), "Lateral load testing of large drilled shafts after blast-induced liquefaction", 4th International Conference on Earthquake Geotechnical Engineering, Paper no 1141, June 25-28, Thessaloniki, Greece
- Valsamis A., Bouckovalas G. & Dimitriadi V., (2007), "Numerical evaluation of lateral spreading displacements in layered soils", 4th International Conference on Earthquake Geotechnical Engineering, Thessaloniki, Greece, June 25-28
- Valsamis A., "Numerical simulation of single pile response under liquefaction-induced lateral spreading", PHD Thesis, N.T.U.A.
- Youd L. T., Hansen M. C. and Bartlett F. S. (2002), "Revised multilinear regression equations for prediction of lateral spread displacement", Journal of Geotechnical and Geoenvironmental Engineering, Vol. 128, No. 12, December 1, pp 1007-1017.

Ground movements during tunnel construction by EPB method along the southern extension of Athens Metro Line 2, Greece

Mouvements de terre pendant la construction du tunnel avec la méthode EPB pour l'extension sud de la Ligne 2 du Métro d'Athènes, Grèce

Elena Papageorgiou

Civil Engineer, M.Sc, Attiko Metro S.A., Greece, epapageorgiou@ametro.gr

Nikolaos Boussoulas

Civil Engineer, M.Sc, Attiko Metro S.A., Greece, nboussoulas@ametro.gr

Fotios Karaoulanis

Civil Engineer, M.Sc, Doctoral Candidate, Aristotle University, Greece, fkar@civil.auth.gr

Stefanos Tsotsos

Prof. of Geot. Eng., Aristotle University, Greece, stsotsos@civil.auth.gr

ABSTRACT

This work is based on a significant number of field records, monitoring data of ground movements and data from the EPB machine used for the excavation of the southern extension of Athens Metro Line 2. Several issues concerning shield tunnelling operation are addressed, while the interaction between ground response and influencing factors during shield advancement is studied, with promising conclusions for the continuance of the present work.

RÉSUMÉ

L'article suivant présente et essaie d'évaluer les rapports d'instrumentation des mouvements de terre et les données provenant de la machine EPB utilisée pour le creusement du tunnel de l'extension sud de la Ligne 2 du Métro d'Athènes. Un nombre considérable de questions concernant l'opération des machines de creusement est examiné, ainsi que la relation entre les mouvements de terre et les facteurs qui influencent les déformations pendant le creusement. L'article présente aussi des conclusions intéressantes pour les études futures.

Keywords : shield tunnelling, Athens Metro, ground movements

1 INTRODUCTION

In recent years, during shield tunnelling (usually associated with closed face machines) the produced ground movements have been greatly reduced due to technological innovations, mainly associated with the face pressure and grouting control. As a result, shield tunnelling with closed face machines is gaining in popularity in developed urban areas and geotechnical engineers are facing the challenge of accurate ground movement prediction.

On this complex geotechnical topic, Professor Robert Mair, introducing the discussion session 3-3 for underground works in urban areas during the XVth ICSMGE (2001), underlined that, when using pressurized face TBMs, the modern tunnelling technology is ahead of our understanding of the fundamental mechanics and that, although the applied techniques improve stability, we cannot yet reliably quantify their effects on ground movements. Furthermore, Professor Mair asked whether geotechnical engineers know enough about the mechanical engineering aspects of TBMs to fully evaluate the influence of face and grouting pressure on ground movements. Also, he asked whether it is possible to evaluate their influence when tunnelling in heterogeneous ground conditions.

This paper, based on various field records and monitoring data of ground movements, as well as on data from the EPB machine which is used along the southern extension of Line 2 of Athens Metro from the existing terminal station of Aghios Dimitrios towards Elliniko, aims at the better understanding of the functioning of shield tunnels, as well as the clarification of the interaction between ground response and influencing factors during shield advancement.

2 MECHANISM OF GROUND DEFORMATION DURING THE TBM SHIELD PASSING THROUGH

Ground deformation due to shield tunneling can be divided in two parts, one that originates from the stress release at the cutting face and at the tail when the shield is passing through, the other being the subsequent deformation occurring after the shield has passed through. The above situation can be expressed with the following equation:

$$\delta_t = \delta_i + \delta_s \quad (1)$$

where:

δ_t = total deformation

δ_i = deformation due to stress release when the shield is passing through

δ_s = subsequent δ_t occurring after the shield has passed through

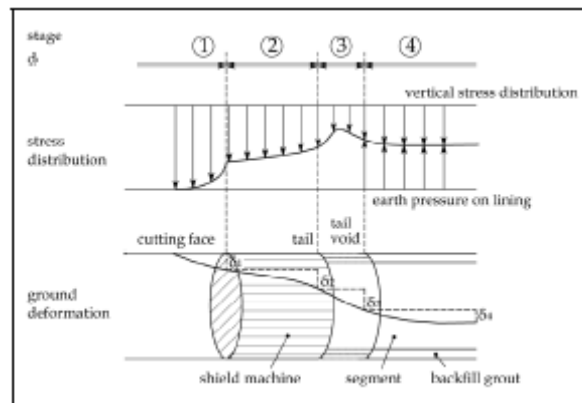


Figure 1. Deformation components during the various stages of shield tunneling (Hashimoto et al. (1999)).

Taking into consideration the different mechanisms of deformation during the various stages of shield tunnelling, Hashimoto et al. (1999) and Bai et al. (2000), distinguish four deformation components instead of two, dividing δ_i , into 3 parts, δ_1 , δ_2 and δ_3 , as is shown in Figure 1.

1st stage, δ_1 Deformation that occurs in front of the cutting face due to the unbalance between earth pressure and shield face pressure.

2nd stage, δ_2 Deformation that occurs while the body of the shield is passing through, mainly due to the disturbance of the surrounding ground and the friction between the shield body and the ground or due to decrease in the soil modulus.

3rd stage, δ_3 Deformation that occurs immediately after the shield has passed through, due to stress release by tail void or sometimes due to the excessive back-fill grouting pressure (ground heave).

4th stage, δ_4 Long term deformation caused by consolidation of the disturbed ground. This last component is a considerable portion of the total deformation, especially in cases of soft clay.

It is remarkable that, according to Bemmebarek et al (2000), one more immediate settlement component is distinguished between δ_1 and δ_2 , at the time of passage of the shield face.

Furthermore, the δ_2 mechanism is differentiated, when the shield is of conical shape (eg. 3 cm along the length of the shield) which facilitates the control of shield position, reduces soil – shield friction, but, due to the gap in the shield shape, conditions for additional direct movement can be created.

In recent bibliography, numerous shield tunnelling cases were described and interesting field observations were pointed out, providing useful information, technical notes, recommendations, and various meaningful approaches for movement prediction. The following are some indicative conclusions:

- In modern shield tunnelling technology, when the earth balance at the cutting face is carefully controlled, the deformation δ_1 is significantly reduced. However with EPB machines it is often difficult to control face pressures.
- In the case of the second Heinenoord tunnel, where slurry tunnelling was used in soft clays, the proportions of the δ_i were 15% prior to shield arrival, 35% from the tapered shield and 50% from the tail void. The conclusion, based not only on the experience from the specific tunnel, but from general practice, is that tail grouting influences the magnitude as well as the shape of the settlement trough. Specifically for EPB machines, the initial percentage of 50%, according to *Bai et al. (2000)*, is reduced to 20% – 30%.
- Movement predictions using various computational methods often offer promising approaches, but there remains a constant need to check and calibrate them with field observations, especially at the early stages of construction.
- In general, the shape of the settlement trough under free field conditions can be simulated by the normal distribution curve. It is characteristic that in the case of four subway lines in the Taipei basin (*Chang et al. 2000*), where the normal distribution curve was fitted by the least square method on the recorded settlement data, the values of the coefficient R^2 were as a rule greater than 0.8, with the highest value being 0.96 and the lowest 0.37.
- Ground movements are very sensitive to tunnelling progress. In order to measure this progress, an index was introduced by *Chang et al. (2000)*, namely the Ground Loss Index (GLI), defined as the sum of the division of back fill volume by tail volume and the division of chamber pressure by the in-situ stress at tunnel depth.

3 EVALUATION OF GROUND MOVEMENTS

The detailed analysis of tunneling construction using TBM and the evaluation of ground movements require the solution of an intricate soil – structure interaction problem, which may prove a rather exhausting task. This occurs because numerous complex factors are involved, such as ground excavation, overcut or annular space between the external side of the lining segments and excavation side, face support by pressure application, installation of rings and grouting of annular space.

In order to overcome this obstacle, a simplified model was proposed by *Oteo & Sagaseta (1982)* and applied to actual cases. According to this model, the maximum settlement at the surface above the tunnel axis, δ_{max} , can be expressed as:

$$\delta_{max} = \psi(0.85 - \nu)\gamma \frac{D^2}{E} \quad (2)$$

where:

- D : tunnel diameter,
- γ : density,
- ν : Poissons ratio,
- E : an average Young's modulus,
- ψ : an overall factor $\psi \leq 1$. The value of this coefficient according to the previous paragraph, depends on various shield characteristics and operational parameters.

In Figure 2, ψ values scatter; their large range and the influence of shield velocity are shown.

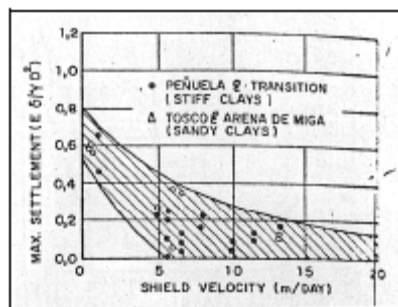


Figure 2. Influence of shield advance rate according to *Oteo & Sagaseta (1982)*.

A similar relationship is included in a recent article on settlements induced by tunneling, presented by the working group "Research" ITA/AITES Report (2006),

$$s_{max} = \kappa \lambda \frac{\gamma R^2}{E} \quad (3)$$

where κ and λ depend on construction method, ground stresses, tunnel geometry, workmanship and experience.

On the other hand, in many published works ground movements are evaluated using numerical 2D or 3D analyses, based on different approaches simulating tunneling process. In the most common 2D cases, the methodologies described are based either on the use of a stress release factor λ , (λ -method) or on the assumption that the support forces are reduced until a particular volume loss value is computed (VL-method). The capability of both approaches depends mostly on the accepted values of λ and VL correspondingly, as well as on the used constitutive model for ground behavior, and on the ground modulus and K_0 values. The use of 3D analyses, in addition to the increase in computational time, requires the realistic estimation of large uncertainties concerning the interaction between the shield and the soil and the magnitude and distribution of tail void after grouting.

Interesting experimental relationships, between recorded ground movements and influencing factors related to shield tunneling operation, have been recently proposed. Thus, according to *Chang et al. (2000)* the Ground Loss Ratio is determined with the following formula (see Figure 3(a)):

$$\text{Ground Loss Ratio} = 16.70 (\text{GLI})^{-2.60} \quad (4)$$

However, results from other work sites, with different geological – geotechnical conditions and other types of boring machines, differ significantly (*Emeriault et. al*).

For that matter, *Chang et al. (2000)* clarify that the coefficients in Equation 4 should be carefully adjusted, if the formula is to be applied in other locations than the one proposed for.

Another interesting experimental relationship for the estimate of tunnel radial convergence is presented in Figure 3(b). The index ITBM in this figure is defined as the ratio $TQ2/Th/ROP$, where TQ is the cutterhead torque (kNm), Th is the thrust (kN) and ROP is the penetration rate (m/h).

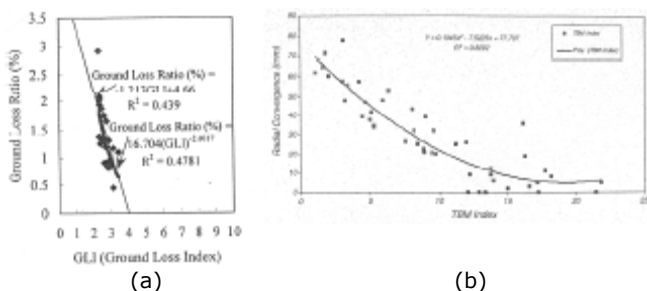


Figure 3. (a) Ground Loss Ratio versus Ground Loss Index according to Chang et al. (2000). (b) The relationship between ITBM and Tunnel Radial Convergence for different areas of the Ghomroud tunnel excavated length, according to Farrock & Rostami (2008).

4 EXPERIENCES FROM EPB TUNNELING ALONG THE SOUTHERN EXTENSION OF ATHENS METRO LINE 2

The double track tunnel of the Athens Metro extension from the existing southern terminal station of Aghios Demetrios towards Elliniko (Figure 4), was constructed during 2007 – 2008, by the Joint Venture “Aktor S.A. – Siemens A.G. – Vinci Constructions Grands Projets”. A Herrenknecht EPB machine was used to excavate 4.65 km of tunnel alignment, with the whole project being 5.5 km long. The diameter of the cutterhead was 9.49 m, but with the added use of regulated cutting tools controlled overexcavation was sometimes effected, reaching up to a tunnel diameter of 9.53 m. The tunnel was lined with rings made by 8 precast concrete segments, with an external diameter of 9.18 m and a thickness of 0.35 m. During tunneling, the influencing factors, used in Equation 4 and in the equation of the ITBM index, were monitored with sensors placed in the excavation chamber, such as face pressure, the quantity of grouting used to fill tail voids, tunneling rate, cutterhead torque and cutterhead thrust.



Figure 4. Map of Athens Metro, where the southern extension is shown.

The encountered geology is multilayered along the alignment, as the ground profile along the whole project usually consists of 3 to 5 layers. In total, 17 ground layers are encountered and classified in separate geological formations, the most important being:

- Athens clay schist – metasandstone – metasilstone
- Marly limestone with variable composition
- Products of weathering and erosion.

It is noticeable that the average Compression Modulus of the main formations varies between 900MPa (marly limestone) and 100MPa (products of weathering).

The following observations, (a) that the average tunnelling rate was 10m/day and (b) that the maximum measured ground settlement was 17 mm, while along 80% of the whole alignment the recorded settlements were lower than 5 mm, strongly indicate that the applied EPB tunneling method must be considered successful.

In the present work, in order to study the interaction between settlements, ground properties and tunneling parameters, a particular section of approximately 300 m length was selected.

Along this particular section the measured settlements varied significantly, with remarkably high values monitored in some locations.

In Figure 5 the following monitoring and computed data are plotted:

- The settlements above the tunnel axis (Figure 5(a)).
- The computed weighted value of an imaginary uniform soil profile modulus, E_w (Figure 5(b)). This modulus is suitable for use in equations (2) and (3). E_w is defined as the unique value of Young’s Modulus for a homogeneous idealized elastic material, which stands for the in-situ multilayer ground profile. The E_w value is estimated using a systematic algorithm based on the following:
 - The Compression Modulus of each layer, determined in the geotechnical investigation and evaluation carried out during the Predesign and Design phase of the Project.
 - The thickness and position of each layer with respect to the tunnel position (Karaoulanis & Tsotsos (2008)).
 - The variability of stress conditions around the tunnel (extension, compression, unloading), as shown in Figure 6.
 - The strain magnitude, which decreases with distance from the excavated area.

The detailed description of the E_w determination process lies beyond the scope and the intentions of the present work.

In the following figures (Figures 5(c)-5(f)) GLI, GLI independent components and ITBM values, as described above, are plotted against chainage for the above mentioned section of 300 m, which is located at approximately the center of the studied alignment

An intensive effort was made, based on the measured data of Figure 5, to examine the possible relationship between settlements and the various tunneling parameters. The conclusion of this work was that, for the specific data, all the considered sets of values seem to be practically unrelated, as the correlation coefficients computed with the aid of smoothing splines and moving averages techniques are low.

5. CONCLUSIONS

Reviewing the available experience from the interpretation of the above work, the following observations were formulated:

- In cases where the measured settlements are not significantly higher compared with the observed measurement error, the determination of an experimental relationship must be considered as unfeasible or at least unreliable.

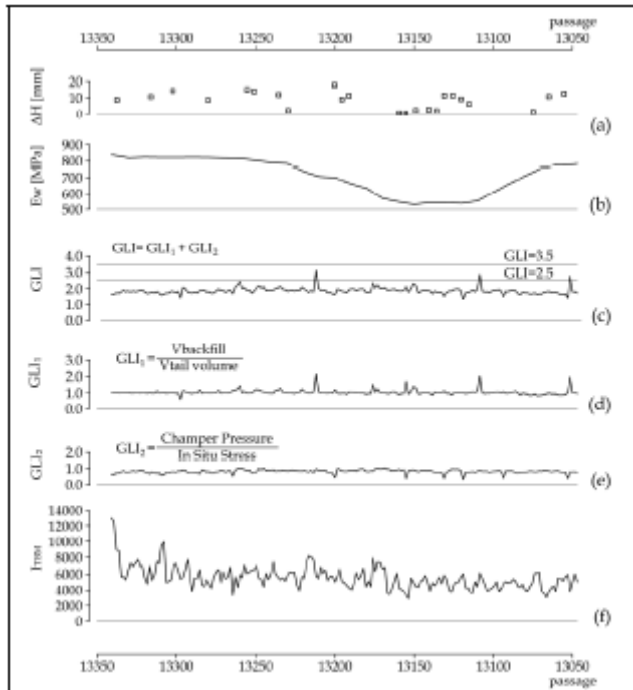


Figure 5. Settlements, E_w , GLI and ITBM values for the area of interest.

- According to Figure 5, GLI values lied between 1.5 and 2.3 and the range of the volume loss was between 0.05 and 0.4%, while the application of Equation 4 leads to values between 2.0% and 3.0%. This large discrepancy confirms the fact that relationships such as the one presented in Equation 4 are valid only under geotechnical conditions comparable to the ones of the equation data. It is important to notice that, concerning the GLI computation, questions and difficulties arise, as the value of the in-situ stress at tunnel depth and the value of the chamber pressure with respect to time show successive peaks and valleys due to reasons that are not yet determined. Furthermore, the surface displacements do not depend alone on the operational conditions, as is shown in Figure 5, but also on the conditions along a surrounding area of appropriate width.
- According to Figures 5(a) 5(b), as well as the results of the application of Equation 2, the highest measured values of settlement correspond to ψ values between 0.6 and 0.8. This observation indicates that the application of relationships for values of ψ approaching 1.0, forms an upper limit for ground settlements.

The combination of the above remarks guides us towards a more general approach, as shown in Figure 7. However, the determination of a more general relationship, requires a more developed database, enriched with data from various works and different ground conditions, as expressed by E_w .

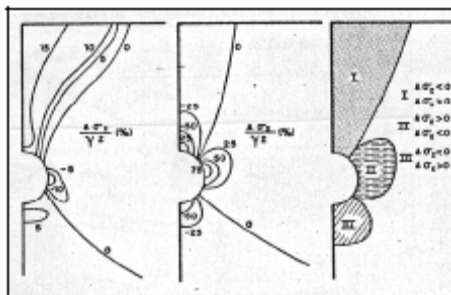


Figure 6. Stress paths around the tunnel according to Oteo & Sagaseta (1982).

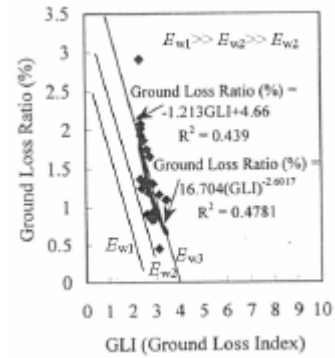


Figure 7. Ground loss ratio versus ground loss index for various E_w values.

ACKNOWLEDGMENTS

The authors gratefully acknowledge the Athens Metro Management's permission to publish this case history. The arguments and conclusions presented in this paper express only the personal opinion of the authors and do not necessarily depict the official view of ATTIKO METRO S.A. Also, Fotios E. Karaoulanis wishes to acknowledge financial support from the Greek State Institute of Scholarships (I.K.Y.); contract/grant number: 4506/05.

REFERENCES

Bai, Y., Liu, Q.W. and Zhao, J. 2000. Deformation analysis based on shield tunneling and soil conditions with case studies from Shanghai Metro tunnels. Tunnels and Underground Structures, Zhao, Shirlaw & Krishnan (eds), Balkema, Rotterdam, pp.527-534, 2000.

Benmebarek, S., Kastner R. and Ollier C. 2000. Reducing settlement caused by shield tunneling in alluvial soils. Geotechnical Aspects of Underground Construction in Soft Ground, Kusakabe, Fujita & Miyazaki (eds), Balkema, Rotterdam, pp.203-208, 2000.

Chang, C.T., Wang J.J. and Chen Y.W. 2000. Factors influencing the ground loss due to tunnels driven by EPB shield. Geotechnical Aspects of Underground Construction in Soft Ground, Kusakabe, Fujita & Miyazaki (eds), Balkema, Rotterdam, pp.209-212, 2000.

Emeriault, F., Bonner-Eymard T., Vanoudheuden E., Petit G., Robert J., Lamballerie J.Y. and Reynaud B. 2005. Ground movements induced by Earth-Pressure Balanced, Slurry Shield and Compressed-Air tunneling techniques on the Toulouse subway line B. Underground Space Use: Analysis of the Past and Lessons for the Future - Erdem & Solak (eds) London, pp.841-847, 2005.

Farrokh, E. and Rostami J. 2008. Correlation of tunnel convergence with TBM operational parameters and chip size in the Ghomroud tunnel, Iran. Tunnelling and Underground Space Technology 23, pp.700-710, 2008.

Hashimoto, T. Nagaya J. and Konda T. 1999. Prediction of ground deformation due to shield excavation in clayey soils. Soils and Foundations 39, pp.53-61, 1999.

ITA/AITES Report 2006 on Settlements induced by tunneling in Soft Ground. Tunnelling and Underground Space Technology 22, pp.119-149, 2007.

Karaoulanis, F. and Tsotsos S. 2008. Numerical analysis of tunnel excavations in layered soils. 6th GRACM International Congress on Computational Mechanics, Thessaloniki, 19-21 June 2008.

Mair, R.J. and Standing, J.R. 2001. Discussion Session 3.3. Underground work in urban areas including its impact on

existing infrastructure. Proceedings of the Fifteenth International Conference on Soil Mechanics and Geotechnical Engineering, Vo. 4, p.2715, 2001.

Oteo, C.S. and Sagaseta, S. 1982. Prediction of settlements due to underground openings. International Symposium on Numerical Models in Geomechanics, pp.653-659, Zurich, 1982.

Numerical simulation of the pore pressure regime in landslides with underdrainage

Simulation numérique du régime de pression des pores dans des glissements avec sous-drainage

Bardanis, M., Cavounidis, S., Dounias, G.
Edafos Consulting Engineers S.A., Athens, Greece

ABSTRACT

Large palaeo-landslides with considerable movements have sometimes caused the burial of permeable formations by the landslide mass. The pore pressure regime established in the landslide material where it overlies these permeable formations is strongly non-linear with depth. A close to hydrostatic pore pressure may be maintained down to a considerable depth, followed by a sharp drop upon approaching the base of the landslide material, to reach the pore pressure of the underlying permeable strata. This pore pressure profile is known as underdrainage profile. The paper presents the results of numerical analyses investigating the effect of inhomogeneity and anisotropy of the coefficient of permeability and infiltration from the ground surface. In order for such a non-linear pore pressure profile to exist in landslide materials there must be considerable infiltration from the ground surface and the coefficient of permeability of the landslide material must decrease with depth. This decrease is often due to the increase in vertical stress in the landslide material and also due to the orientation of clay particles along the slip surface, which may be located immediately above the upper boundary of the buried permeable formation.

RÉSUMÉ

Les paléo-glissements de grande taille avec des mouvements importants dès qu'ils apparaissent pour la première fois, peuvent mener quelquefois à l'enterrement des formations perméables par la masse glissante. Le régime de la pression de pores établi dans le matériel de l'éboulement, quand ceci recouvre ces formations perméables, est fortement non-linéaire avec la profondeur. Le profil de la pression de pores est considéré comme un profil de sous-drainage, vu que une pression de pores considérable peut être soutenue dans les matériaux du glissement jusqu'à une profondeur importante, avant que ça diminue dramatiquement à la base du matériel de glissement pour atteindre la valeur de la pression de pores dans la formation perméable enterrée. Cet article présente les résultats des analyses numériques qui investiguent l'effet de l'inhomogénéité et de l'anisotropie du coefficient de perméabilité et infiltration de la surface. Pour qu'un tel profil non-linéaire de pression de pores existe dans les matériaux de glissement, il faut qu'une infiltration considérable ait lieu à la surface et que le coefficient de perméabilité des matériaux de glissement diminue avec la profondeur. Cette diminution est souvent due à l'augmentation de la pression verticale dans les matériaux de glissement et aussi due à l'orientation des particules de l'argile au long de la surface du glissement qui peut être située immédiatement au dessus de la frontière supérieure de la formation perméable enterrée.

Keywords : Landslides, pore pressure, underdrainage, non-linearity, coefficient of permeability

1 INTRODUCTION

Large scale palaeolandslides with considerable movements often lead to the burial of permeable formations such as river gravel. The latter seems to be the formation most frequently buried by landslide materials, as rivers eroding the toes of valley slopes cause destabilization and movement of the landslide mass towards the toe. Bardanis et al. (2006) presented examples of two landslides in Greece, the toe of which has covered old river beds, while Dounias &

Dede (2006) presented an example of a landslide the toe of which had covered permeable sandstones. The common characteristic in all three cases is that within the low permeability landslide materials an underdrainage pore pressure profile is established which is in equilibrium with the lower pore pressure in the underlying permeable formation and the infiltration condition at the ground surface. The paper presents the general shape of such pore pressure profiles, investigates numerically the factors causing their development (coefficient of permeability, infiltration boundary condition) and concludes with a summary of the parameters that need to be determined numerically before proceeding with simulations of the effect of drainage measures on the pore pressure regime of the landslide. The importance of this type of pore pressure profile lies in that it may be employed in a drainage scheme consisting of vertical large diameter wells drilled from the ground surface and extending down into the permeable formation. These wells allow a decrease of the pore pressure at the slip surface, which is often located just above the boundary between permeable formations and landslide materials.

2 PORE PRESSURE REGIME

The general form of an underdrainage pore pressure profile in low permeability landslide materials overlying a permeable formation in equilibrium with a much lower pore pressure is presented in Fig. 1. This is a theoretical profile drawn by considering the field measurements on three different cases (Bardanis et al, 2006; Dounias & Dede, 2006). The profile follows essentially the hydrostatic pore pressure distribution from a shallow depth from the ground surface down to a small distance from the boundary between low and high permeability materials and then the pressure drops considerably to the much lower value in the underlying permeable formation. When river gravel is buried, it often communicates with the existing river bed and its pressure reflects the water level in the present river.

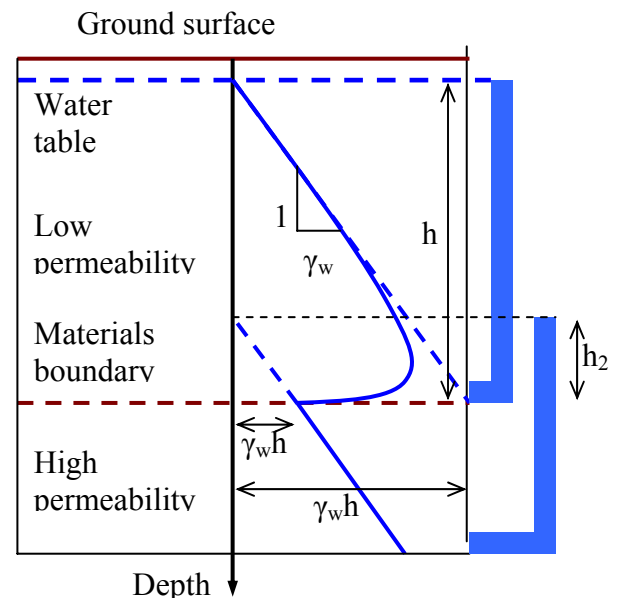


Fig. 1. Pore pressure distribution with depth in low permeability soil overlying higher permeability layer under lower pressure.

Similar pore pressure profiles have been reported by Kennard & Reader (1975), Vaughan & Wallbancke (1975), and Vaughan (1994), who attribute their presence to the decrease in the coefficient of permeability k with depth as a result of stress increase with depth and the corresponding decrease of void ratio. Bromhead & Vaughan (1980), Vaughan et al. (1983) and Vaughan (1989) have

investigated the effect of various types of distributions of the coefficient of permeability on the pore pressure profiles.

The underdrainage profiles reported in the aforementioned references however are characterised by a gradual decrease in the pore pressure that begins at quite a large distance from the interface between low permeability and high permeability material. Bardanis et al. 2006 have reported underdrainage pore pressure profiles exhibiting a decrease in the pore pressure at a much smaller distance from the interface between low and high permeability formations. These profiles were observed in landslide materials overlying permeable formations like old river beds, and the decrease in pressure was observed in the sub-layer lying only 2-3m above the interface, which contained the slip surface. In the vicinity of the slip surface the coefficient of permeability in the vertical direction k_v is expected to decrease even to a lower value than the one corresponding to the stress level at that depth as a result of the orientation of the clay particles parallel to the slip surface turning the slip surface into an impermeable "membrane" that inhibits the movement of pore water from the landslide material into the underlying permeable layer.

3 NUMERICAL ANALYSIS OF SEEPAGE

A simplified model was used instead of the actual landslide geometry, in order to illustrate the conclusions derived from the analysis. The problem was investigated numerically using the finite element method (FEM) as this is incorporated into SLIDE (Rocscience Ltd.). The geometry of the simplified example is presented in Fig. 2. The numerical model consisted of 415 quadrilateral eight-noded elements with degrees of freedom on pore pressure and seepage velocity. The landslide modelled has a length of 120m, a maximum depth of 17m, and a depth of the buried river bed of 5m. The landslide mass in Fig. 2 lies within BCDEFG, the permeable layer lies within DEFHIJK, and under them an intermediate layer was introduced down to LMNO, under which the rockbed was introduced as an impermeable layer.

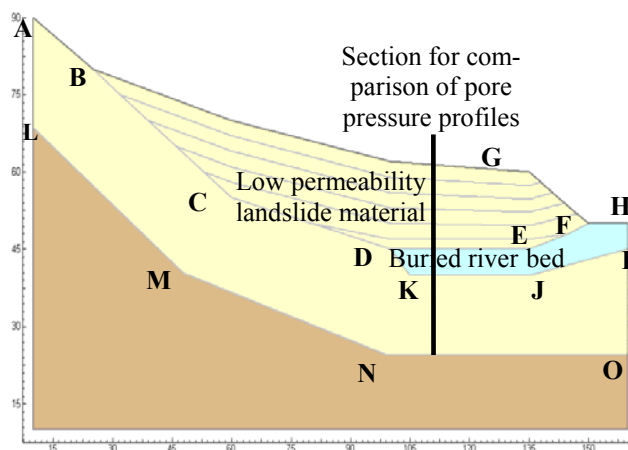


Fig. 2. Assumed simplified geometry.

4 HOMOGENEITY AND ANISOTROPY OF THE COEFFICIENT OF PERMEABILITY

The effect of the coefficient of permeability on the pore pressure profile was first investigated. Initially a unique value of the coefficient of permeability was investigated. Five different values of the coefficient of permeability were introduced into the model for the landslide materials (10^{-8} , 10^{-9} , 10^{-10} , 10^{-11} & 10^{-12} m/s, while the coefficient of permeability of the permeable layer was set at 10^{-4} m/s). None of these values allowed the prediction of the underdrainage profile and a linear hydrostatic distribution from the ground surface all the way to the bottom of the model was obtained.

After this stage, inhomogeneity was introduced in the coefficient of permeability of the landslide material. As inhomogeneity cannot be introduced directly into SLIDE, this was modelled by introducing separate layers into the landslide material in the model of Fig. 2, each having a different value of k . The layers were parallel to the ground surface in the part where the permeable layer is covered. The layers do not continue to be parallel to the ground surface at the toe of the landslide as the toe is formed by the erosion caused by the river and therefore a fair assumption is that the coefficient of permeability corresponds to a void ratio consistent with the stress regime before the erosion of the toe.

The coefficient of permeability profiles with depth that were introduced are presented in Fig. 3. Due to the introduction of inhomogeneity with different layers, these linear profiles were introduced as step profiles, with k values for each layer corresponding to the middle of each layer from the linear distribution. A linear distribution of the logarithm of the coefficient of permeability with vertical effective stress and therefore depth was assumed. The general form of such a relation is described by Eq. 1, where a is the coefficient of proportionality.

$$\log k = a \cdot \sigma'_v \quad (1)$$

For all distributions for the coefficient of permeability, the same value of k was assumed for the depth at the middle of the landslide materials (10^{-8} m/s) and only the coefficient of proportionality a was changed. Five values of a were introduced: a) -0.050, b) -0.075, c) -0.100, d) -0.125, and e) -0.150 (Fig. 4). In a real problem the value of k may be determined from field and laboratory permeability measurements. Once again none of these values allowed the prediction of the underdrainage profile and a linear hydrostatic distribution from the ground surface all the way to the bottom of the model was obtained. Inhomogeneity of the coefficient of permeability by itself therefore does not allow the prediction of underdrainage profiles.

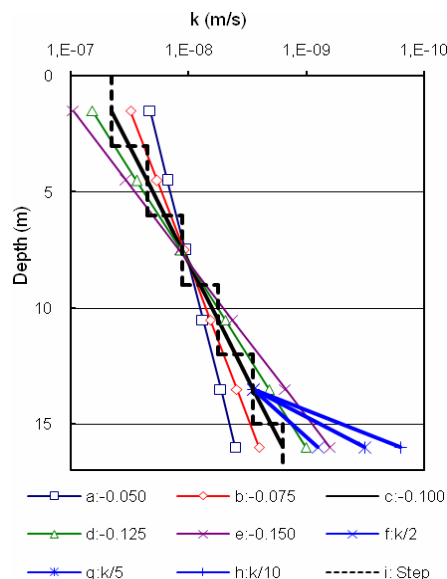


Fig. 3. Tested distributions of coefficient of permeability with depth for the landslide material.

In the last set of analyses investigating the effect of the coefficient of permeability, a decrease in the value of k was introduced for the lowest sub-layer of the landslide materials right above the permeable soil layer. The k -profile used in these analyses was profile c in Fig. 3 (where factor a corresponds to real data for totally weathered siltstone from north-western Greece, -Bardanis et al. 2006). The decrease in the value of k was introduced only in the

vertical direction, while in the horizontal direction the value of k was kept constant, at the value corresponding to k -profile c for this depth. k_v was decreased 2 times (profile f), 5 times (profile g), and 10 times (profile h) over k_h . The latter was assumed to remain constant, equal to the value corresponding to the void ratio for the stress level at that depth, while the former was assumed to decrease as a result of the orientation of clay particles parallel to the slip surface. Once again the observed pore pressure profile could not be predicted, indicating that further decrease of k_v at the sub-layer containing the slip surface does not alone allow the prediction of underdrainage profiles.

5 EFFECT OF THE BOUNDARY CONDITIONS

The next set of analyses involved the investigation of the boundary condition at the ground surface of the landslide. Infiltration is affected by slope inclination, altitude, soil type and its degree of saturation near the surface, presence and type of plants covering the ground surface etc. Attempting to model in detail the infiltration condition along the ground surface is an almost impossible task. Therefore, a single value of infiltration was introduced into each of the analyses.

The results of these analyses are presented in Fig. 4. For a constant value of the coefficient of permeability in the landslide material, the presence of an infiltration condition at the ground surface has no effect at all (Fig. 4a). For inhomogeneously permeable landslide materials an underdrainage profile is actually predicted, as the larger the decrease of k with depth the closer the predicted profile comes to the theoretical one (Fig. 4b). Also, as may be seen in Fig. 4c, the larger the decrease of k_v in the lowest sublayer the better the theoretical profile is predicted. Finally, controlling for the value of infiltration allows essentially an exact prediction of the theoretical profile which deviates from it only because a step k -distribution was introduced rather than a continuous one.

6 THE PORE PRESSURE REGIME IN THE PRINOTOPA LANDSLIDE, EPIRUS, GREECE

The Prinotopa landslide is located on the path of Egnatia Highway, close to the city of Metsovo in the region of Epirus in north-western Greece. The toe of the landslide practically coincides with the northern bank of the Metsovitikos river, which in the area of the landslide has been diverted to the south by the movement of the landslide mass. The considerable movement of the landslide mass of this palaeolandslide has led to the burial of the old river bed of the Metsovitikos river. Still the buried river bed is hydraulically connected to the present river bed. The maximum depth of the slip surface is in the order of 50m, determined by a large number of inclinometer readings, and it is found in the area where the landslide material overlies the buried river bed. There, the slip surface is located approximately 1-2m above the buried river bed.

The landslide materials consist of siltstone, totally weathered into sandy silty clay with occasional limestone boulders which have been mixed with the landslide materials. The prevailing fines of the landslide material have on average: $w_L=40\%$, $I_p=21$, $\gamma_d=18.5 \text{ kN/m}^3$, and a void ratio ranging from 0.24 to 0.87. The values of the coefficient of permeability measured in-situ, using ceramic tip piezometers with the piezometer tips at various depths, vary from $6.3 \times 10^{-10} \text{ m/s}$ to $3.7 \times 10^{-7} \text{ m/s}$. Measured k values are plotted with depth in Fig. 5, along with the continuous and stepped distribution that was used to model the landslide material. Dry unit weight increased with depth while void ratio and coefficient of permeability decreased with depth. The buried river bed consisted of coarse gravel with sand.

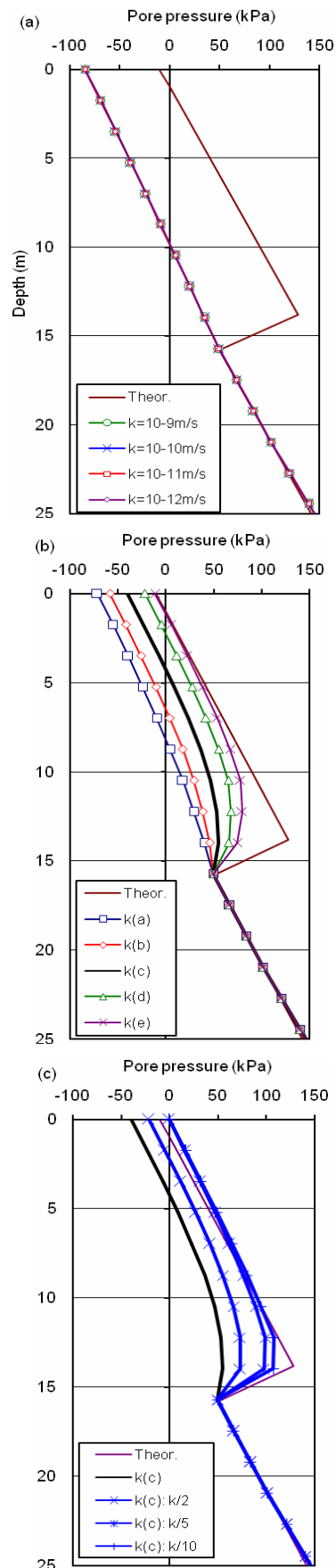


Fig. 4. Theoretical distribution of pore pressure with depth compared to predicted by FEM analyses after introduction of infiltration from the ground surface with: a) homogeneous with depth coefficient of permeability, b) coefficient of permeability decreasing with depth, and c) coefficient of permeability decreasing with depth with further decrease at the zone of the slip surface (distributions of coefficient of permeability with depth as shown in Fig. 3).

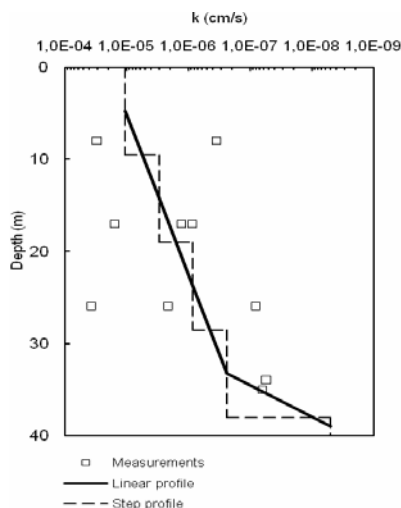


Fig. 5. Coefficient of permeability at various depths in Pri-notopa landslide.

A part of the stabilisation measures of the landslide consisted of large vertical wells drilled from the ground surface down to 4-5m into the buried river bed. These wells would drain the landslide material down into the permeable material of the buried river bed, by reducing the high pressures in the vicinity of the slip surface. For the design of this drainage system, the initial condition of the underdrainage pore pressure profile needed to be modelled, essentially as a benchmarking exercise of the numerical model that would yield parameters necessary to carry out the analysis of the drainage wells. The results of the analysis are presented in Fig. 6. Introducing the stepped distribution of the coefficient of permeability shown in Fig. 5 and an even infiltration of 1.3×10^{-9} m/s at the ground surface (which is consistent with rainfall, evaporation and transpiration data for the area) allowed a good prediction of the pore pressure profile. In agreement with the results of the numerical analysis in the theoretical model, anisotropy of the coefficient of permeability was introduced in the sub-layer of the landslide material containing the slip surface ($k_v = 1/10$ of k_h).

7 CONCLUSIONS

In order for an underdrainage pore pressure profile to be predicted in landslides underlain by permeable formations, the following should be considered:

- i) Inhomogeneity of the landslide material must be introduced. This corresponds to a decrease of k with depth, which is consistent with increasing stress level with depth in landslide materials.
- ii) A further decrease of k must be introduced for the zone containing the slip surface. This may be introduced by anisotropy of k , with a much lower value in the vertical direction than in the horizontal, which is consistent with the orientation of clay particles in the vicinity of the slip surface.
- iii) When landslide materials are highly disturbed, anisotropy should not be introduced throughout their mass but only in the zone containing the slip surface. Introducing anisotropy in the whole landslide mass may not alter the results of the benchmarking exercise but it may result in misleading predictions when the drainage measures are introduced at the following stage of numerical investigation.
- iv) Introducing inhomogeneity in the landslide mass and anisotropy in the vicinity of the slip surface does not allow the prediction of an underdrainage profile, as the fundamental requirement is the introduction of

infiltration as a boundary condition at the ground surface. The actual value of infiltration, and the length along the ground surface in the model that it is applied, is more the result of a back analysis rather than exact calculation. If records of rainfall and evaporation are available, the mean value of their difference seems like a good starting point for the analyses investigating the value of infiltration to be carried out.

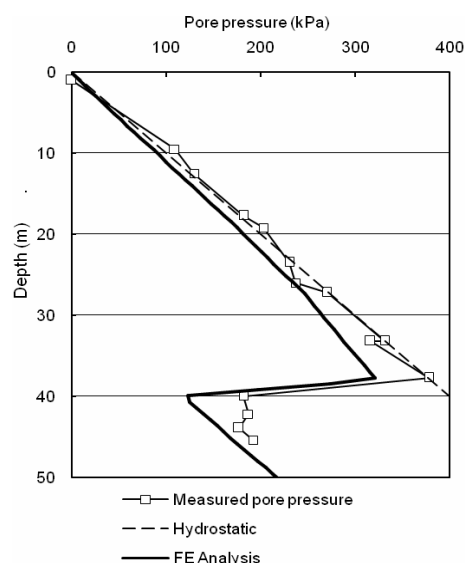


Fig. 6. Measured and predicted by FEM initial pore-pressure profile.

REFERENCES

- Bardanis, M., Dounias, G., Cavounidis, S. (2006), "Examples of low permeability landslide materials with underdrainage from Greece", Proc. 5th Hellenic Conf. on Geot. & Geoenv. Engng, Xanthi, Greece, Vol. II, pp. 603-610 (in Greek).
- Bromhead, E.N., Vaughan, P.R. (1980) "Solutions for seepage in soils with an effective stress dependent permeability", Proc. Conf. Num. Methods for Non-linear Problems, Vol 1, pp. 567-578.
- Dounias, G., Dede, V., (2006), "Stabilisation of the '93 landslide at the Evinos reservoir with drainage galleries", Proc. 5th Hellenic Conf. on Geot. & Geoenv. Engng, Xanthi, Greece, Vol. III, pp. 35-42 (in Greek).
- Kennard, M.F., Reader, R.A. (1975) "Cow Green dam and reservoir", Proc. Instn Civ. Engrs, Part 1, 58, May, pp. 147-175.
- Vaughan, P.R. (1989) "Non-linearity in seepage problems-theory and field observations", De Mello Volume, Sao Paulo, Edgar Blucher, pp. 501-516.
- Vaughan, P.R., Kennard, R.M., Greenwood, D.A. (1983) "Squeeze grouting of a stiff fissured clay after a tunnel collapse", Proc. 5th Eur. Conf. Soil Mech., Helsinki, Finland, Vol 1, pp. 171-176.
- Vaughan, P.R., Wallbancke, H.J. (1975) "The stability of cut and fill slopes in boulder clay", Proc. Symp. Engng Behaviour of Glacial Materials, Birmingham, Midland Society for Soil Mechanics and Foundation Engineering, pp. 209-219.

Probabilistic analysis in slope stability

Analyses Probabilistes de stabilité des pentes

M. Kavvasas, M. Karlaftis, P. Fortsakis, E. Stylianidi
National Technical University of Athens, Greece

ABSTRACT

Geotechnical design is, perhaps, the civil engineering subject most dominated by uncertainty. Although partly due to limited field investigations, the main reason of this uncertainty is the highly heterogeneous and anisotropic nature of ground materials. Deterministic design methods as required by design codes, attempt to account for ground uncertainty by adopting conservative values of ground parameters and relatively large safety factors. This paper performs probabilistic analyses of soil slopes using Monte Carlo simulation in order to investigate the effect of these assumptions on the calculated probability of failure of the slopes. For slopes in saturated cohesive materials under undrained conditions an analytical solution is proposed while for drained conditions parametric analyses are performed. It is shown that slopes designed according to Eurocode 7 (EN1997-1) correspond to probabilities of failure up to 12%. Based on the results of these analyses, diagrams are proposed for the estimation of the probability of failure as a function of the geometrical, geotechnical and support parameters of the slope.

RÉSUMÉ

Le calcul géotechnique est probablement l'endroit le plus incertain de génie civil à cause de l'hétérogénéité et l'anisotropie du sol. Les calculs déterministes, après les demandes des codes et règlements, adoptent des valeurs conservatrices pour les paramètres du sol et des facteurs de sécurité assez élevés, pour dépasser ces incertitudes. L'article performe des analyses probabilistes de stabilité des pentes avec la simulation de Monte Carlo pour étudier l'approche précédente. Dans un tel contexte, la stabilité des pentes dans un milieu saturé et cohésive se divise en conditions non drainé, où une solution analytique est proposée, et en conditions drainé, avec des analyses paramétriques. Il est montré que la stabilité des pentes en fonction de Eurocode 7 (EN1997-1) donne de probabilité d'échec de 12%. Basé sur les résultats, des diagrammes sont proposés pour l'estimation de la probabilité d'échec en fonction des paramètres géométrique, géotechnique et soutènement de la pente.

Keywords : Probabilistic analysis, Slope stability, Eurocode 7, Monte Carlo Simulation

1 INTRODUCTION

Despite the uncertainties involved in slope stability problems, the civil engineering profession has been slow in adopting probabilistic techniques (e.g. El-Ramly et al. 2002). All design codes, including Eurocode 7 (2004), attempt to account for ground uncertainty by adopting conservative (characteristic) values of ground parameters and relatively large safety factors.

In order to investigate the stochastic characteristics of slopes designed according to the methodology proposed by Eurocode 7, parametric analyses are performed for a very wide range of geometrical, geotechnical and support parameters of soil slopes. The investigated slopes have height and inclination which provides marginally adequate safety according to the requirements of Eurocode 7 for the ultimate limit state (ULS) of overall stability, using planar failure surfaces and the Mohr-Coulomb failure criterion.

Since slope failure on a planar surface is a force equilibrium problem the distributed forces acting on the slope surface (typically support measures such as nails, anchors, geotex-

tiles, etc.) can be represented by a single concentrated force (F).

Ground strength parameters are considered as random variables following truncated normal distribution. Cohesion and friction angle are considered to be statistically uncorrelated. Unit weight, geometrical and support parameters are considered as deterministic variables.

A probabilistic analysis is then performed for these slopes using Monte Carlo simulation to determine the probability distribution of the safety factor and the corresponding probability of failure (p_f) of the slope (i.e., when the safety factor is less than unity) as a function of the problem parameters.

For the case of slopes in saturated cohesive soil under undrained conditions, an analytical solution is presented for the calculation of the probability of failure.

2 SLOPE DESIGN ACCORDING TO EUROCODE 7

According to Eurocode 7, the overall stability of slopes must be verified in ultimate limit states GEO and STR using one of the three Design Approaches (DA). In Greece, Design Approach 3 (DA-3) is used for slope stability problems (National Annex 2007). The relevant partial factors are presented in Table 1.

Table 1. Partial factors of safety according to Eurocode 7 (DA-3)

	Set	Partial factor
Permanent favourable actions, γ_G	A2	1.00
Angle of shearing resistance, γ_{φ} (applied to $\tan\varphi$)	M2	1.25
Effective cohesion, γ_c	M2	1.25
Undrained shear strength, γ_{cu}	M2	1.40
Earth resistance, $\gamma_{R,e}$	R3	1.00
Model uncertainty factor*, γ_M		1.10

* for usual unfavourable hydraulic conditions (National Annex 2007)

Since slope stability problems usually involve a large volume of soil, failure depends on the distribution of the mean values of soil strength parameters (Frank et al 2004). Therefore the relevant characteristic values are determined from the following formulae (Schneider 1999).

$$c'_{k} = m_{c'} - 0.50 V_{c'} \cdot m_{c'} \quad (1)$$

$$\varphi'_{k} = m_{\varphi'} - 0.50 V_{\varphi'} \cdot m_{\varphi'} \quad (2)$$

$$c_{u,k} = m_{c_u} - 0.50 V_{c_u} m_{c_u} \quad (3)$$

where $m_{c'}$, $m_{\varphi'}$, m_{c_u} are the mean values and $V_{c'}$, $V_{\varphi'}$, V_{c_u} the coefficients of variation of the geotechnical strength parameters.

The probabilistic analysis proposed is based on the conservative assumption that the standard deviation of the mean value of soil strength parameters equals the standard deviation of the original variable. This assumption results in larger probability of failure and has been adopted because it is difficult and computationally very cumbersome to analytically consider spatial averaging in parametric analyses.

According to Eurocode 7, the design parameters entering the calculations are obtained by dividing the characteristic values by the corresponding partial factors $\gamma_{\varphi'}$, $\gamma_{c'}$ and γ_{c_u} .

$$c'_{d} = c'_{k}/\gamma_{c'} \quad (4)$$

$$\varphi'_{d} = \varphi'_{k}/\gamma_{\varphi'} \quad (5)$$

$$c_{u,d} = c_{u,k}/\gamma_{c_u} \quad (6)$$

3 SLOPES IN SOIL

A wide range of slopes was analysed using the following ranges of geometrical, geotechnical and support parameters:

Table 2. Range of analysed parameters

Parameters	Range of values	Number of values
Slope height, H, m	5-40	8
Soil unit weight, γ , kN/m ³	21	1
Cohesion mean value, m_c , kPa	0-150	31
Friction angle mean value, m_ϕ , deg	20-40	11
Force parameter $F/(\gamma H^2)$	0-0.15	7
Number of slopes examined		19096

Assuming a planar failure surface at an inclination (θ) with respect to the horizontal, the factor of safety (FS) is calculated from Equation 7 (Duncan & Wright 2005).

$$FS = \frac{2 \cdot c' \frac{H}{\sin\theta} + \gamma H^2 \frac{\sin(\beta - \theta)}{\sin\beta} \cdot \frac{\tan\phi'}{\tan\theta} + 2F \sin(\theta + \omega) \tan\phi'}{\gamma \cdot H^2 \cdot \frac{\sin(\beta - \theta)}{\sin\beta} - 2F \cos(\theta + \omega)} \quad (7)$$

where (β) is the slope inclination and (ω) is the angle of the support force (F).

The analysis procedure is illustrated in Figure 1. FS_{det} is the deterministic value of the safety factor calculated from Equation 7 using the design values of all parameters.

The adopted coefficients of variation of the ground parameters are: cohesion $V_{c'} = 0.40$ (Schultze 1972), friction angle $V_{\phi'} = 0.12$ (Fredlund & Dahlman 1972).

Among the analysed slopes, 10890 are marginally safe according to Eurocode 7, i.e., they satisfy the relationship $FS_{det} = \gamma_M$. For these slopes, a probabilistic analysis is performed using Monte Carlo simulation to determine the probability of failure.

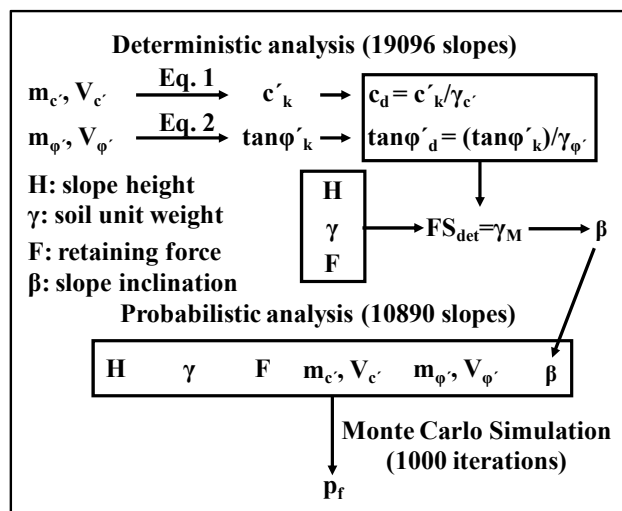


Figure 1. Analysis flow chart

Figure 2 presents the distribution of p_f for all slopes analysed. The range of p_f is very large (0-12%) considering that all slopes are marginally safe according to the same deterministic methodology (Eurocode 7). The probability of failure is not uniformly distributed in this range but appears to follow an exponential distribution. Furthermore, about 30% of the slopes have $p_f > 5\%$, a value which can be considered as an acceptable limit.

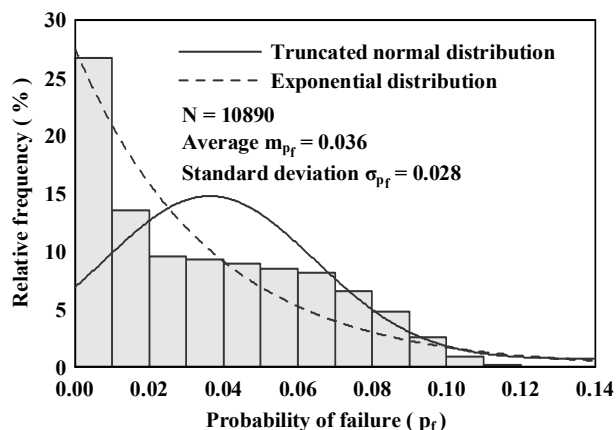


Figure 2. Distribution of the probability of failure for slopes in soil

It was thus attempted to correlate the calculated p_f with the following normalized parameters for the cohesion : $m_c / \gamma H$ and the support force : $F / \gamma H^2$, while the friction angle is considered to be statistically insignificant. Table 3 shows the calculated correlation coefficients:

Table 3. Correlation coefficients of p_f and input parameters

	$\tan\phi'$	$m_c / \gamma H$	$F / \gamma H^2$
p_f	-0.25	0.91	-0.48

The best fit was obtained for the following formula as shown in Figure 3.

$$p_f = 0.087 + 0.33 (1 - F / \gamma H^2) (m_c / \gamma H) \quad (8)$$

The above relationship shows that an increase of the support force decreases the probability of failure of the slope, because the support force is a deterministic favourable action. On the contrary, an increase of the cohesion increases p_f because cohesion has high variability. Therefore, slopes in overconsolidated plastic clays have higher p_f than slopes in sandy or gravelly clays when designed with the same deterministic methodology.

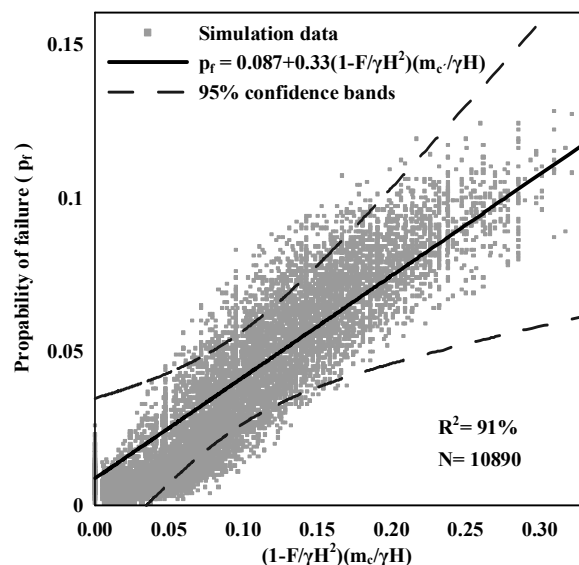


Figure 3. Correlation of the calculated probability of failure (p_f) of 10890 typical slopes in soil with input strength (m_c) and support (F) parameters

4 SOILS UNDER UNDRAINED CONDITIONS

Short-term stability of slopes in fully saturated clays is controlled by the undrained shear strength (c_u) and is commonly analysed using total stresses: $c=c_u$ and $\phi_u=0$. The undrained shear strength of clays has relatively high variability of the order $V_{cu}=0.40$ (Harr 1987; Kulhawy 1992).

The deterministic factor of safety (FS_{det}) under undrained conditions assuming a planar failure surface is given by the formula (Duncan & Wright 2005):

$$FS_{det} = \frac{2 \cdot \frac{c_{u,k}}{\gamma_{cu}} \cdot \frac{1}{\gamma H}}{\frac{\sin(\beta - \theta) \cdot \sin \theta}{\sin \beta} - \frac{F}{\gamma H^2} \cdot \sin 2\theta} \quad (9)$$

Using Monte Carlo simulation, as above, the correlation factors between the probability of failure and the dimensionless parameters $m_{cu}/\gamma H$ and $F/\gamma H^2$ are -0,03 and 0,02 respectively, indicating that the mean value of the undrained shear strength (m_{cu}) and the stabilizing force (F) are not correlated with the probability of failure of the slope.

The critical angle of the failure plane (θ_{cr}) is obtained by setting the derivative of FS with respect to the angle θ equal to zero, which gives:

$$\frac{\sin(\beta - 2\theta_{cr})}{\sin \beta \cdot \cos 2\theta_{cr}} = \frac{2F}{\gamma H^2} \quad (10)$$

Consequently, the critical angle θ_{cr} does not depend on the undrained shear strength c_u and it is a deterministic variable.

By setting the denominator of Equation 9 equal to A, the total deterministic factor of safety ($FS_{det,total}$) is :

$$FS_{det,total} = \frac{2c_{u,k}}{A\gamma H} \quad (11)$$

i.e., the factor of safety is proportional to the random variable c_u while all other dependencies are deterministic. Hence, it is feasible to express the stochastic factor of safety through an analytical solution.

The total stochastic factor of safety ($FS_{st,total}$) is expressed by using undrained shear strength c_u as a stochastic variable which follows the truncated normal distribution :

$$FS_{st,total} = \frac{2c_u}{A\gamma H} \quad (12)$$

By replacing the value A from Equation 11, Equation 12 gives :

$$FS_{st,total} = \frac{FS_{det,total}}{c_{u,k}} \cdot c_u \quad (13)$$

The standard deviation of the undrained shear strength is expressed as:

$$\sigma_{cu} = V_{cu} \cdot m_{cu} \quad (14)$$

Finally, the expression of the $FS_{st,total}$ using Equations 3 and 14 is :

$$FS_{st,total} = \frac{FS_{det,total}}{m_{cu}(1-0.5 \cdot V_{cu})} \cdot c_u \quad (15)$$

According to the principles of statistics, $FS_{st,total}$ follows normal distribution as it is a linear combination of the stochastic variable c_u . The mean value ($mFS_{st,total}$) and the standard deviation ($\sigma FS_{st,total}$) of $FS_{st,total}$ are:

$$mFS_{st,total} = \frac{FS_{det,total}}{1-0.5V_{cu}} \quad (16)$$

$$\sigma FS_{st,total} = \frac{FS_{det,total} \cdot V_{cu}}{1-0.5V_{cu}} \quad (17)$$

The probability of failure of slopes in cohesive materials under undrained conditions is expressed as:

$$p_f = p(FS_{st,total} < FS_{min} = 1) \quad (18)$$

Transforming in standard normal distribution and using Equations 16 and 17, the expression of p_f is:

$$p_f = \text{Erf} \left(\frac{1 - 0.5V_{cu} - FS_{det,total}}{FS_{det,total} \cdot V_{cu}} \right) \quad (19)$$

The relationship between the p_f and the $FS_{det,total}$ for various values of V_{cu} is illustrated in Figure 4. It is concluded that in this case, p_f is determined only by the value of $FS_{det,total}$ and V_{cu} which depends on the heterogeneity of the geomaterial.

It is observed that an increase of the value of $FS_{det,total}$ results in a significant decrease of the value of p_f for $FS_{det,total} < 2$ and does not induce a considerable decrease in p_f for $FS_{det,total} > 2$, because of the decreasing inclination of the curves.

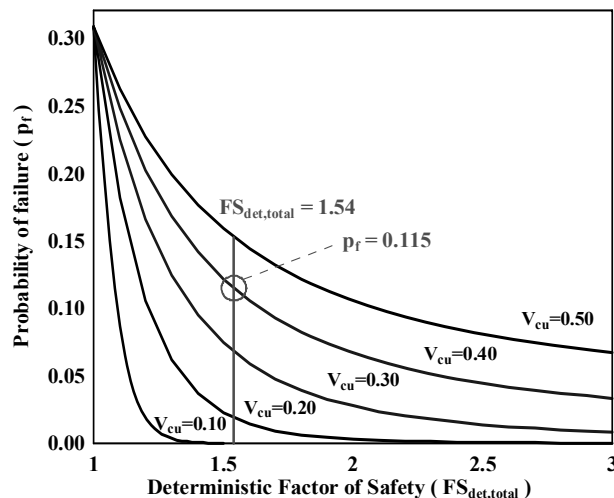


Figure 4. Probability of failure as a function of the deterministic factor of safety (FS_{det}) and the variability index of c_u (V_{cu}) for slopes in cohesive soil under undrained conditions

According to Eurocode 7, $FS_{det,total}$ is equal to $\gamma_M \cdot \gamma_{cu} = 1.1 \cdot 1.4 = 1.54$. Thus, all slopes that are designed to the ultimate limit state according to Eurocode 7 and have $V_{cu}=0.40$ are characterized by a probability of failure equal to 11.5%, independently of other characteristics.

5 CONCLUSIONS

The level of safety in geotechnical projects, usually expressed by the Safety Factor in Design Codes, can be better described by the probability of failure using stochastic analyses which account directly for problem uncertainties. Geotechnical problems can be analysed stochastically without added difficulties, since such analyses do not require more data, time and effort (El-Ramly et al. 2002).

The present paper investigates the stochastic characteristics of soil slopes designed according to Eurocode 7 using parametric probabilistic analyses. A closed-form analytical solution is also obtained for undrained analyses of slopes in cohesive materials.

It is shown that the probability of failure of soil slopes, in general, can be estimated from the geometrical parameters of the problem, the unit weight and cohesion of the material and the value of the retaining force. The probability of failure, for the same value of the deterministic Safety Factor ($FS_{det,total}$) can be decreased with the use of support elements (e.g. anchors, geotextiles etc) which are characterized by a very low strength variability. For the slopes designed according to Eurocode 7 probability of failure varies from 0 to 12% percent, while 30% of the slopes correspond to values of p_f larger than 5%.

In the case of undrained analyses, the Safety Factor can be calculated by an analytical expression and is proportional to the undrained shear strength (c_u). It is thus possible to determine the required deterministic Safety Factor ($FS_{det,total}$) for a given probability of failure (p_f) and vice versa. It is shown that for slopes designed according to Eurocode 7, the probability of failure under undrained conditions is 11.5% ($V_{c_u}=0.40$).

REFERENCES

- Duncan, J.M., & Wright, S.G., 2005. *Soil Strength and slope stability*. New Jersey: John Wiley and Sons
- El Ramly, H., Morgenstern, N.R. & Cruden, D.M., 2002. Probabilistic slope stability analysis for practice. *Canadian Geotechnical Journal*, Vol. 39, pp. 665-683.
- Eurocode 7, 2004: EN1997-1, Geotechnical Design – Part 1: General Rules. Bruxelles: CEN.
- Frank, R., Bauduin, C., Driscoll, R., Kavvas, M., Krebs Ovesen, N., Orr, T. & Schuppener, B., 2004. *Designer's Guide to EN 1997-1 Eurocode 7: Geotechnical design-General rules*. London: Thomas Telford Ltd.
- Fredlund, D.G. & Dahlman, A.E., 1972. Statistical geotechnical properties of glacial lake Edmonton sediments, in *Statistics and Probability in Civil Engineering*. London: Hong Kong University Press, distributed by Oxford University Press.
- Harr, M.E., 1987. *Reliability based design in civil engineering*. New York: Dover Publications INC.
- Kulhawy F.H., 1992. On the evaluation of soil properties, *ASCE Geotechnical Specialty Publication*, Vol. 31, pp. 55-115.
- National Annex, 2007: Greek National Annex to EN 1997-1, Athens Greece: ELOT.
- Schneider, H.R., 1999. Determination of characteristic soil properties. *Proceedings of the 12th European Conference on Soil Mechanics and Foundation Engineering*, Amsterdam, Balkema, Rotterdam, Vol. 1, pp. 273-281.
- Schultze, E., 1972. Frequency distributions and correlations of soil properties, in *Statistics and Probability in Civil Engineering*. London: Hong Kong University Press, distributed by Oxford University Press.

ΠΡΟΣΕΧΕΙΣ ΓΕΩΤΕΧΝΙΚΕΣ ΕΚΔΗΛΩΣΕΙΣ

Για τις παλαιότερες καταχωρήσεις περισσότερες πληροφορίες μπορούν να αναζητηθούν στα προηγούμενα τεύχη του «περιοδικού» και στις παρατιθέμενες ιστοσελίδες.

Submarine Mass Movements and Their Consequences, 4th International Symposium, Austin, Texas, November 8 – 11, 2009,

www.beg.utexas.edu/indassoc/dm2/Conference2009

2nd International Conference Geosynthetics Middle East - Waterproofing Systems and Reinforced Structures, 10 and 11 November 2009, Dubai / UAE, www.skz.de



5th Congress on Forensic Engineering November 11 – 14, 2009, Washington DC

content.asce.org/conferences/forensics2009/index.html

ASCE's Technical Council on Forensic Engineering welcomes your input on topics, tracks, short courses, or special symposia.

Every year, structures and other engineered facilities suffer damage and performance problems because of natural and manmade disasters, unanticipated loading conditions, poor design, lack of maintenance, and poor construction practices.

As TCFE celebrates 25 years of service, we invite the public to join us as we reflect on a quarter century of construction pathology – understanding why and how structures fail.

Suggested topics

Structure

- Buildings
- Bridges
- Parking structures, stadiums, and other special purpose structures
- Temporary structures
- Industrial structures
- Progressive Collapse
- Vibration

Failures During Construction

- Cranes
- Scaffolding
- Shoring
- Construction phase loading
- Protecting adjacent structures

Extreme Loading

- Blast
- Impact
- Fire
- Seismic

Building Envelope

- Façades

- Roofs
- Foundation waterproofing
- Thermal performance
- Water and moisture management
- Performance and durability of materials and systems

Environmental

- Indoor air quality
- Mold

Geotechnical

- Soil stability
- Foundation settlement/failure

Professional Practice

- Ethics
- The legal arena and the role of the expert
- Working with the insurance industry
- Conducting the right investigation for your client

Education

- Case studies in forensic engineering education
- Historical Failures
- Educators' experiences

Forensic Investigations

- Tools and techniques (e.g. visual assessment, inspection openings, non-destructive testing, load testing, simulated weather)
- Investigation methodology and approach
- Case studies

Repairs and Remediation

- Structural repair
- Strengthening



12th International Conference of ACUUS «Using the Underground of Cities: for a Harmonious and Sustainable Urban Environment», November 18-19, 2009, Shenzhen City (China), www.acuus.qc.ca/coming.html

6th WBI-International Shortcourse «Rock Mechanics, Stability and Design of Tunnels and Slopes», November 26 to 30, 2009, Christmas market time, WBI - head office, Aachen, Germany, www.wbionline.de

5th Colloquium "Rock Mechanics - Theory and Practice" with "Vienna-Leopold-Müller Lecture", November 26th and 27th, 2009, christine.cerny@tuwien.ac.at

Stuva Tagung'09 – Stuva Conference'09 "Tunnels – Key to Sustainable Mobility", 1-3 December 2009, CCH Hamburg, Germany, www.stuva.de/STUVA-Conference-09.tagung.0.html?&L=1

International Symposium on Geotechnical Engineering, Ground Improvement, and Geosynthetics for Sustainable Mitigation and Adaptation to Climate Change including Global Warming, 3 to 4 December 2009, Bangkok, Thailand, www.set.ait.ac.th/acsiq/conference

International Symposium on Ground Improvement Technologies and Case Histories (ISGI09), 9 to 11 December 2009, Singapore, ISGI09@nus.edu.sg

Conference on Improving the Seismic Performance of Existing Buildings and Other Structures, 9 – 11 December 2009, San Francisco, USA, www.atc-sei.org

13th International Conference on Structural & Geotechnical Engineering, Cairo, Egypt, 27-29 December 2009, www.icsge2009.com

GeoFlorida - Advances in Analysis, Modeling & Design, February 20-24, 2010, West Palm Beach, Florida, USA content.asce.org/conferences/geoflorida2010/index.html

CAVING 2010 Second International Symposium on Block and Sublevel Caving, 20 - 22 April 2010, Perth, Australia, www.caving2010.com

CPT'10 2nd International Symposium on Cone Penetration Testing, May 9 - 11, 2010, Huntington Beach, California, USA.



17SEAGC

**THE SEVENTEENTH SOUTH ASIAN
GEOTECHNICAL CONFERENCE**
Taipei, Taiwan, May 10 - 13, 2010
www.17seagc.tw

The SEAGC is the official conference of the Southeast Asian Geotechnical Society. The objectives of the Conference are to promote good liaison and cooperation with member countries in SEAGS and its relationship with other international and related societies in the exchange of information for tackling common areas of interests in Geotechnical Engineering; gather the pioneers of the Society and to look at the development, advancement and achievements and put them on record for the benefits of engineers, and others who are interested in Geotechnical Engineering; provide an opportunity for engineers to publish their works and networks with others and provide an excellent opportunity for participants who are members of engineering profession to meet socially and exchange information and ideas pertaining to the profession. Since the 1st SEAGC held in Bangkok in 1967, sixteen conferences were held in Singapore, Kuala Lumpur, Hong Kong, Taipei and Bangkok. This is the fourth time that Taipei will host the Conference, and it is solemn by the supports of AGSSEA and ISSMGE. The 17SEAGC has a three-day in-house program consisting the Keynote, Guest and Special Lectures and Plenary and Discussion Sessions that cover through the themes of this conference. A number of Special Sessions supported by TC and ATC committees on Natural Hazard Mitigations, Geotechnical Code Development as well as a Forum on geotechnical industry/academia dialogue are scheduled. Finally, technical tours are arranged for attendees to visit NTU/NTUST/NCREE laboratories and large-scale construction sites around Taipei. As the host of 17SEAGC, the SEAGS allied with TGS warmly welcome all the society members and international friends to join us in Taipei.

Dr. Chung-Tien Chin, President, SEAGS
Prof. Horn-Da Lin, President, TGS

Main Theme: Geo-engineering for Natural Hazard Mitigation and Sustainable Development

Conference Topics

1. Site characterization and laboratory testing
2. Ground improvement and reinforcement
3. Design, construction and performance of foundations
4. Ground excavations and tunnelling
5. Land-slide and debris-flow hazard mitigation and rehabilitation
6. Geotechnical earthquake engineering
7. Geo-environmental engineering
8. New generation design code developments
9. Geo-information and land reclamation technologies

Contact
Techniques
Secretary General, 17SEAGC
Prof. Der-Wen Chang
Department of Civil Engineering, Tamkang University, Tamsui, Taiwan 25137
Tel: +886 (2) 2623-4224
Fax: +886 (2) 2620-9747
E-mail: dwchang@mail.tku.edu.tw

Administration
17th SEAGC Secretariat
Ms. Shaan Hsieh
Elite PCO
4Fl., No.158, Jingye 1st Rd., Taipei 10462, Taiwan
Tel: +886 (2) 8502-7087 ext. 13
Fax: +886 (2) 8502-7025
E-mail: seagc2010@elitepco.com.tw



ITA - AITES 1010 World Tunnel Congress and 36th General Assembly "TUNNEL VISION TOWARDS 2020", Vancouver, Canada, May 14 - 20, 2010, www.wtc2010.org

12^o Διεθνές Συνέδριο της Ελληνικής Γεωλογικής Εταιρείας, Πάτρα, 19 - 22 Μαΐου 2010, www.synedra.gr

78th ICOLD Annual Meeting & International Symposium "DAMS AND SUSTAINABLE WATER RESOURCES DEVELOPMENT", 23 - 26 May 2010, Hanoi, Vietnam, www.vncold.vn/icold2010

IX International Conference on Geosynthetics, Guarujá, Brazil, 23 - 27 May 2010 - www.igsbrasil.org.br/icg2010

Fifth International Conference on Recent Advances in Geotechnical Earthquake Engineering and Soil Dynamics and Symposium in Honor of Professor I. M. Idriss, May 24 - 29, 2010, San Diego, California, USA, 5geoeqconf2010.mst.edu

11th International Conference "Geotechnical Challenges in Urban Regeneration", 26th - 28th May 2010, ExCel London, www.geotechnicalconference.com/page.cfm/Link=20

Tenerife 2010 Cities on Volcanos, 3rd International Workshop on Rock Mechanics and Geo-engineering in Volcanic Environments, Canary Islands, 31st of May and 1st of June 2010, www.citiesonvolcanoes6.com

BRATISLAVA 2010 14th Danube-European Conference on Geotechnical Engineering, Bratislava, Slovakia, 2nd - 4th June 2010, www.decge2010.sk

NUMGE 2010 7th European Conference on Numerical Methods in Geotechnical Engineering June 2 - 4, 2010, Trondheim, Norway, www.ivt.ntnu.no/numge2010

2010 MOSCOW - International Geotechnical Conference GEOTECHNICAL CHALLENGES IN MEGACITIES, 7 - 10 June 2010, Moscow, Russia www.GeoMos2010.ru

International Conference Underground Construction Prague 2010 Transport and City Tunnels, 14 - 16 June 2010, Prague, Czech Republic, www.ita-aites.cz

Rock Mechanics in Civil and Environmental Engineering, European Rock Mechanics Symposium (EUROCK 2010) ISRM Regional Symposium on Rock Mechanics, Lausanne, Switzerland, 15 - 18 June 2010, lmr.epfl.ch

7th International Conference on Physical Modelling in Geotechnics, Zurich, Switzerland, 28 June - 1 July 2010, www.icpmg2010.ch

ER2010 Earth Retention Conference 3, August 1 - 4 2010, Bellevue, Washington, USA, content.asce.org/conferences/er2010

Isap Nagoya 2010 - The 11th International Conference on Asphalt Pavements, August 1 to 6, 2010, Nagoya, Japan, www.isap-nagoya2010.jp

ISRS V The 5th International Symposium on In-Situ Rock Stress, August 25-28, 2010 Beijing, China, www.rockstress2010.org



Pipelines Conference 2010
August 28 - September 1, 2010
Keystone Resort & Conference Center
Keystone, (Dillon) Colorado

content.asce.org/conferences/pipelines2010/call.html

The worldwide market and demand for infrastructure materials and constantly changing economic times has forced agencies, engineers, manufacturers, contractors, and operators to evaluate the management, safety, design, operation, and maintenance issues when designing, constructing, maintaining, and operating water, wastewater, oil, gas, and other pipeline infrastructure.

All stakeholder parties associated with pipelines face the immense challenge of "climbing the peak" toward "renewal, rehab, and reinvestment" in their aging infrastructure.

Professional organizations must provide forums for discussion of these issues to enhance the civil engineer's knowledge of state-of-the-art techniques related to pipeline engineering, rehabilitation, safety, and risk management as pipeline infrastructure is planned, designed, constructed, and operated. The American Society of Civil Engineers (ASCE) continues to remain at the leading edge in ensuring the public's safety and confidence that pipeline infrastructure is cost effective and secure so the public can maintain their quality of life moving forward with confidence into the future. For this reason, the Pipeline Division, in cooperation with the Pipeline Infrastructure Committee will hold a technical specialty conference for Pipelines Conference 2010 in Keystone, Colorado, focusing on advances in pipeline rehabilitation, risk management, safety, integrated asset management, and pipeline engineering and construction.

This specialty conference is an excellent opportunity to assert leadership in the field of pipeline engineering through a collaborative effort related to advances in pipeline planning, design, construction, materials, condition assessment, corrosion protection, rehabilitation, vulnerability analysis, asset management, regulations, risk assessment, and business decisions associated with pipeline systems, and public and environmental safety. Papers, workshops, and panel discussions will be organized to cover special topics and recent regulatory initiatives in the water, wastewater, oil, and gas pipeline industries.

Pipelines Conference 2010 will be held in Keystone, Colorado, and is expected to draw interest from all facets of the industry— owners, consultants, academia, contractors, and manufacturers— and participants from around the world.

The following are suggested pipeline topics and subdivisions to match the conference theme:

Infrastructure Evaluation

Assessment Inspection
PCCP Monitoring & Rehabilitation
Corrosion Control/Monitoring
Leak Detection & Monitoring
Pipeline Location Technologies
Case Histories/Studies
Condition Assessment
Asset Management
Forensics
Life Cycle Cost Analysis
Geographic Information Systems

Pipeline Durability

Material Selection
Research and Development
Pipeline Performance
Case Histories/Studies

Operation and Maintenance

Water Quality Regulations
Case Histories/Studies
Valve Changes
ROV

Planning

Case Histories/ Studies
Technology Evaluation
Environmental Mitigation
Gas/Oil Regulatory Update

Risk Management

Construction and Safety Trend Analysis
Risk Assessment
Regulatory Initiatives
Hazard Assessment

Hydraulic Design

Transient Analysis
Hydraulic Modeling
Case Histories/Studies

Construction

Construction Management
Trenchless Technology
Pipeline Rehabilitation
Case Histories/Studies
Pipeline Installation
Construction Inspection
Storm Water Pollution Prevention Plans
Claims Analysis
Construction Safety

Design

Seismic
Pipeline Crossings
Appurtenance Design
Codes and Regulations

Specialty

Student Papers
Engineer's Without Borders
Projects

For technical program questions, contact the Technical Program co-chairs:
Tom Roode, P.E. tom.roode@denverwater.org
George Ruchti gruchti@acipco.com



14th European Conference on Earthquake Engineering,
Ohrid, FYROM, August 30 – September 3 2010,
www.14ecee.mk

Geologically Active 11th IAEG Congress, 5 – 10 September
2010, Auckland, New Zealand, www.iaeg2010.com

GBR-C 2k10 - 3rd International Symposium on Geosyn-
thetic Clay Liners, 15 - 16 September 2010, Würzburg,
Germany



**II International Congress on Dam
Maintenance and Rehabilitation
28th-30th September 2010, Zaragoza, Spain
www.damrehabilitationcongress2010.com**

In October of 2002, SEPREM (Sociedad Española de Presas y Embalses, or Spanish Society of Dams and Reservoirs), in collaboration with the Dirección General del Agua del Ministerio de Medio Ambiente y Medio Rural y Marino (Water Directorate of the Ministry of the Environment), organized in Madrid (Spain) the First International Congress on Dam Maintenance and Rehabilitation. The bulleting which announced the Congress stated the following:

"Dams, like every human artefact immersed in Nature, are originally conceived to stand against a number of actions. After their construction, dams are subject to a series of external agents and processes which tend to deteriorate the qualities with which they were originally conceived to stand against these actions. Deterioration processes may affect the foundation on which the dam rests, the materials with which it was built, or result in deterioration of the outlet works. Reservoir sedimentation or water quality issues within the reservoir also give raise to problems that must be addressed. In addition to the previous issues, it will be necessary in many cases to respond to increased safety standards, either in the structural or hydrological fields.

Criteria to establish how dams and reservoirs deteriorate and the magnitude of this deterioration vary from country to country, but it is clear anyhow that works of maintenance, rehabilitation, retrofit and decommissioning constitute more and more an important field of activity in every country which has in place a system of dams of certain age, among which Spain is notorious. Dam Owners will necessarily have to increase their budget allocation to keep their facilities in proper order. A substantial number of scientists and engineers, as well as consulting and contracting companies will be involved in these activities".

The time passed since the Congress, far from making these words less valid, has only made them more evident and pressing, making some related concepts more obvious such as the incidence of climatic change in the management of water resources, and the need for sustainability. In view of all this, SEPREM, again in collaboration with the Dirección General del Agua del Ministerio de Medio Ambiente y Medio Rural y Marino announces and has the pleasure to invite you to attend the Second International Congress on Dam Maintenance and Rehabilitation, to take place in Zaragoza (Spain) during September 2010.

This Congress will serve as a forum, not only to exchange knowledge and debate experiences of the diverse and complex field of dam maintenance and rehabilitation, but also to share the techniques and preventive activities which may prevent or delay the need for major capital maintenance. The Congress will also serve to convey the experience of the Spanish practitioners and companies to the international community of professionals in this field.

Congress Topics

**SECTION 1.
GROUNDWORK AND PERIODIC MAINTENANCE**

to include:
Applicable legislation and standards. Current status and future tendencies. Adequacy of existing dams to policy changes.
Monitoring, inspection and diagnosis activities. Evaluation of the behaviour.
Conservation and maintenance. Periodic performances in the watershed, reservoir and dam.
Programming of extraordinary investments.

**SECTION 2.
CONCERNING RESERVOIR CAPACITY, WATER RESOURCES
MANAGEMENT AND HYDRAULIC PERFORMANCE**

to include:
Water resources management and sustainability. Climate Change.
Reservoir siltation and sediment contamination. Proceedings for qualitative and quantitative recovery.
Flood control and hydrological safety. Proceedings for outlet work rehabilitation, improvement in spillway performance and remedial measures.
Alternative solutions. Freeboards and storage limitations.
Dam heightening. Measures to withstand crest overspill.

**SECTION 3.
CONCERNING STABILITY AND STRUCTURAL BEHAVIOUR**

to include:
Old dams. Upgrading proceedings to present standards and needs.
On-going deterioration processes. Long term performance.
Remedial measures.
Safety regarding seismic activity. Proceedings to meet current standards for seismic activity.
Conservation and remedial measures in reservoir, foundation and dam (earth dam, gravity dam, arch dam, etc.).

E-mail: sepremzaragoza2010@tileasa.es
TILESA OPC, S.L.
Londres 17- 28028 Madrid
Tel: +34 913612600 - Fax: +34 913559208
www.damrehabilitationcongress2010.com



International Symposium on Geomechanics and Geotechnics: From Micro to Macro 10 – 12 October 2010, Shanghai, China, geotec.tongji.edu.cn/is-shanghai2010

11th International Symposium on Concrete Roads, Seville (Spain) 13th - 15th October 2010, www.2010pavimentosdehormigon.org

ARMS – 6 ISRM International Symposium 2010 and 6th Asian Rock Mechanics Symposium "Advances in Rock Engineering", New Delhi, India, 23 – 27 October 2010, www.cbip.org



2nd International Conference on Geotechnical Engineering - ICGE 2010 Innovative Geotechnical Engineering October 2010, Hammamet, Tunisia

Contact person: Imen SAID

- Phone : (216) 22 14 66 34
- E-mail: imen_said@yahoo.fr
- Adress : National Engineering School of Tunis , ENIT, BP 37, Le Belvédère 1002, Tunis Tunisie



7 – 10 November 2010, San Fransisco, USA
www.icse-5.org

The International Conference on Scour and Erosion is a respected event in the technical conference calendar for engineers, scientists, decision makers and administrators who provide services in the areas of scour and erosion. Its importance and reputation has grown through the technical successes of the first four conferences:

- College Station, Texas, USA(2002)
- Singapore (2004)
- Amsterdam, The Neterlands (2006)
- Tokyo, Japan (2008)

Now at its 5th meeting, the conference will to highlight the multi-disciplinary nature of scour and erosion problems and solutions, which require approaches that merge expertise in a wide variety of fields. Contributions discussing emerging theoretical developments, field and laboratory studies, field applications of technology, and case histories are especially encouraged. The conference will span three days with keynote speakers in plenary sessions followed by concurrent sessions. ICSE-5 will also offer short courses before the conference and technical tours following the conference. Additional events which will help you to renew acquaintances and meet new colleagues include a welcome reception and a networking reception with posters in the Exhibition Hall.

Conference Topics

- Scour of foundations
- Cohesive scour
- Scour in gravel, sand, and silt
- Rock scour
- Unknown foundations
- Levee scour
- Dam scour
- Bridge scour
- Erosion of soils
- Laboratory measurement of erosion properties and countermeasures
- Field studies / inspection
- Case histories
- International guidelines and practices
- Scour risk management
- Numerical modeling
- Physical model tests
- Internal dam erosion
- Pressure scour
- Debris scour
- General degradation and aggradation
- Pier and abutment scour
- Scour depth prediction
- Scour of underwater pipelines
- Scour of offshore platforms
- Countermeasure selection and design
- Stream stability/meander migration
- Scour monitoring
- Scour and stream ecology (e.g., habitat enhancement)



ISFOG 2010 2nd International Symposium on Frontiers in Offshore Geotechnics, 8 – 10 November 2010, Perth, Western Australia, w3.cofs.uwa.edu.au/ISFOG2010

6ICEG 2010 - Sixth International Congress on Environmental Geotechnics, November 8 - 12, 2010, New Delhi, India www.6iceg.org

5th International Conference on Earthquake Geotechnical Engineering, Santiago, Chile, 17 – 20 January 2011, www.5icege.cl

International Conference on Tunnelling and Trenchless Technology, 1-3 March 2011, Kuala Lumpur (Malaysia), www.iem.org.my/external/tunnel/index.htm

WTC2011 Helsinki, AITES-ITA 2011 World Tunnel Congress and 37th General Assembly, 21-25 May 2011, Helsinki, Finland, www.ril.fi/web/index.php?id=641

XIV Asian Regional Conference Soil Mechanics and Geotechnical Engineering, Hong Kong, China, 23 - 28 May 2011

XV African Regional Conference on Soil Mechanics and Geotechnical Engineering Maputo, Mozambique, 13 - 16 June 2011.



**Fifth International Symposium on Deformation
Characteristics of Geomaterials (IS-Seoul 2011)
31 August - 3 September 2011, Seoul, Korea**

Contact person: Prof. Dong-Soo Kim
Dept. of Civil & Environmental Eng., KAIST
305-701 Daejeon, Korea
• Phone: 82-42-350-3619
• Fax: 82-42-350-3610
• E-mail: dskim@kaist.ac.kr



XV European Conference on Soil Mechanics and Geotechnical Engineering, 12 - 15 September 2011, Athens, Greece,
www.athens2011ecsmge.org

24th WORLD ROAD CONGRESS, 25 - 30 September 2011,
Mexico City, Mexico

XIV Panamerican Conference on Soil Mechanics and Geotechnical Engineering (October) & V PanAmerican Conference on Learning and Teaching of Geotechnical Engineering & 64th Canadian Geotechnical Conference, Toronto, Ontario, Canada, 2 - 6 October 2011

Beijing 2011, 12th International Congress on Rock Mechanics, 16 - 21 October 2011, Beijing, China,
www.isrm2011.com

ΗΛΕΚΤΡΟΝΙΚΑ ΠΕΡΙΟΔΙΚΑ



**INTERNATIONAL SOCIETY FOR
SOIL MECHANICS AND GEOTECHNICAL ENGINEERING**
www.issmge.org

Κυκλοφόρησε το Τεύχος Vol. 3, Issue 3 του ISSMGE Bulletin (Σεπτέμβριος 2009) με απολογισμό του ήδη απεθάντος προέδρου της ISSMGE Prof. P. Seco e Pinto, παρουσίαση των δραστηριοτήτων Τεχνικών Επιτροπών (TC) και εθνικών ενώσεων, άρθρο – case history με τίτλο "Case History Some aspects of the M6.3 April 6 2009, L'Aquila, Italy, earthquake" και άλλα ενδιαφέροντα νέα. Επίσης παρουσιάζεται νεκρολογία για τον Γιάννη Βαρδουλάκη.



www.geoengineer.org

Κυκλοφόρησαν τα Τεύχη #57 και #58 του Newsletter του Geoengineer.org (Σεπτέμβριος και Οκτώβριος 2009) με πολλές χρήσιμες πληροφορίες για όλα τα θέματα της γεωτεχνικής μηχανικής. Υπενθυμίζεται ότι το Newsletter εκδίδεται από τον συνάδελφο και μέλος της ΕΕΕΕΓΜ Δημήτρη Ζέκκο [secretariat@geoengineer.org].



International Society for Rock Mechanics

ISRM

newsletter

www.isrm.net/adm/newsletter

Κυκλοφόρησε το Τεύχος No. 7 - Σεπτέμβριος 2009 Newsletter της International Society for Rock Mechanics.



**INTERNATIONAL TUNNELLING AND
UNDERGROUND SPACE ASSOCIATION**

ita@news n°30

www.ita-aites.org/cms/index.php?id=486

Κυκλοφόρησε το Τεύχος No. 30 - Σεπτέμβριος 2009 των ita@news της International Tunnelling Association.



**British Tunnelling Society Newsletter
September 2009**

www.britishtunnelling.org.uk



**International Journal of
Geoenvironment Case Histories
Volume 1, Issue #3, October 2008**

In this issue:

Thomas D. Richards Jr. **Discussion of: "Design Process of Deep Soil Mixed Walls for Excavation by Casandra J. Rutherford, Giovanna Biscontin, Demetrious Koutsotas, and Jean-Louis Briaud, Volume 1, Issue #2, pp. 56-72"**

John B. Burland, Michele B. Jamiolkowski, Carlo Viggiani **Leaning Tower of Pisa: Behaviour after Stabilization Operations**

Jean-Louis Briaud, Brad Smith, Keun-Young Rhee, Hugh Lacy, Jennifer Nicks **The Washington Monument Case History**

Vladimir M. Ulitsky, Alexey G. Shashkin, Constantin G. Shashkin, Michael B. Lisyuk **Reconstruction of Konstantinsky Palace in a Suburb of Saint Petersburg**

ΕΕΕΕΓΜ

Τομέας Γεωτεχνικής
ΣΧΟΛΗ ΠΟΛΙΤΙΚΩΝ ΜΗΧΑΝΙΚΩΝ
ΕΘΝΙΚΟΥ ΜΕΤΣΟΒΙΟΥ ΠΟΛΥΤΕΧΝΕΙΟΥ
Πολυτεχνειούπολη Ζωγράφου
15780 ΖΩΓΡΑΦΟΥ

Τηλ. 210.7723434
Τοτ. 210.7723428
Ηλ-Δι. secretariat@hssmge.gr ,
geotech@central.ntua.gr
Ιστοσελίδα www.hssmge.org (υπό κατασκευή)

«ΤΑ ΝΕΑ ΤΗΣ ΕΕΕΕΓΜ» Εκδότης: Χρήστος Τσατσάνιφος, τηλ. 210.6929484, τοτ. 210.6928137, ηλ-δι. pangaea@otenet.gr

«ΤΑ ΝΕΑ ΤΗΣ ΕΕΕΕΓΜ» «αναρτώνται» και στην ιστοσελίδα www.hssmge.gr